The role of actin in hyphal tip growth

A thesis submitted in partial fulfilment of the requirements for the

Degree

of Doctor of Philosophy in Biochemistry

in the University of Canterbury

by Sandy H.Y. Suei

University of Canterbury

2008

In memory of Sandra Jackson

Table of contents

Acknowledgement

I am greatly appreciative to my supervisor Dr. Ashley Garrill, who has made an enormous contribution to this thesis, helping me develop my scientific brain, discovering my talent in this field, and most importantly, always having faith in me. I also deeply thank him for allowing me to watch soap dramas during lunch breaks, listening to all my lala ideas, always asking for gossips, putting Jazz on really loudly, telling me never work too hard and having his permission to swear in the lab.

I am especially grateful to have had Dr. Sandra Jackson as a co-supervisor as she made my supervisory team so much cooler by contributing her knowledge and her optimistic personality. Most of all, I thank her for always passing on directions where Ashley was hiding from me.

I would also like to thank my later co-supervisors Dr. Juliet Gerrard and Dr. Drusilla Mason for their support and care.

Huge thanks to these on-campus boys and girls who bear with me to accomplish this monstrous degree:

Sophie Walker is a great tutor, lab member, coffee mate, and listens to all my dramas. Kenny Chitcholtan taught me how to dance in the lab (or be his pole) with kinky boots. Jason Song and Angie Sin helped me with molecular work. Claudia Lang is my beloved progress watcher. Tina Yang is my gossip source and gym mate. Laura Rolston is the most amazing proof reader. Craig Galilee is helpful in technical support, material ordering, and always telling me off. Matt Walters helped with poster design and my pretty pictures on the PhD webpage. Manfred Ingerfeld for confocal techniques and always be there on Friday afternoons. Jackie Healy kindly helped me with western blots and charged Ashley for it. Gerald Cuthbert for fixing every single broken piece that has a wire in it.

Great thanks to my off-campus family and friends:

My parents for their life time scholarship plus all the love and support. Allen Suei always tells me to study more and driving home at 180km/hr will do. Angel Lin for keeping me awake during coffee deficient periods whenever she's at work. Jenny Teng helped creating the prize winning poster at IMC8 and her not-so-special 3D poses. Mu-Han Chio helped with the presentation of Fig 6.1 in this thesis.

Abstract

This thesis investigates whether there are alternative mechanisms of tip growth in invasive and non-invasive hyphae of the fungus *Neurospora crassa*. The cytoskeleton protein actin is thought to play a pivotal role in hyphal tip growth, performing a multitude of tasks, one of which may be the provision of a resistive force to counter turgor pressure.

An Actin depleted zone (ADZ) was the dominant feature of invasive hyphal tips, which was largely absent from non-invasive hyphae. The Spitzenkörper was slightly larger in invasive hyphae but this size difference alone was thought insufficient to account for the exclusion of filamentous actin (F-actin) from the tip. The actin nucleating protein formin was found at sites where actin nucleation is occurring, while cofilin, a protein that severs F-actin, was found to localise where F-actin disassembly was likely to be occurring. It is suggested that these proteins are likely to play a role in controlling a dynamic cytoskeleton, rearrangements of which are required for the two modes of growth. Invasive hyphae were found to generate a higher turgor than non-invasive hyphae.

These results suggest that the F-actin rearrangements facilitated by cofilin give an ADZ that may play a role in invasive hyphal tip growth; possibly through a reduction of tip resistance; thus enabling the provision of a greater protrusive force by turgor.

Abbreviation

ABP(s)	Actin binding protein(s)
ADF	Actin depolymerizing factor
ADZ	Actin depleted zone
ADP	Adenosine diphosphate
ATP	Adenosine triphosphate
ANOVA	Analysis of Variance
ARP	Actin related protein
BLAST	Basic Local Alignment Search Tool
bp	Base pair
BSA	Bovine serum albumin
Cc	Critical concentration
EGTA	Ethylene-diamine-tetra-acetic acid
F-actin	Filamentous actin

G-actin	Globular actin
GFP	Green fluorescent protein
HEPES	4-(2-Hydroxyethyl)piperazine-1 -ethanesulfonic acid
IgG	Immunoglobulin G
kDa	Kilo Dalton
PAGE	Polyacrylamide gel electrophoresis
PBS	Phosphate buffer saline
PIPES	Piperazine-N, N'-bis (2-ethanesulfonic acid)
PYG	Peptone- Yeast extract- Glucose
RT-PCR	Real Time- Polymerase Chain Reaction
SEM	Standard error of the mean
SD	Standard deviation
v/v	Volume/ volume
w/v	Weight/ volume

List of Figures

List of Tables

Chapter 1 : General Introduction

1.1 Fungi

The Fungal kingdom (fungi; *Latin*, mushroom) is a grouping of heterotrophic eukaryotes that are diverse and ecologically widespread. While to date, only around 0.1 million species have been described, it is estimated that there may be as many as 1.5 million species, which would rank second only to the insects among the eukaryotes in terms of species diversity (Borkovich et al. 2004; Campbell & Reece 2005). They are one of the most important and essential components for the welfare of ecosystems, as they break down organic materials and recycle nutrients. This service is beneficial to their symbiotic partners such as plants, as well as in agriculture, forestry and food production.

Cytologically, fungi are most distinguishable from other cell walled organisms in that their major cell wall component is chitin, which is a strong, but flexible nitrogen containing polysaccharide. On the other hand, the major polysaccharide of plant and oomycete cell walls is cellulose. While fungi are heterotrophic organisms like animals, they differ from these in that they display absorptive nutrition (i.e., they digest food

externally by secreting exoenzymes to the surrounding environment and then take up the small organic compounds that are formed upon breakdown of more complex molecules). This allows fungi to colonise numerous diverse habitats and display a number of different lifestyles. For example, saprophytic fungi decompose non-living organic materials; while parasitic fungi absorb nutrients from living hosts (some of these can be pathogenic). Mutualistic fungi absorb nutrients from their host in what is typically a reciprocal manner.

The predominant morphological form of filamentous fungi, such as the ascomycete *Neurospora crassa*, which is the focus of this thesis, is a tubular cell called a hypha that grows by a type of polarised growth called tip growth. This growth is fundamental to fungal morphogenesis (Gow 1989). Hyphae elongate in a linear fashion, but the process of branching gives rise to new axes of polarity. These give rise to new hyphal tips and generate the dominant vegetative fungal morphological form, the mycelium (Glass et al. 2004; Riquelme & Bartnicki-Garcia 2004).

The oomycetes such as *Achlya bisexualis*, which are used for numerous comparisons in this thesis, share a similar morphology, but are phylogenically distant to fungi. The phylogenetic detachment of fungi and oomycetes is reflected by the taxonomic

differences in their biochemistry, cell structures, cell wall compositions, and development. However, the fact that they show great similarity in biological activities suggests the convergent evolution across the phylum (Money et al. 2004).

Concurrent with tip growth and branching are the processes of nuclear division, septation and cytokinesis that together contribute to the formation of multicellular or septate hyphae (Garrill 2000; Wendland 2001). Polarity and thus morphology can be influenced through developmental and environmental stimuli (Oh 1997; Kumar et al. 2005; Ma et al. 2006).

Hyphae can be septate (if fungal) or coenocytic (if oomycete). The septa of septate hyphae are cross walls that make fungal mycelia multicellular structures. In contrast, an oomycete mycelium consists of one continuous cytoplasmic mass, which is multinucleate. Some fungi form specialised hyphae, such as parasitic/mutualistic fungi which use haustoria to penetrate cell walls and mutualistic fungi that utilise mycorrhizae to deliver phosphate ions and minerals to plants.

Fungal hyphae are able to grow rapidly (i.e., speeds up to 12 μm/min) (Lopez-Franco et al. 1994). They extend their tips into new territory to compensate for their lack of

motility by focusing their energy and resources on extending hyphal length. Proteins and synthesised materials are channelled through cytoplasmic streaming to the extending hyphal tip. The structure of the mycelium benefits fungi by maximising the ratio of its surface area to its volume, hence increasing feeding efficiency (Campbell & Reece 2005).

1.2 Tip growth

As detailed above, tip growth is a form of cell growth that is characterised by localised expansion at the apex of cells. In addition to fungal hyphae, tip growth occurs in several other cell types including oomycete hyphae, plant root hairs, pollen tubes and algal rhizoids (Heath 1995b). It involves numerous processes, such as cell wall and membrane synthesis/deposition, cytoplasmic migration, organelle positioning within the cytoplasm, and the yielding of the tip region to a protrusive force (Steinberg 1998; Heath & Steinberg 1999; Gupta & Heath 2000; Heath 2000, 2001; Chitcholtan & Garrill 2005). All of these are extremely dynamic processes, and to ensure constancy of shape, require the cooperating actions of a range of proteins (Sone & Griffiths 1999; Heath 2000; Heath & Skalamera 2001). Although tip growth has been extensively researched, there have been, to the best of this author's knowledge, no studies examining how growth mechanisms may change when filamentous fungi grow invasively (i.e., through material). As invasive hyphae penetrate through solid media, it is likely that there are compensatory mechanisms to allow for a greater force required for growth relative to non-invasive hyphae, which extend through liquid media. In oomycetes, there have been indications that rearrangement of cytoskeletal actin creating an ADZ may be required for such growth (Walker et al. 2006).

1.3 The processes of tip growth

1.3.1 Cell wall/plasma membrane synthesis and deposition

During tip growth, synthesis and deposition of apical cell wall and plasma membrane is necessary as an extending hypha has an ever increasing surface area. Thus, these processes are essential and must be regulated to sustain tip expansion and maintain a hypha of constant shape. These processes involve the action of wall vesicles that are thought to contain enzymes and precursors involved in the biosynthesis of cell wall and plasma membrane. They are thought to play a role in exocytosis with the depositing of wall materials/proteins and in endocytosis, which functions to actively recycle membrane. Wall vesicles can aggregate (along with a population of F-actin) into a structure referred to as a Spitzenkörper (German for apical body), which has been hypothesised to act as a vesicle supply centre (VSC). This is specifically located at the apex of growing hyphae or sub-apical branching sites (Bartnicki-Garcia et al. 1989).

Actin cables and filaments (as described below) are likely to direct the delivery of vesicles to sites of growth (Virag & Griffiths 2004). This is suggested by the subapical swelling observed when hyphae are treated with latrunculin, which inhibits the formation of filamentous actin, and hence de-localises vesicle delivery (Heath et

al. 2003). Furthermore, actin and myosin (a motor protein associated with movements along actin filaments) mutants contain accumulations of vesicles, but display a loss of polarised growth. The role of F-actin in the Spitzenkörper is unclear, although it is possible that it could enable movement of the Spitzenkörper to allow directional changes in growth.

1.3.2 Cytoplasmic migration

In hyphal tip growth, the cytoplasm migrates along with the integrated organelles to maintain an apical mass of cytoplasm in the hyphae. This may be analogous to cytoplasmic movements in amoebae (reviewed in Heath & Steinberg 1999). The likeness is suggested by the presence of apical adhesion, actin-based cytoplasmic protrusive and contractile systems (Heath 2000). The movement of cytoplasm, thus, might involve contractions via calcium and F-actin-mediated systems and would be predominantly unidirectional towards the tip (reviewed in Heath & Steinberg 1999).

1.3.3 Organelle positioning

While the cytoplasm migrates with the growing tip, within that cytoplasm organelles retain a characteristic position relative to the growing tip. Thus, dictyosomes are located closer to the hyphal tip than are mitochondria, which in turn are closer to the

tip than nuclei. In more subapical regions, vacuoles predominate. The retention of these positional relationships involves interaction between the respective organelles and cytoskeleton proteins. To cite one relevant study, Suelmann and Fischer (2000) have observed GFP-labelled nuclei, which show asynchronous and bidirectional movement (with velocity up to 0.67 μm/s), and this and other studies have suggested that nuclear positioning in growing hypha may result from a balance of counteracting cytoskeletal motor proteins (Xiang & Morris 1999; Freitag et al. 2004). Vacuoles are dynamic lysosomal compartments of fungi, again these are motile with vectoral transportation occurring along the cytoskeletal elements (reviewed in Cole et al. 1998; Steinberg 1998). Compelling evidence suggests that the spatial organisation is largely dependant on F-actin (reviewed in Walker & Garrill 2006).

1.4 Actin

1.4.1 Role and structure

Actin is an almost ubiquitous protein that is involved in an assortment of fundamental processes in eukaryotic cells. Actin exists in two distinct forms, globular monomeric G-actin and filamentous F-actin, the monomer has a molecular weight of 42- 47 KDa (reviewed in Cooper 1991). The primary sequence of actin has been described in a variety of organisms (Vorobiev et al. 2003). This protein appears to be highly conserved across phyla with less than a 5% difference between yeast and human. The actin protein in *N. crassa* contains 375 amino acid residues with a molecular weight of approximately 42 KDa (Tinsley 1998). Mutation study in *N. crassa* actin (act^1) results in multiple defects in tip growth and branching (Virag & Griffiths 2004).

The sequence identity of *N. crassa* in comparison to several other organisms is shown in Table 1.1 demonstrates the conservation of actin across the phylum, although *N. crassa* shares similar morphology and growth mode to oomycetes and yeasts, they are phylogenically more related to animal than plant. Detailed comparative protein sequence alignment is included in Appendix 1.1.

Table 1.1 Similarity in sequence identity between actin genes in different organisms.

	Actin	*Aspergillus nidulans* (ascomycete)	*Achlya bisexualis* (oomycete)	*Saccharomyce cerevisiae* (yeast)	*Homo sapiens* (animal)
N. crassa	Identity	99%	82%	90%	86%
	Positives	100%	93%	96%	94%

Note: positives suggest the extent to which nucleotide/protein sequence are related.

Although most yeasts and filamentous ascomycetes only express a single actin gene, most other higher eukaryotes express several actin isoforms. They are generally classified into alpha, beta and gamma according to their isoelectric point (reviewed in Pollard & Cooper 1986). Alpha actins are usually expressed in muscular cells, while the beta and gamma isoforms are more apparent in non-muscle cells.

An actin monomer (G-actin) consists of a single polypeptide. The tertiary structure of this protein contains a large and a small domain (Vorobiev et al. 2003). These domains can be further divided into four sub-domains (Figure 1.1). There are two structural features particularly important to the F-actin dynamics. Firstly, there is a high affinity ATP/ADP binding site in a central cleft that normally contains a cation (i.e., Ca^{2+} or Mg^{2+}). Within this cleft, nucleotide hydrolysis occurs and is of particular significance with respect to F-actin dynamics. Secondly, the monomer is longitudinally asymmetrical with different functional groups exposed, which give an intrinsic structural polarity when they associate to form F-actin. Due to biochemical

differences inferred by these different functional groups, monomers associate/ dissociate at the respective ends of an actin filament (termed the barbed or plus (+) and pointed or minus (-) ends) at different rates. One facet of actin dynamics, a process that is referred to as treadmilling occurs when monomers dissociate from the pointed end of a filament at the same rate as monomers associate at the barbed end. As described by Carlier (1998), this phenomenon is a consequence of nucleotide hydrolysis. G-actin with a bound ATP molecule typically associates at the barbed end of a filament; the ATP is then hydrolysed as more ATP actin monomers are added to the barbed end. This has the effect of creating filaments that have ATP associated with the subunits at the barbed end of the filament and ADP associated with the subunits at the pointed ends (as shown in Figure 1.2). During the process of treadmilling, ATP-actin association at the barbed end occurs concurrently with ADP-actin dissociation at the pointed end. The rapid association/dissociation influences the critical concentration (Cc) of the free monomers at the two ends. At the steady state, the rate of actin dissociation from the pointed end is equal to the rate of association from the barbed end. Therefore, the concentration of actin monomer in the medium is maintained as the rates of actin assembly of both ends are identical. Consequently, this results in an actin filament of constant length and a dynamic pool of G-actin (Fig. 1.2) (reviewed in Walker & Garrill 2006).

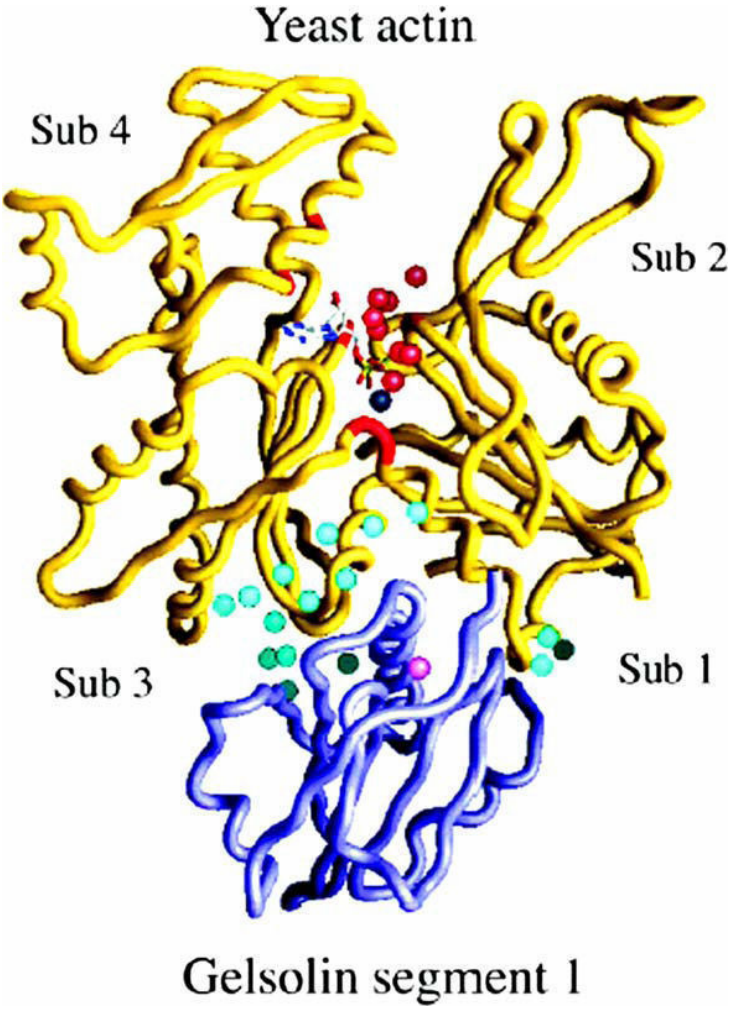

Figure 1.1 Representative three-dimensional structure of actin from yeast that is conjugated with gelsolin segment-1 (blue) to aid in crystallisation. An actin monomer is composed of four sub-domains (Sub 1~4) and contains a nucleotide (ATP/ADP) binding cleft (red) associated with a divalent cation (black) and a water molecule (light blue) (Reproduced from Vorobiev et al. 2003).

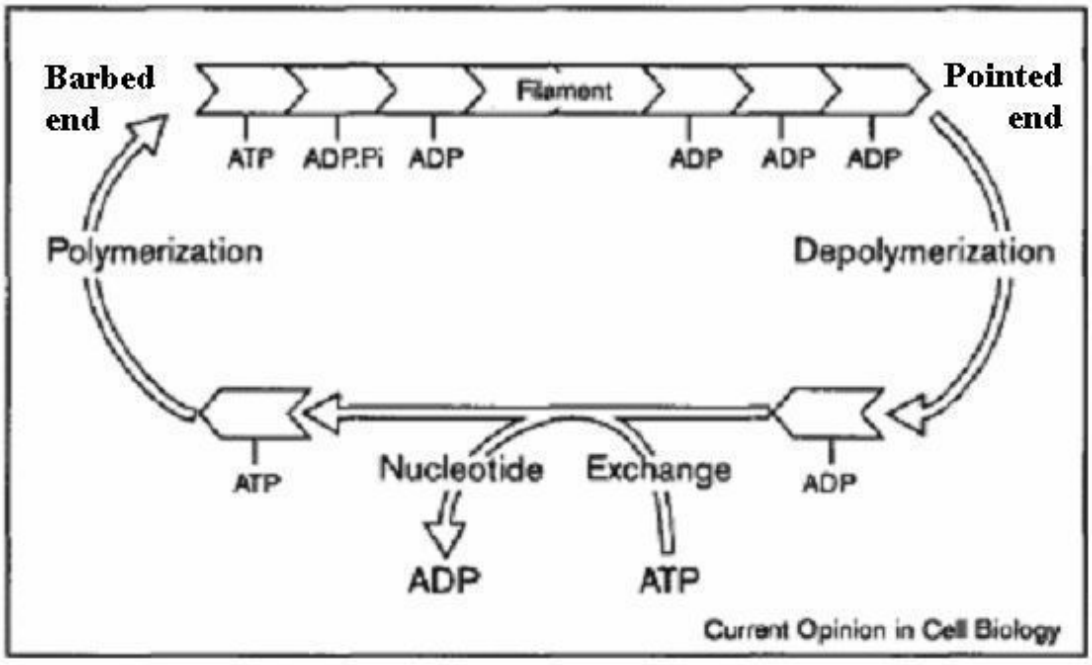

Figure 1.2 Treadmilling cycle of F-actin at the steady state.

At the steady state, the net rate of actin filament growth is zero. $[\text{ATP-G-actin}]_{\text{conc.}}$ in the medium is equal to the dissociation rate at the pointed end; this balances the association rate at the barbed end (Carlier 1998).

Actin filaments (F-actin) are comprised of two long-pitched helical strands that twist every 13 subunits along one strand with a diameter of approximately 7 nm (reviewed in Walker & Garrill 2006). It is likely that these measurements are only approximations, as in a cell, the rotation of strands may be affected by cross-linking. The actin cytoskeleton is a dynamic entity that undergoes rapid and extensive modification in response to cellular requirements. This is achieved mainly through its interaction with a large family of actin binding proteins (ABPs), which are described in more detail below.

1.4.2 Organisation and distribution

The distribution of actin that is observed in an organism varies depending upon different stages of the life cycle, the species that is being observed, and the methodology that has been used to preserve and/or visualise such a dynamic structure. In tip growing organisms, actin filaments normally form an actin cap or patches/plaques and cables. In filamentous fungal species, the most common arrangements are distinct peripheral patches/plaques at or close to the hyphal tips/branching sites. Similarly in yeasts, actin localises predominantly at the sites of bud formation in budding yeast and both growing ends in fission yeasts. These arrangements are comparable to those observed in other tip growing systems, studies

on pollen tubes have revealed a prominent cortical actin fringe composed of longitudinally orientated F-actin (Lovy-Wheeler 2005) and root trichoblasts show an actin cap at the tip during root hair initiation (Braun et al. 1999). In oomycetes, another group of hyphal organisms, albeit one that is phylogenetically very distant from the fungi, actin is present as an apical cap, although this can contain an actin depleted zone, a structure that is described in greater depth later (Walker et al. 2006; Walker & Garrill 2006). The positioning of actin at sites of growth has been cited as crucial to morphogenesis, cytokinesis, septation, and movement and positioning of organelles (reviewed in Walker & Garrill 2006).

Actin cables are a commonly observed arrangement of actin in all organisms, although they vary in length. These are formed by microfilament bundles and act as the conveyer for organelle transportation. Actin cables are typically aligned parallel along the longitudinal axes of filamentous fungal hyphae and extend in a polarised manner in both fungi and yeasts.

1.5 The role of actin binding proteins (ABPs)

As detailed above, actin plays a multitude of roles in eukaryotic cells such as acting as a major determinant of cell morphology. Yet, these various roles could not be achieved by actin alone. This is where a group of accessory proteins, the actin binding proteins (or ABPs), are required to regulate the equilibrium between monomeric G-actin and the polymeric F-actin, to nucleate the formation of F-actin, to sever and break filaments and to bundle and crosslink filaments to each other or to other cytoskeletal elements or cellular structures. They also act as motor proteins producing contractile force or moving cargoes around the cell (Ayscough 1998; Carlier et al. 2003; Mogilner & Oster 2003a, 2003b).

Numerous actin binding proteins appear to share a conserved actin-binding domain that binds actin in the hydrophobic cleft between sub-domains 1 and 3 (Dominguez 2004) (Fig. 1.1). This may to some extent explain why actin is thought to participate in more protein-protein interactions than any other known protein. With respect to the dynamics of actin filaments and the roles that the ABPs play, the processes that occur at the actively growing site of motile cells have been well studied (as shown in Fig 1.3). Such assembly functions to expand the plasma membrane in structures such as lamellipodia (Pollard & Borisy 2003) and in fungi (Steingerg 2007), which involves

the activities of various ABPs. The turnover of actin is also regulated by the activities of profilin, proteins of the Wiskott-Aldrich syndrome protein (WASP) family that activate actin polymerisation cascade from Arp 2/3, and capping proteins (Braun et al. 1999; Blanchoin et al. 2000; Baluška et al. 2001; Higgs & Pollard 2001; Winder 2003).

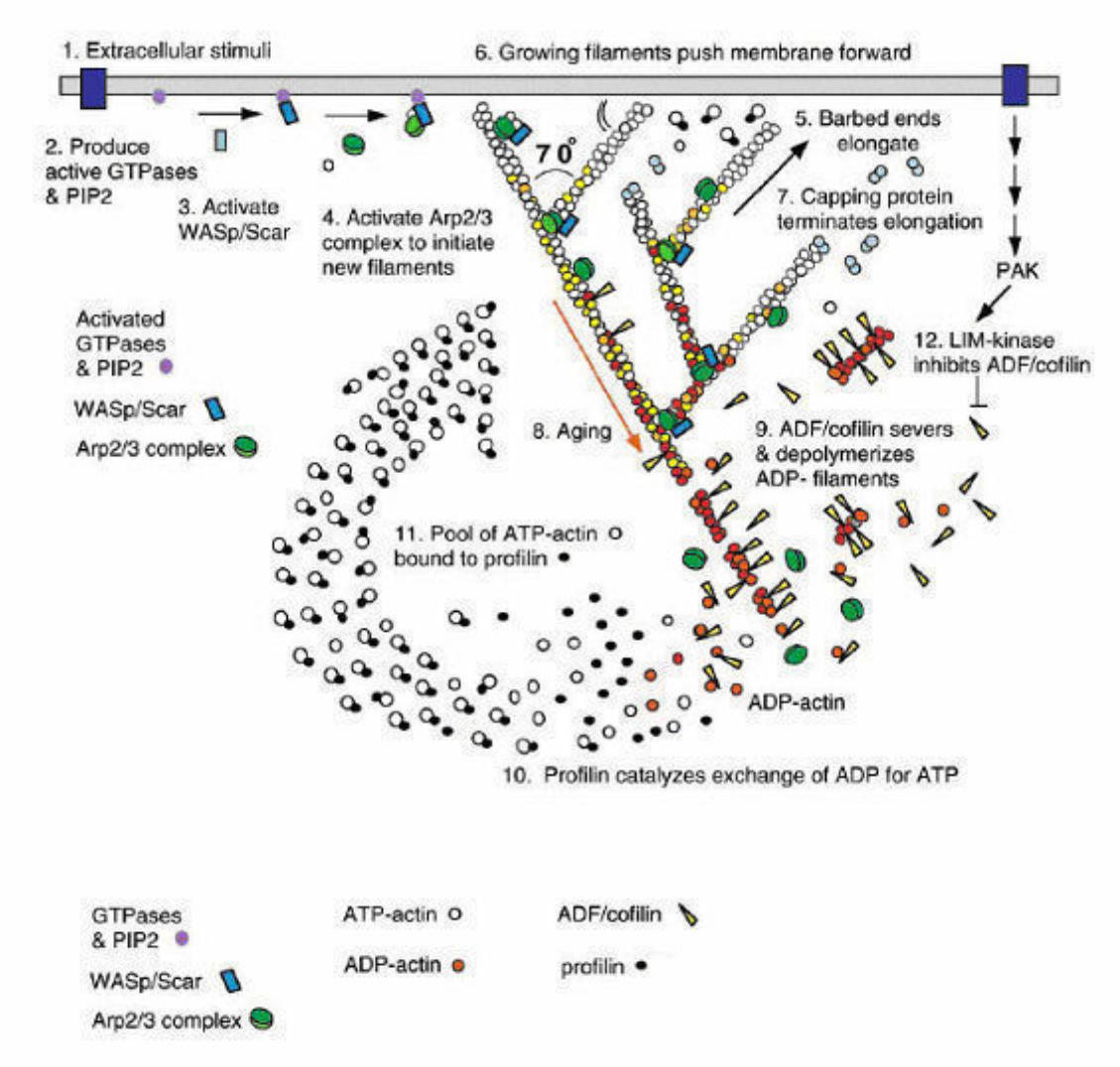

Figure 1.3 Dendritic Nucleation/Array Treadmilling Model of the Leading Edge

(1) Extra-cellular signals activate receptors. (2) The associated signal transduction pathways produce active Rho-GTPases and PIP2 that (3) activate WASP proteins. (4) WASP proteins bring together Arp2/3 and G-actin to branch from a pre-existing filament. (5) Rapid growth at the barbed end of the new branch (6) pushes the membrane forward. (7) Capping protein terminates growth within a second or two. (8) Filaments age by hydrolysis of ATP bound to each actin subunit (white subunits turn

yellow) followed by dissociation of the phosphate (subunits turn red). (9) ADF/cofilin promotes phosphate dissociation, severs ADP-actin filaments and promotes dissociation of ADP-actin from pointed ends. (10) Profilin catalyzes the exchange of ADP for ATP (turning the subunits white), returning subunits to (11) the pool of ATP-actin bound to profilin, ready to elongate barbed ends as they become available. (12) Rho-GTPases also activate PAK and LIM kinase, which phosphorylates ADF/cofilin. This tends to slow down the turnover of the filaments (Pollard & Borisy 2003).

The discovery of the seven-subunit protein, the Arp2/3 complex, was a key stage in understanding the mechanisms underlying actin organisation. This nucleates filaments and also the branching out of filaments from a pre-existing actin filament at a characteristic 70º angle (Machesky 1994; Svitkina & Borisy 1999; Cooper & Schafer 2000; Volkmann et al. 2001; Robinson et al. 2001; reviewed in Higgs & Pollard 2001) by linking the pointed end of the new filament to the side of an older filament (Welch et al. 1998). This process is facilitated by the WASP family, which also binds to proteins thought to provide signals for actin polymerisation (Prehoda et al. 2000; Feijó et al. 2004).

Formin on the other hand, facilitates *de novo* nucleation of the actin filaments from monomers or short actin filaments with the aid of profilin. It also prevents the binding of capping proteins at the barbed end (i.e., growing end) of filaments. Formin is an actin polymerising protein that functions independently of the Arp2/3 complex (Sagot et al. 2002a). Formins play a crucial role in actin organisation that influences downstream cytoplasmic activities, such as directional vesicle transportation and septation. Comparisons of formins between various species have revealed a number of domains in the protein that appear important to the regulation of actin (Schmitz et al. 2006). The FH2 domain, which is responsible for actin nucleation, is found to be the

most conserved domain. Studies showed that mutation in yeast formin, Bni1p, caused filamentous actin to undergo significant rearrangement (Sagot et al. 2002b). Aberrant expression of the *Arabidopsis* formin homologues, AtFH8, resulted in the inhibition of F-actin coordinated root hair elongation (Deeks et al. 2005).

Conversely, cofilin/ADF acts to depolymerise actin filaments by severing them, providing free barbed ends and consequently accelerating the binding of capping proteins and the recharge of ADP-actin (Blanchoin et al. 2000). The actin dynamics that underlie cell motility and morphogenesis require the disassembly of F-actin as well as its assembly. The ADF family enhances the turnover of actin by regulating the rate constants between polymerisation and depolymerisation by severing to create more ends and/or increasing the rate of subunit loss from the ends (Lappalainen & Drubin 1997; Carlier 1998; Bamburg et al., 1999). However, severing is more likely to occur on long filaments, as there appears to be little severing activity on short filaments (Carlier & Pantaloni 1997). A number of members in this family have been identified that mediate F-actin disassembly in other eukaryotes, invertebrate depactin, porcine ADF or destrin, cofilin, *Acanthamoeba* actophorin, *Drosophila* twinstar or D-61, unc-60A/B from *Caenorhabditis*, *Xenopus* Acs, and *Toxoplasma* ADF that shares 30-40% protein sequence identity (Cooper & Schafer 2000; Dos Remedios et

al. 2003). In addition to its severing property, destrin not only stabilises F-actin, but also has an actin assembly-promoting activity in the absence of ATP (Tokuraku et al. 2001).

Enhanced interaction of yeast cofilin and actin has been shown to occur at an alkaline pH (Du & Frieden 1998). There is data suggesting that *N. crassa* hyphae either have a pH gradient or an alkaline cytoplasmic pH (Robson et al. 1996; Parton 1997). A pH gradient is pertinent in that this, along with a Ca^{2+} gradient may play a role in regulating ABPs that are likely to play a role in tip growth in plant cells (reviewed in Holdaway-Clarke & Hepler 2003).

Capping proteins function to stop the elongation of filamentous actin by binding at the barbed ends. They regulate the speed, length and availability of the free barbed ends in order to cause movement at the cell periphery. It has been shown that loss of capping protein leads to increased F-actin, but decreases in motility (reviewed in Schafer 2000). Their binding to the freshly cut barbed ends can be facilitated by cofilin/ADF (Balcer et al. 2003).

The role of actin binding proteins cofilin and formin are of particular interest in this

thesis. In the *Neurospora* genome, there are three genes related to cofilin (NCU01587, NCU10777, and NCU08053) and three genes related to formin (NCU03062 (similar to formin binding protein FNB3), NCU01431 (cytokinesis protein sepA), and NCU00600 (protein RHO3)). More specifically, the NCU01587 gene encodes a potential cofilin/ADF-like protein that has an estimated molecular weight of around 17kDa, which sits in the middle of the protein size range in this family of around 14~21kDa (Carlier et al. 2003). The NCU01431 (cytokinesis protein sepA) gene has a conserved FH2 domain and the estimated weight is around 197kDa, which is similar to the size of formin from human origin (180kDa). These *Neurospora* proteins may probably be related to cofilin and formin, however, none have been further investigated to date.

The sequence identity of the hypothetical genes of cofilin and formin in *N. crassa* in comparison to several other organisms is shown in Tables 1.2 and 1.3, respectively. Cofilin gene alignments showed a similar degree of conservation although less conserved than actin (Table 1.1) across the phylum. They are typically conserved within an internal epitopic region around amino acid number 80-120. Formin gene alignments were found to be less conserved across the phylum compared to cofilin and actin. These genes showed high similarities around two internal epitopic regions,

which are amino acid number 400-800 and 1200-1500. Neither cofilin nor formin genes have yet been identified in *Achlya bisexualis*. Detailed comparative protein sequence alignment of cofilin and formin is included in Appendix 1.2 and 1.3, respectively.

Table 1.2 Similarity in sequence identity between cofilin in different organisms.

	Cofilin	*Aspergillus nidulans* (ascomycete)	*Achlya bisexualis* (oomycete)	*Saccharomyce cerevisiae* (yeast)	*Homo sapiens* (animal)
N. crassa	Identity	38%	-	38%	33%
	Positives	59%	-	62%	58%

Table 1.3 Similarity in sequence identity between formin in different organisms.

	Formin	*Aspergillus nidulans* (ascomycete)	*Achlya bisexualis* (oomycete)	*Saccharomyce cerevisiae* (yeast)	*Homo sapiens* (animal)
N. crassa	Identity	56%, 71%	-	38%, 28%	19%
	Positives	71%, 83%	-	56%, 49%	40%

Note: The percentages are subjected to amino acid sequence 400-800 and 1200-1500, respectively.

1.6 Turgor pressure

Most cells have a greater concentration of solutes in the cytosol than the surrounding medium, which consequently causes water influx along with the potential to result in swelling of the cell or even bursting. The existence of cell walls, which are able to restrain swelling cells, is one of the solutions that have evolved to overcome this problem. Net water fluxes become zero when the internal hydrostatic pressure, also known as turgor pressure, balances off the osmotic pressure. Turgor pressure has been cited as the main/most relevant driving force in cell expansion.

With respect to the relationship between turgor and growth, there have been a number of pertinent studies, despite which the actual relationship remains unclear. For instance, some organisms have been shown to grow in the absence of measurable turgor (Harold et al. 1996, Money and Harold 1992; Money 1994). Others report that turgor is necessary, but not sufficient to account for observed apical extension rates (Kaminskyj et al. 1992). Therefore, the role of turgor is still yet to be clarified within and among species (reviewed in Harold 2002).

1.7 Summary/ Hypothesis

Tip growth, the dominant growth of fungi, is a complex process that is likely to involve the actin cytoskeleton. This is suggested by the high concentration of actin in growing regions and the fact that perturbation of actin affects growth rates. There is evidence to suggest that, at least in oomycete hyphae, the actin cytoskeleton is rearranged when hyphae grow into agar (this modelling invasive growth). In such cases, an actin-depleted zone (ADZ) is present at the extreme tip of the cell. In contrast, the majority of the oomycete hyphal tips growing on the agar (i.e., on top of the surface) have an intact actin cap (Walker et al. 2006). The exact role of this dynamic rearrangement of the actin cytoskeleton is unknown but clearly it may well play some role in invasive hyphal growth. The fact that invasive growth is likely to underlie the pathogenicity of many hyphal organisms means that an understanding of the relevance of this ADZ is of paramount importance.

It has been suggested that the ADZ may be a mechanism that allows greater tip yielding, which would be a requirement for invasive growth. However, previous results showed no difference in burst pressures between invasive and non-invasive hyphae of *A. bisexualis* (Walker et al. 2006), although the surrounding agar may possibly lead to an overestimation of invasive tip strength.

1.8 Objectives

Further experiments need to be carried out to investigate in more detail the prevalence of the ADZ and its exact role in invasive growth. All of the above work pertaining to an actin depleted zone has been carried out on oomycetes and there is a need for comparative studies on the filamentous fungi. The ascomycete *Neurospora crassa* is chosen in this study, since it is a long-standing model fungal system that has been fully sequenced (Borkovich et al. 2004) with the planned availability of knockouts (Colot et al. 2006). Furthermore, the composition of the ADZ needs to be clarified.

This thesis hypothesises that:

- An ADZ is present in hyphal organisms other than the oomycetes
- That the ADZ in fungi (if present) is an area that will contain collections of wall vesicles
- That the ADZ in fungi will contain actin depolymerising factor (ADF).
- That actin nucleating proteins such as formin is likely to present at the tips of non-invasive hyphae and will be largely absent in the ADZ.
- The turgor pressure at the tips of fungi will differ in invasive hyphae compared to non-invasive hyphae.

In testing these hypotheses the proposed work will help gain a better understanding of an extremely important mode of growth in an ecologically and economically very important group of organisms. With the presence of an ADZ in the fungi, the work raises important questions regarding convergent evolution of similar processes in two distinct phylogenetic lineages (i.e., the oomycetes and the fungi).

Chapter 2: An F-actin depleted zone is present at the tip of invasive hyphae of *Neurospora crassa*

2.1 Introduction

2.1.1 F-actin in hyphal tip growth

Actin has long been suggested to play a pivotal role in hyphal tip growth in fungi, establishing and maintaining cell morphology, transporting secretory vesicles, enabling cell motility and cytokinesis (Vorobiev et al. 2003). Its importance was first suggested by a characteristic tip-high localisation as described in Chapter 1 (Heath et al. 2000). Evidence suggests that microfilaments reinforce the hyphal tip of oomycetes, as the disruption of the F-actin cap using a UV micro-beam results in hyphae that are prone to bursting (Jackson & Heath 1990). There is also evidence suggesting the attachment of F-actin to possible wall-membrane linking molecules, which would allow for the F-actin to resist turgor (Kaminskyj & Heath 1996; Chitcholtan & Garrill 2005).

F-actin distribution has largely been visualised by chemical fixation of hyphae followed by phalloidin and/or antibody staining. However, the fixatives used can have

a profound influence of the quality of the staining. Yu *et al* (2004) found that a combination fixative of 0.5% methylglyoxal and 4% paraformaldehyde provides a more complete staining of F-actin compared to the use of paraformaldehyde alone (as has been used in many other studies) and any other combinations. This improvement is likely gained from the cross-linking capabilities of methylglyoxal, which allowed Yu *et al* (2004) to differentiate two distinct distributions of F-actin present in the hyphal apex of the oomycete *Achlya bisexualis*. Approximately half of the hyphae examined had a continuous apical cap, whereas the other half showed an F-actin depleted zone. In addition, they observed two types of cytoplasmic organization at the growing hyphal tip, firstly a clear smooth zone that was present and which the authors suggested may correlate to the F-actin depleted zone and secondly a less smooth area that presumably contained organelles and which was suggested to represent the continuous cap. These two organizations appeared interchangeable thus presumably represent dynamic changes that are occurring at the tip. The discovery of this F-actin depleted zone raised a critical question of our understanding of the fundamental tip growth mechanisms, given earlier descriptions of tip high concentrations of F-actin.

In subsequent work Walker *et al* (2006) discovered that the occurrence of the F-actin depleted zone appeared to be associated with invasive growth in two species of

oomycete, namely *Achlya bisexualis* and *Phytophthora cinnamomi*, in which the F-actin depleted zone was present in 70% and 74% of invasive but only 9% and 20% of non-invasive hyphae, respectively. TEM results showed that the F-actin depleted zone was unlikely to represent areas of vesicle accumulation. Measurements of turgor indicated no significant increase in turgor pressure under invasive conditions. It was therefore suggested that a reduction of F-actin at the tips, as evidenced by the presence of the F-actin depleted zone, could, along with cell wall softening, increase tip yielding and thus play a role in invasive hyphal growth. This would allow a greater protrusive force in the absence of turgor increases (Walker et al. 2006).

2.1.2 Vesicle supply centre (VSC or Spitzenkörper)

The Spitzenkörper (SPK) is a common, but not universal component of growing hyphal tips. In species where it is present, it is thought to play a role in tip growth (Bartnicki-Garcia et al. 1995; Löpez-Franco & Bracker 1996; Riquelme et al. 1998). While the exact composition of the SPK is unknown, it is thought to be comprised largely of vesicles (Löpez-Franco & Bracker 1996). Previous reports also suggest the presence of actin (Degousee et al. 2000; Heath et al. 2000; McDaniel & Roberson 2000). This actin is thought to be distinct from the population of actin that forms plaques, the most common form of the tip-high actin populations. The relationship

between possible different populations of actin and also with the SPK is largely unknown.

It has been suggested that the Spitzenkörper may act as a Vesicle supply centre (VSC). Bartnicki-Garcia and co-workers (1989) have presented models for tip growth that assumes a gradient along the hypha of vesicles that deliver 'wall units' to the expanding wall, which arises by the forward movement of a VSC (i.e., the Spitzenkörper) that emits vesicles in all directions. The frequency of impacts with the plasma membrane will then create the required gradient of additional 'wall units' to generate the hyphal form. A crucial aspect of the VSC hypothesis is that it puts the control of the gradient in wall deposition in the cytoplasm (Bartnicki-Garcia et al. 1995). The visualisation of the Spitzenkörper in living cells has been possible through the use of amphiphilic styryl dyes, such as FM4-64, and its behaviour indicates that it could play a significant role in determining the direction of growth (Torralba & Heath 2001; Torralba et al. 2001, 2002; Hickey et al. 2002). With respect to the current thesis, with an apparently large collection of vesicles, the positioning of the Spitzenkörper relative to the growing apex could affect the distribution of actin at the tip and vice versa.

In view of the above, an investigation is described in this chapter detailing the distribution of actin in invasive and non-invasively growing hyphae. This is coupled with a comparison of the hyphal morphologies as well as the Spitzenkörper. Results are discussed with reference to the problems that the growing hyphae encounter during invasive growth.

2.2 Materials and Methods

2.2.1 Cell maintenance and culture preparation

The *N. crassa* wild type strain 74-OR23-1A was obtained from the international collection of micro-organisms from plants (Auckland, New Zealand, ICMP Number 7781). Hyphae were grown on 2% agar (Agar bacteriological, Oxoid LTD) containing Vogel's minimal medium (Vogel 1956, 1964) (Appendix 2) with 1.5% (w/v) sucrose and overlaid with scratched cellophane in a 20˚C incubator. Prior to subculture, scratched cellophane squares were boiled in distilled water three times for 5 minutes each time and autoclaved to remove manufacturing residues. Scratched cellophane was used here for several reasons; the use in non-invasive culture was primarily to prevent hyphae growing invasively. The cellophane layer also prevents invasive hyphae growing out of the focal depth. In addition, hyphae seemed to adhere to the material and were easily transferred.

2.2.2 Immunofluorescence and immunostaining

Prior to experiments hyphae were cut 1 cm behind the growing edge of the mycelia on a stock plate that had been inoculated 24 hours previously and placed in a welled slide. For invasive experiments, hyphae were overlaid with 2% low melting point agar (Sigma). For experiments comparing the response of the F-actin distribution to agar

strength, 4% overlays were used in addition to the 2% overlays. The agar was cooled almost to the point of it setting prior to pouring to lessen any heat damage to the hyphae and then overlaid with Vogel's broth. Non-invasive hyphae were directly overlaid with Vogel's broth. After a 2 hour recovery period hyphae were checked to ensure that normal growth had resumed and that their morphology indicated that they were healthy. Healthy hyphae were then fixed in a mixture of 4% paraformaldehyde (ProSciTech, Thuringowa Central, Queensland, Australia) and 0.5% methylglyoxal (Sigma) made up in saline solution (60 mM PIPES (Sigma) pH 6.8, 2 mM EGTA, 2 mM $MgCl_2$, 137 mM NaCl, 6 mM NaN_3, 0.268 mM KCl) for 30 minutes at room temperature. Fixed hyphae were rinsed five times, each for 5 minutes duration using a washing solution (0.05% Tween-20 (Bio-Rad) in saline solution). The cell wall was then degraded for 45 seconds with a digesting solution (1 mg/ml Driselase and 1.6 mg/ml β-D-glucanase in saline solution) as described by Virag & Griffiths (2004) and the membranes permeabilised with 0.1 % (v/v) Triton X-100 (Bio-Rad) in saline solution for 10 min. The hyphae were rinsed with washing solution twice after both digestion and permeabilisation. The hyphae were then blocked for 30 minutes (3.5% skimmed milk powder in saline solution), and washed with washing solution four times for 5 minutes.

For imaging of F-actin, the thus prepared hyphae were incubated overnight at 4 °C with 1:500 dilutions of anti-actin antibody conjugated with FITC, which is a monoclonal IgG2a isotyped antibody conjugated with FITC raised against a synthetic actin c-terminal peptide (AC40) in mouse (Sigma-Aldrich). Hyphae were rinsed ten times for 5 min; using washing solution prior to observation and in addition anti-fading solution (containing 0.1% (w/v) of *p*-phenylenediamine dihydrochloride) was added to prevent photo bleaching.

Preparations were examined using an Olympus IX70 microscope with Nomarski differential interference contrast (DIC). The epifluorescent optics utilised a 100 X 1.35-NA objective, dichroic mirror, and a fluorescein or rhodamine long-pass emission set (U-MWG and U-MWIBA) for FM4-64 and appropriate filter sets (U-MWU and U-MWIBA) for immunofluorescence. Images were collected using a cooled Cool-Snap camera and processed using Adobe Photoshop. Statistical analyses were carried out using PRISM. All experiments have been carried out a minimum of three times.

The volume occupied by any F-actin depleted zone (ADZ) was estimated by approximating the tips of hyphae to be the elliptic parabolas. The distance from the tip

to the first prominent actin staining was taken as the length and the width of a hypha was measured where the first prominent staining was evident. Faint staining observed in the area that was presumed to represent the Spitzenkörper was not measured. The height was assumed to be equal to the width.

2.2.3 Control experiments

2.2.3.1 Fixatives comparison in invasive hyphae

To examine the ability of different fixatives on resolving the ADZ, hyphae were fixed and treated as described above. In addition, one set of hyphae were fixed not with the combination fixative, but with 4% paraformaldehyde alone.

2.2.3.2 The motility of the antibody

Non-invasive hyphae were fixed as described above. These were then overlaid with 2% low melting point agar. These hyphae were then treated with an antibody and observed as described above.

2.2.3.3 Cytoplasmic streaming

To assess the time taken for fixation to occur invasive and non-invasive hyphae were

prepared and fixed as described above. After addition of the fixative the time taken for the movement of organelles to cease was recorded. Cytoplasmic streaming can be seen readily with organelles being carried in the streaming cytoplasm. Organelles that were monitored could be mitochondria, vacuoles and nuclei. Preparations were examined by a Zeiss IM35 light microscope with a Zeiss F-LD20/O, 25 Phase objective.

2.2.4 Growth rates

Growth rates of invasive and non-invasive hyphae were calculated using two different methods. Initially, invasive and non-invasive hyphae were prepared as described in 2.1.1. Growth was monitored at 10-minute intervals using a light microscope as described above. In the second methodology that was used, the growth was monitored at 1-minute intervals for 20 minutes using an Olympus IX70 microscope with Nomarski differential interference contrast (DIC) microscope with a 100 X 1.35-NA objective. The distances grown were recorded and measured using Image Pro Plus and the growth rates were calculated using PRISM. The outlines of the cell images taken while monitoring growth at each interval were superimposed onto each other using Photoshop.

2.2.5 Visualisation of the Spitzenkörper using FM4-64

Invasive and non-invasive hyphae were prepared as described above. Once growth had resumed they were covered with Vogel's broth containing 5 μM FM4-64 (Molecular Probes). FM4-64 is a membrane sensitive styryl dye that shows red fluorescence upon incorporation into the endocytic vesicle membrane. After 7 minutes of loading with FM4-64, hyphae were observed using the epifluorescent microscope as described above.

2.3 Results

2.3.1 Organisation of cytoskeletal actin

Two distinct patterns of actin staining were observed in *N. crassa* hyphae that had been chemically fixed with the combination fixative of methylglyoxal and formaldehyde. In one of these staining patterns, F-actin was located primarily at the hyphal tip; in the other, staining was more abundant in subapical regions. The relative abundance of these staining patterns differed depending on whether the hyphae were growing invasively or non-invasively. Approximately 86% of non-invasive hyphae (43 out of 50) had staining predominantly in the region 0–5 μm from the tip (Fig. 2.1A, B, and C). The remaining 14% of non-invasive hyphae had subapical staining.

By contrast, 91% (86 out of 94 hyphae) of the invasive hyphae had no obvious tip high concentration of F-actin staining (Fig. 2.1D, E). In these hyphae, the staining was largely absent from the beginning of the tip and was more common in subapical regions. This F-actin deficient area at the hyphal tip has, in previous studies on oomycetes, been referred to as the F-actin depleted zone (Yu et al. 2004), a term that will continue to be used in the present work on a fungus. While the tip area was largely depleted of F-actin, in some of these hyphae there was some very faint staining visible at just back from the beginning of the tip (Fig 2.1D, E). The remaining

9% of invasive hyphae (8 out of 94) showed a tip high concentration of F-actin staining. The F-actin depleted zone extended further back from the tip in hyphae growing invasively through 4% agar (an average $\pm$ SEM of 4.0 $\pm$ 0.2 μm behind the tip (n=20)) compared to those growing invasively through 2% agar (an average $\pm$ SEM of 3.2 $\pm$ 0.1 μm behind the tip) and those growing non-invasively (an average $\pm$ SEM of 2.9 $\pm$ 0.2 μm behind the tip)). The average volumes of the actin-depleted zones in these hyphae were 68, 60 and 42 μm^3, respectively. Ninety five percent of hyphae (20 out of 21) examined in 4% agar had an actin-depleted zone (Fig 2.2).

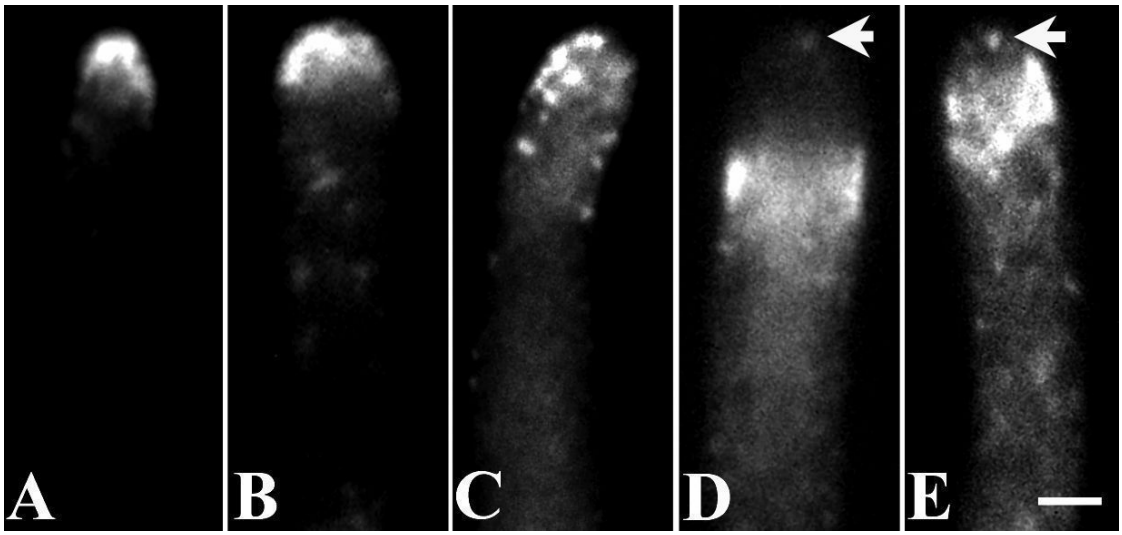

Figure 2.1 F-actin staining patterns observed in non-invasive (A, B, C) and invasive (D, E) hyphae of the ascomycete *Neurospora crassa*. The non-invasive hyphae had prominent clouds of F-actin staining (A, B) or F-actin plaques (C) in the tip region. This contrasts with the invasive hyphae which had an F-actin depleted zone in the tip with prominent subapical staining (D, E). Within the F-actin depleted zone there was however some faint staining (arrows in D and E). All are near the median focal plane epifluorescent images. Bar = 3.5 μm.

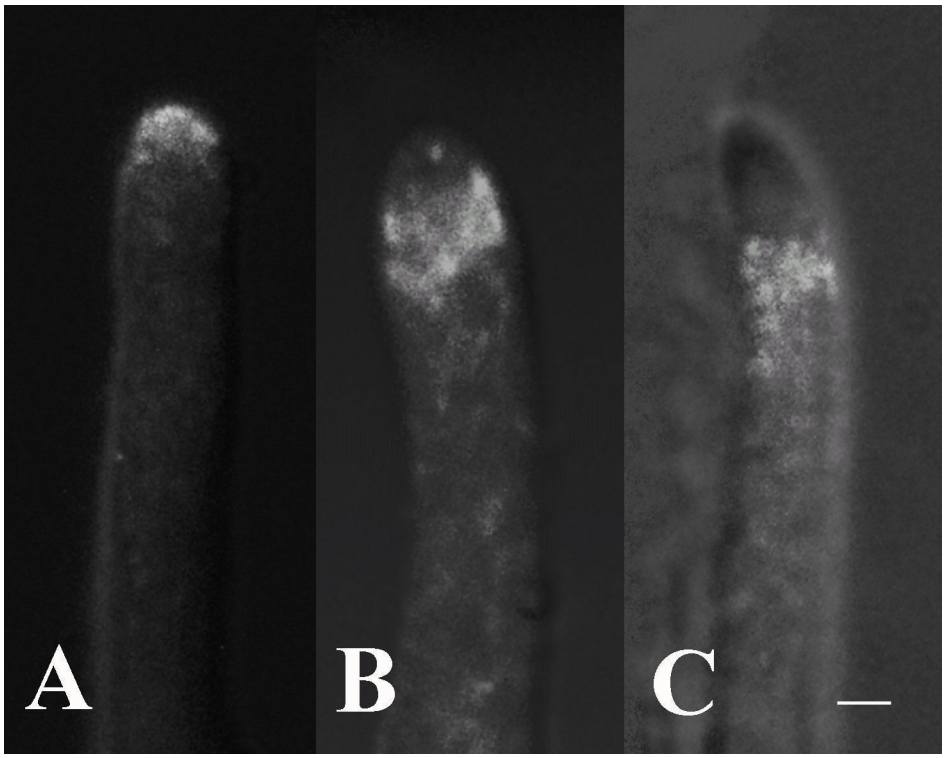

Figure 2.2 Superimposed fluorescent and DIC images of F-actin staining patterns observed in non-invasive (A) and invasive hyphae with 2% (B) and 4% (C) low melting point agar overlay. The non-invasive hyphae (A) had prominent F-actin staining at the hyphal tip. The invasive hyphae with 2% agar overlay (B) had an ADZ with an estimated volume of 60 μm^3, which increased to 68 μm^3 when agar concentration increased to 4% (C). Bar = 3.5 μm.

DIC images of fixed/unfixed hyphae showed no apparent differences in morphology between invasive and non-invasive hyphae (Fig 2.3). In addition, the morphology between the fixed and unfixed hyphae does not appear to differ for both the invasive and non-invasive hyphae. The morphology of the hyphae is also comparable between different treatments and an untreated control. This is important because with poor fixation, differing morphology and inconsistencies in the cytoplasm would occur, which may contribute to artifactual distributions of F-actin.

To ensure that the invasive hyphae were actually growing in, rather than on, the surface of the agar prior to fixation and/or live imaging, the microscope was initially focused on the surface of the agar and then the focal plane was lowered such that only those hyphal tips in the agarose were examined. Following this, the microscope was lightly tapped, and any hyphae on top of the agar tended to jiggle; those within the agar were largely immobile and as such were regarded as growing invasively.

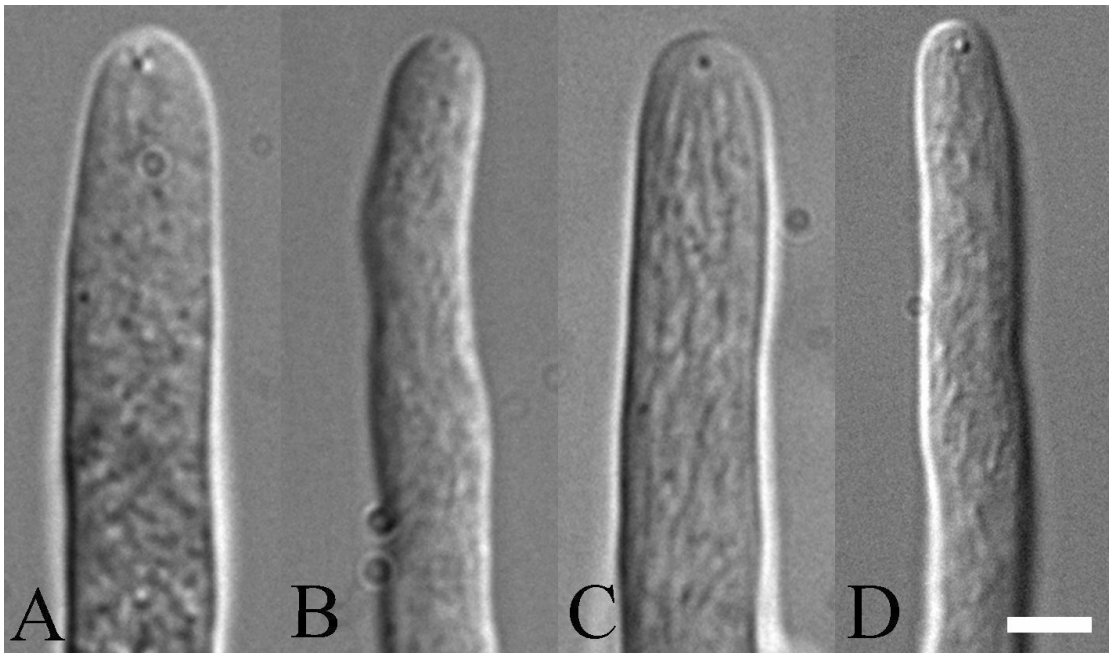

Figure 2.3 DIC images of fixed non-invasive (A) and invasive (B) hyphae and unfixed non-invasive (C) and invasive (D) hyphae of *Neurospora crassa*. The appearance of the cytoplasm was not significantly altered by fixation. Bar = 5 μm.

2.3.2 The ability to resolve the ADZ

2.3.2.1 Fixative comparison

Subsequent experiments were carried out with the aim of examining the effects of different fixative solutions and their ability to preserve and better stain actin in invasive hyphae. The two fixative solutions examined differed in that one contained 4% paraformaldehyde with 0.5% methylglyoxal (Fig 2.4A) and the other was only 4% paraformaldehyde (Fig 2.4B). The combination of paraformaldehyde and methylglyoxal gave brighter fluorescence and a more detailed actin network was evident (Fig 2.4A and Fig 2.1A-D) than with paraformaldehyde alone (compared to Fig 2.4B). The pattern of the staining was also more consistent with a combination of paraformaldehyde and methylglyoxal, as 89% of the invasive hyphae (n= 109) had an ADZ. In contrast, only 28% of the hyphae fixed with paraformaldehyde alone (n= 83) showed an ADZ and importantly a more variable actin staining pattern in the subapical regions. This is taken as indicative of poorer overall fixation. In hyphae fixed with paraformaldehyde alone, fading of the stain was rapid to the extent that on some occasions, the staining faded away prior to or almost at once as hyphae were observed. This indicates that F-actin structure was less well preserved by paraformaldehyde alone, leading to less staining. There was no apparent morphological difference in DIC images between hyphae fixed with the two fixatives.

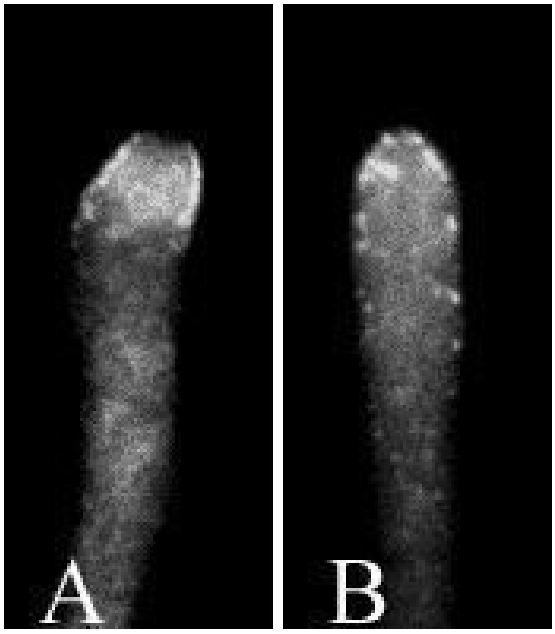

Figure 2.4 F-actin staining patterns observed in invasive hyphae of the ascomycete *Neurospora crassa* that were fixed with a combination of paraformaldehyde and methylglyoxal (A) and paraformaldehyde alone (B). Hyphae fixed with the combination of paraformaldehyde and methylglyoxal showed more consistent staining than those fixed with paraformaldehyde alone, which tended to fade rapidly after exposure to the fluorescence light.

2.3.2.2 Does antibody penetration through the agar affect the staining of the invasive hyphae?

An additional control experiment was carried out to test whether the difference in staining between invasive and non-invasive hyphae was due to the inability of the anti-actin antibody to permeate the agar media and stain the tips of invasive hyphae. The non-invasive hyphae were fixed, overlaid with 2% low melting point agar and then incubated with the antibody. One such hypha is shown in Figure 2.5. The hyphae treated in this way showed the same staining pattern as non-invasive hyphae that had not been overlaid with the 2% low melting point agar. This indicates that the F-actin depleted zone that was observed in the invasive hyphae was not caused by a lack of antibody permeating through the agarose. The abundant subapical staining that was observed in invasive hyphae (Figure 2.1 D, E) would also support this.

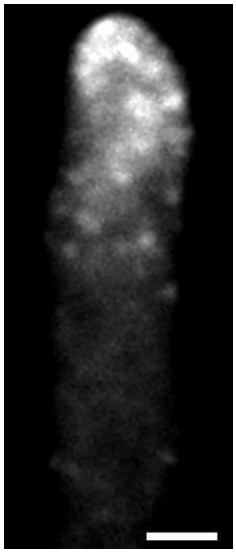

Figure 2.5 A non-invasive hypha that was fixed and then overlaid with LMP agar prior to staining. F-actin staining was located in the tip region. This indicated that the staining observed in invasive hyphae was not due to the inability of the anti-actin antibody to permeate agarose media. This is a near median focal plane epifluorescent image. Bar = 3.4 μm.

2.3.2.3 The Effect of Fixative

In an attempt to discount the possibility that the difference in staining pattern between invasive and non-invasive hyphae was due to slower rates of fixation of the invasive hyphae (due to slow permeation rate of the fixative through the agar), we investigated the time that it took for organelle movements in cytoplasmic streaming to stop after the fixative was added. Mean times ($\pm$ SD) for such cessation were 104 $\pm$ 18 seconds for non-invasive hyphae (range = 68 to 129 seconds) (n=17) and 113 $\pm$ 25 seconds for invasive hyphae (range = 74 to 168 seconds) (n=17). The mean values were not significantly different statistically (t-test $P>0.05$).

2.3.2.4 Growth rate

The growth rates of hyphae using the first technique for measuring growth rate (as described in the Materials and Methods section 2.2.4) were calculated. The average growth rate $\pm$ SEM of the non-invasive hyphae was 8.7 $\pm$ 1 μm min^{-1} (mean growth rate $\pm$ SEM, n=10) whereas the invasive hyphae had an average growth rate $\pm$ SEM of 10.3 $\pm$ 1 μm min^{-1} (n=10). These values were not significantly different statistically (t-test $P>0.05$). The results obtained using the second method of determining growth rates were also calculated. The average growth rate $\pm$ SEM of the non-invasive hyphae was 5.1 $\pm$ 0.5 μm min^{-1} (n=48), whereas the invasive hyphae had an average

growth rate (± SEM) of 4.7 ± 0.5 μm min^{-1} (n=48). These values were again not statically different (t-test P>0.05). The differences in growth speed between the two methods was probably due to the location of the microscope used for the second method which was in a dark room with slightly lower temperature, which is approximately 18° while using the first methodology the temperature was 20° .

In order to compare hyphal morphologies of growing invasive and non-invasive hyphae, representative superimposed images are shown in Figure 2.6A-J. Both non-invasive and invasive hyphae were divided into 5 groups according to their respective growth rates, from 0-3 μm min^{-1} (Fig 2.6A and F), 3.1-6 μm min^{-1} (Fig 2.6B and G), 6.1-9 μm min^{-1} (Fig 2.6C and H), 9.1-12 μm min^{-1} (Fig 2.6D and I), and 12.1-15 μm min^{-1} (Fig 2.6E and J). There was an obvious difference between the shape of the hyphal tips between and within groups in both invasive and non-invasive hyphae. However, the average hyphal diameter of the faster growing hyphae is significantly larger than those slower growing ones.

Figure 2.6 Representative superimposed images of non-invasive (A-E) and invasive (F-J) hyphae. Hyphae were divided into 5 groups according to the growth rates, from the slowest growing hyphae (A and F) to the fastest growing ones (E and J) (actual growth speeds of these groupings are given in the text). There was no obvious difference of the shape of the tips between each group. However, the faster growing hyphae did have a wider average hyphal diameter than those slower growing ones. In addition, there is no significant difference in hyphal diameter in each pair of groups between invasive and non-invasive hyphae.

2.3.3 The presence of Spitzenkörper

To evaluate whether the ADZ is associated with differences in the level of vesicle accumulation in the tip region the membrane sensitive dye FM4-64 was used to monitor vesicle distribution in the tips of living *N. crassa* hyphae. This dye has previously been used to monitor apical vesicle clusters or Spitzenkörper in a range of fungi (Fischer-Parton et al. 2000). Both non-invasive and invasive hyphae rapidly took up FM4-64 with internal apical accumulations, which were assumed to be the Spitzenkörper, first visible around 20 seconds to 1 minute after application. Optimal staining was observable around 7 minutes after exposure to the dye, thus, this was used as the benchmark time at which the Spitzenkörper of invasive and non-invasive hyphae were compared. The dye was not removed after incubation in order to avoid the distraction of solute equilibrium by replacing other media. The remaining free dye in the solution did not affect the observation, since FM4-64 only fluoresces after binding to the membrane. A change in morphology was observed after 3 minutes of exposure under fluorescent light. Therefore, all images were taken within 0~3 minutes after exposure to fluorescent light.

In order to distinguish between vesicle distribution at the tips of invasive and non-invasive hyphae, and to discount any differences that may have been accountable

to different widths of hyphae, the ratio of the width of Spitzenkörper over the width of the hyphae 10 μm away from the tip was calculated. The non-invasive hyphae had an average ratio of 0.26 (n= 94 hyphae) (Fig. 2.7 A), whereas the average of the invasive hyphae was 0.33 (n= 96 hyphae) (Fig. 2.7 B). Statistical analyses (t-test) showed that the two ratios had a significant difference ($P<0.01$). There was no obvious morphological difference between non-invasive and invasive hyphae. Hyphal diameters 10 μm back from the tip showed no significant difference with average diameters $\pm$ SEM of 9.9 $\pm$ 0.2 μm for the non invasive hyphae (n=62) and 9.5 $\pm$ 0.1 μm for the invasive hyphae (n=61).

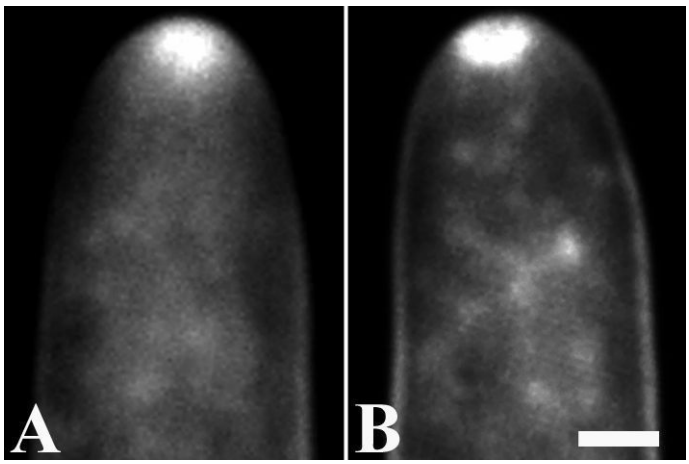

Figure 2.7 A non-invasive (A) and an invasive (B) hypha that had been exposed to the membrane sensitive dye FM4-64. Both hyphae show an accumulation of vesicles or Spitzenkörper close to the tip. Overall the width of the Spitzenkörper relative to hyphal diameter was slightly larger in invasive compared to non-invasive hyphae. Hyphae were imaged near the median focal plane. Bar= 3.3 μm.

2.4 Discussion

The results of the actin immunostaining provide evidence for the presence of an F-actin depleted zone in the tips of the invasive hyphae of *N. crassa*. This is largely absent from the non-invasive hyphae. This raises important issues on two levels, firstly, the mechanistics of invasive growth in hyphae, and secondly, in view of reports of an F-actin depleted zone in oomycete hyphae, the issue of convergent evolution of similar processes in two distinct phylogenetic lineages (i.e., the fungi and the oomycetes).

There have been previous reports of F-actin depleted areas in the tip region of some species of fungi (Hoch & Staples 1985; Roberson 1992; Torralba et al. 1998) and oomycetes (Yu et al. 2004; Walker et al. 2006). Heath & Steinberg (1999) have suggested that, in view of other contrary reports of F-actin at the growing tips of fungi and oomycetes, it is unclear whether these subapical distributions are technical artifacts or are real and have functional significance. With respect to technical artifacts, supporting their claims are observations that in fungi, oomycetes, and other tip growing cells, changes to fixatives and fixation conditions can affect F-actin staining patterns (Geitmann & Emons 2000; Yu et al. 2004). This point is especially relevant to the present study in which the different growth conditions necessitate

different conditions of fixation. While we cannot unequivocally discount the possibility that the F-actin depleted zone is an artifact induced by fixation and staining through agar, we propose that this is unlikely for a number of reasons.

Firstly, there was no significant difference in the fixation times for invasive versus non-invasive hyphae. This indicates that the presence of an F-actin depleted zone or the rearrangement of cytoskeletal actin in the invasive hyphae is unlikely due to the impact of longer fixation time. Secondly, an F-actin depleted zone was present in 14% of non-invasive hyphae. If the depleted zone were an artifact caused by the fixation through agar, it will be difficult to explain why non-invasive hyphae had also shown this feature, albeit at a much lower occurrence. Thirdly, there was no obvious difference in the brightness and the number of hyphae stained between invasive and non-invasive hyphae. This similarity of staining quality suggests that the agar does not significantly affect the composition of fixative or antibody reaching the hyphae. In terms of the antibody reaching the hyphae, this is further supported by the result presented in Figure 2.5, which showed the same actin distribution as in non-invasive hyphae following normal immunostaining procedures. Fourthly, there was no observation of a graded transition from F-actin at the tips to subapical F-actin as the focal plane of the microscope was lowered though the agar. If the F-actin depleted

zone were an artifact caused by slower rates of fixation as the fixative permeated the agar, then it could be argued that those closest to the surface of the media should show an actin pattern that is similar to non-invasive hyphae. These data all pointed to the F-actin depleted zone being a true structural component of invasively growing hyphae.

The ability to resolve an F-actin depleted zone is likely due to the use of the combination fixative containing formaldehyde and methylglyoxal. The combination appears to enhance the preservation of the actin network and may make the actin more accessible to antibody staining. Similar observations have been reported earlier by Yu et al. (2004). Interestingly, results indicate that the hyphal diameter increases with increasing growth rates for both invasive and non-invasive treatments. However, no obvious difference in the actual shape of the tips has been observed for hyphae, neither between treatments nor within treatments with a wide range of growth rates. Theoretically, tapered hyphae are considered to be more actively growing than those lesser tapered ones. However, these results suggest that the growth rate is more likely to be related to the size of the hyphae (hyphal diameter) rather than the shape (i.e., taperedness) of the tips as rounded and tapered tips were evenly observed in all growth speed groups. The faster growing hyphae and presumably more actively

growing ones do not necessarily have to have more tapered tips than the slower growing ones. A consistent F-actin distribution was observed in a wide variety of sizes and tip shapes of the hyphae.

This then raises the question of the functional significance of an F-actin depleted zone in invasive hyphal growth. To grow invasively, fungal and oomycete hyphae need to generate a protrusive force which, along with substrate attachment and sufficient enzymatic substrate breakdown, enables them to penetrate through the solid/ semi-solid media. This protrusive force arises from a balance between turgor pressure and tip yielding. Thus, to increase the force hyphae could either increase turgor, or decrease the resistance to turgor (i.e., increase tip yielding). With respect to the first of these possibilities, fungi and oomycetes differ in that fungi are able to turgor regulate, and hence increase their turgor while oomycetes cannot (Lew et al. 2004a). These increases in fungal turgor can be very large and in specialised infection structures the highest recorded cellular pressures was 8 MPa (Howard et al. 1991). Despite these large pressures, in vegetative hyphae it is likely that turgor is only the fuel or driver that enables invasive growth to occur (further investigated in Chapter 5). The main area of control of such growth, along with substrate breakdown, is likely to be tip yielding through changes in the resistance to turgor.

Resistance to turgor in both fungi and oomycetes is offered by the cell wall and the F-actin cytoskeleton. In the oomycetes, changes in the tensile strength of the cell wall, through the secretion of endoglucanases, are thought to enable growth at low turgor (Money & Hill 1997). In addition, the rearrangement of the F-actin cytoskeleton may complement such changes to the cell wall at low turgor and may also play a role in allowing invasive growth in turgid hyphae (Walker et al. 2006). This is based on the observation of an F-actin depleted zone in invasive hyphae of two species of oomycete *A. bisexualis* and *P. cinnamomi*. To resist turgor, F-actin would be required to be linked to a structure such as the cell wall and there have been reports of integrin-like molecules that are capable of such a role in oomycetes (Kaminskyj & Heath 1995a; Chitcholtan & Garrill 2005). Similar molecules are also present in a number of fungi including *N. crassa* (Degousee et al. 2000) raising the possibility that F-actin may also play a role in resisting turgor in fungal hyphae. The observation of an F-actin depleted zone in invasive *N. crassa* hyphae, the size of which changes in response to agar concentration, is consistent with a role in allowing invasive growth through a decreased resistance to turgor.

Another possible explanation for the F-actin depleted zone is that it may simply represent a site of vesicle accumulation. This is unlikely, as firstly, vesicle

accumulation tends to occur in slower growing hyphae and no significant difference was observed in the growth rates between the two treatments. Secondly, images were made of vesicle accumulations at the tips. To image vesicle distribution in the tips of hyphae, the membrane sensitive dye FM4-64 was used. The uptake of this dye has been used to argue for endocytosis in *N. crassa* , in other fungal species, and in pollen tubes (Fischer-Parton et al. 2000; Parton et al. 2001; Atkinson et al. 2002; Read & Kalkman 2003). Although this is an issue of some controversy (Torralba & Heath 2002), its internalisation does represent a means of assessing internal vesicle distribution in live hyphae. The result presented indicates a slightly larger accumulation of vesicles or Spitzenkörper relative to hyphal width 10 µm away from the tips of the invasive hyphae. However, it is unlikely that this increase in the number of vesicles is sufficient to account for the F-actin depleted zone. Similar conclusions have been reached on oomycetes, although this was based on ultrastructural analyses, due to the inability of FM4-64 to label the membranes in oomycetes (Walker et al., 2006).

Previous work has shown the Spitzenkörper to consist of a dense accumulation of vesicles as well as actin and microtubules (Roos & Turian 1977; Howard 1981; Bourett & Howard 1991; Kwon et al. 1991; Roberson & Vargas 1994; McDaniel &

Roberson 1998; Mourino-Perez et al. 2006). Results of the actin immunostaining of the invasive hyphae showed the presence of faint staining at the extreme apical regions of many of those hyphae with the F-actin depleted zone (Fig. 2.1E). It is suggested that this may be indicative of F-actin that is associated with the Spitzenkörper.

In a number of studies, the disruption of F-actin using drugs such as latrunculin B has been shown to lead to tip swelling (e.g. Heath et al., 2003). This is consistent with F-actin restraining the tip against turgor, but leads to the question of why we do not see enlarged tips in invasive hyphae that have an F-actin depleted zone. Latrunculin is likely to disrupt the F-actin cytoskeleton on a large scale and thus treatment with it may not be comparable to the fine rearrangements at the tip that have been suggested in preceeding paragraphs to underlie invasive growth. Furthermore, there is likely to be some restraining of the tip by the substrata itself, which may prevent a change in tip morphology. Images of 2% agar gels using atomic force microscopy have revealed a fine pore structure with an average pore diameter of 364 nm (Courvoisier et al. 1998; Pernodet et al. 1997). Thus hyphae of *N. crassa* with hyphal diameters typically between 5 – 10 μm are likely to have additional support from the cross-linked polysaccharides of the agar media.

In addition to a role in resisting turgor, as a suspected morphogen, F-actin is likely to play a role in the delivery of vesicles to the tip. How then might vesicle delivery to the tip be possible with an F-actin depleted zone? Three possibilities explanations are offered. Firstly, the faint staining observed just subapically may represent a delicate population of F-actin at the tip that may facilitate such delivery. Secondly, as suggested by Heath (2000), there may be additional fine populations of F-actin that are unresolved by our current methodologies. Finally, while our present technology allows only a static image of F-actin distribution, we suggest that the depleted zone is likely to be a dynamic structure. In the tips of oomycete hyphae, a cytoplasmic smooth zone, which has been suggested to possibly correspond to the F-actin depleted zone certainly changes rapidly with time (Yu et al. 2004). Such dynamic rearrangements may allow almost concurrent yielding and vesicle delivery.

Further support for the existence of an ADZ in the tips of hyphae comes from recent work using freeze substitution to preserve actin, and alternately, green fluorescent protein (GFP) to detect actin in live pollen tubes (Wilsen wt al.2006). In these cells, these techniques have revealed a distinct actin distribution consisting of a dense cortical fringe 1 - 5 μm away from the extreme apex and extending basally an additional 5 - 10 μm. This predominant feature, a cortical fringe close to the apex with

extension of finely dispersed longitudinal filaments was found to be relatively consistent irrespective of fixation protocol (Lovy-Wheeler et al. 2005).

In considering all of the above, it should be noted it is not known whether the ADZ in hyphae is an area that is completely devoid of actin. It cannot be discounted that it may be an area that contains delicate and unstabilised F-actin as such populations of actin have been observed in pollen tubes (Gibbon et al. 1999) and algal rhizoids (Hable et al. 2003).

In summary, this chapter presents evidence for an F-actin depleted zone in invasive hyphae of the ascomycete *N. crassa*, a structure that is largely absent from non-invasive hyphae. The size of this depleted zone increases with increasing agar concentration in the media through which the hyphae are growing. The differences in vesicle distribution in invasive and non-invasive hyphae are unlikely to be sufficient to account for the exclusion of F-actin from the F-actin depleted zone and it is suggested that this structure may play a role in invasive hyphal growth by allowing a greater protrusive force at the tip.

Chapter 3: Invasive growth may come about through the action of a cofilin analogue

3.1 Introduction

In Chapter 2, the results presented provide evidence of an ADZ being a dominant feature at the tip of invasively growing hyphae of *N. crassa*. The ADZ is also present in non-invasive hyphae, although it is not nearly as prevalent with an ADZ in 14% of non-invasive hyphae versus 91% of invasive hyphae. The rearrangement of the actin cytoskeleton may be a requirement for hyphae to grow invasively, which is not surprising given the need for a greater protrusive force. The aim of this chapter is to look at the mechanistic details of the rearrangement of actin at the hyphal apex, focusing in particular on hyphae that are able to grow invasively.

It is well documented that the actin cytoskeleton is a dynamic structure and the maintenance/rearrangement of such a structure comes about through the actions of actin binding proteins (ABPs). The assembly and disassembly of F-actin is regulated by ABPs that are responsible for polymerising and depolymerising actin filaments. The Cofilin/actin depolymerising factor (ADF) family are a group of

proteins that as their name suggests, are predominantly responsible for actin depolymerising activities. Most studies investigating the role of these proteins in tip growing systems were carried out in root hairs and pollen tubes. Previous reports suggest that *in vitro*, maize cofilin (ZmADF3) binds G- and F-actin, which increases actin dynamics (Lopez et al. 1996). Jiang *et al* (1997b) further discovered that the distribution of this protein is correlated with areas of actin re-organisation. ZmADF3 was found to be distributed throughout the cytoplasm in the early stages of root hair development. Later on as the root hair emerged, the distribution of microfilaments changed in correlation with the simultaneous redistribution of ZmADF3. These proteins were found to be concentrated at the apex of the emerging root hair and remained there as the tip elongated. These findings suggested that ZmADF3 was present where actin remodelling was occurring. While there is no information available about the exact action of ZmADF3, in other systems the structure and molecular action of cofilin/ADF is fairly well documented (Bowman et al. 2000; Balcer et al. 2003; Paavilainen et al. 2004).

Cofilin is a low molecular weight ABP that ranges from 14- 21 KDa (Carlier et al. 2003); the aforementioned maize protein ZmADF3 has a molecular weight approximately of 17 KDa (Jiang et al. 1997a). The cofilin/ADF family has been

studied extensively both *in vitro* and *in vivo* (reviewed in Bamburg 1999). Members of the family are structurally and functionally conserved among eukaryotes and they are able to bind both G- and F-actin to modulate cytoskeletal actin dynamics. The activity of cofilin/ADF is regulated by reversible phosphorylation of a serine residue in the amino-terminal region, with dephosphorylation leading to cofilin activation. Phosphorylation is controlled by environmental and developmental stimuli associated with changes in the cytoplasm (Djafarzadeh & Niggli 1997). In this case, cofilins are likely to play a dual role in the mechanical properties of actin (reviewed in Carlier 1998). The turnover/rearrangement of F-actin is responsive to a variety of basic cellular processes. F-actin was found to have a 100-200 fold higher turnover *in vivo* than pure actin *in vitro*, suggesting that there are complex regulation processes in place (reviewed in Carlier 1998).

These proteins have three major functions, firstly to sever actin filaments, thus making more free barbed ends available for polymerisation. Secondly, they increase the dissociation rate constant at the pointed end of actin filaments when they are bound. Lastly, they increase the number of actin monomers for assembly at the free barbed ends. Cofilin-mediated depolymerisation has been shown to be accelerated directly upon the binding of the actin interacting protein (Aip1) and indirectly by the

action of the suppressor of ras^{val14} (Srv2) complex in yeast (Bamburg 1999b; Balcer et al. 2003; Pollard & Borisy 2003). For cofilin/ADF to achieve both the severing of F-actin and the recycling of G-actin, the binding of both requires the α-helical domain, although the binding of only F-actin requires the tertiary structure to be in a specific conformation (Jiang et al. 1997b; Ojala et al. 2001).

Cofilin binds to ADP-actin (1:1 ratio) with a higher affinity than ADP-Pi-actin. When bound, it severs F-actin and enhances depolymerisation at parts of the filaments where ADP-actin is present (Nishida et al. 1984). Severing activity appears to be pH dependent *in vitro* and most prominent around pH 7 to 7.5 (Bamburg et al. 1999). However, this optimum may be based on pH-induced structural changes of F-actin rather than a direct pH impact on cofilin itself (Bowman et al. 2000). Electron microscopy showed that there was a change in F-actin conformation by about 5˚, resulting in release of the Pi to enhance the binding of cofilin (Bamburg 1999a; Chen et al. 2000). This unique property consequently changes the F-actin crossover from 35-38 nm to 27 nm, but the length of F-actin remains unchanged. This change in helical twist results in weakening of the lateral and longitudinal actin-actin interaction in a filament, making the filaments more likely to break and subunits more likely to disassociate. This distortion may however also result in the dissociation of Arp2/3

binding at the pointed end, which leads to filament disassembly (Bamburg 1999a; McGough & Chiu 1999; Bobkov et al. 2004). Carlier and Pantaloni (1997) observed a 25 fold increase in F-actin turnover in the presence of cofilin, however, severing ability alone of the protein was insufficient to fully explain this increase. Therefore, they proposed an alternative mechanism where cofilin facilitates the dissociation of G-actin in the rate-limiting step in F-actin disassembly. The presence of cofilin not only establishes the steady state of actin assembly, but also functions to accelerate a rate limiting step of pointed-end depolymerisation (Pantaloni et al. 2001).

The recycling of G-actin involves the action of the Srv2 complex, which is a large multimeric structure that functions as an intermediate in converting cofilin-ADP-actin to profilin-ATP-actin and reprocesses cofilin for subsequent depolymerisation. Apart from the direct mediated actin turnover, cofilins also mediate indirect actin turnover by forming an Aip1-cofilin cap at the freshly cut barbed ends (Balcer et al. 2003). Most freshly cut barbed ends are capped to prevent annealing, and therefore maintain the profilin-actin pool to make profilin available to sequester dissociated G-actin. With this scenario, the dissociation of phosphate from polymerised actin becomes the determining step of deciding the direction of the cycle of actin assembly/ disassembly and recycling (Blanchoin et al. 2000).

In view of the above and of data presented in Chapter 2, an investigation was carried out looking at the location and expression of cofilin in invasive and non-invasive hyphae. Data presented in this chapter demonstrate two distinct distributions of cofilin between invasive and non-invasive hyphae of *N. crassa*, but these two types of hyphae were found to have similar *cof1* (NCU01587) expression levels.

3.2 Materials and Methods

3.2.1 Immunocytochemistry and antibodies

The materials and methods used for preparing, fixing and immunostaining hyphae were as described in Chapter 2, with the exception that the cell walls were digested for 5 min and hyphae were incubated overnight with either a 1:200 dilution of an antibody raised in rabbit against yeast cofilin (kindly supplied by Dr D. Drubin, University of California at Berkeley) or a 1:500 dilution of an affinity purified goat IgG polyclonal antibody (K-15) raised against human cofilin (Santa Cruz Biotechnology Inc). A 1:250 dilution of chicken anti rabbit IgG polyclonal antibody conjugated with Texas Red (Sigma) was used as a secondary antibody for the yeast primary antibody and a 1:1000 dilution of Alexa Fluor® 488 rabbit anti-goat IgG (H+L) conjugate (Molecular Probes) was used as a secondary antibody against the human cofilin primary antibody.

3.2.2 Immunoblotting

Neurospora crassa hyphae were inoculated onto cellophane (prepared as described in Chapter 2) overlaying Vogel's media in a 90mm Petri dish and grown for 24 hours at 20 °C. Hyphae from 40 such dishes were collected, frozen with liquid nitrogen, and ground using a pestle and mortar. The powder obtained was suspended in extraction

buffer (40mM Hepes-NaOH, pH7.5; 250mM sucrose, 4mM $MgCl_2$; 2mM EGTA, 2mM DTT (dithiothreitol); 7mM ß-mercaptoethanol; 10% glycerol; 2mM PMSF (phenylmethylsulphonyl fluoride)) and centrifuged at 10,000*g* for 25 min at 4 °C. Proteins were separated on a NuPAGE® Gel (Invitrogen). After SDS-PAGE, the proteins were transferred to a nitrocellulose membrane (Sigma-Aldrich) in transfer buffer (1.93g tris-Base, 9g glycine per litre solution) at 40V overnight in a 4 °C temperature controlled room. Transferred proteins were stained with 0.1%w/v Ponceau red to check for the homogeneity of the transfer. The nitrocellulose membrane was blocked for 30 min at room temperature and rinsed twice with washing solution, each for 15 minutes, prior to the incubation with the primary goat anti-cofilin antibody at a 1:1000 dilution. Incubation was carried out overnight at a temperature of 4 °C in the dark. The membrane was then visualized using the Western Breeze Immunodetection Kit (Invitrogen).

3.2.3 Real-Time PCR

3.2.3.1 RNA extraction from cell culture

Forty plates of invasive and non-invasive mycelium grown as described in Chapter 2 were collected, frozen immediately in liquid nitrogen and ground prior to extraction. Total RNA was extracted from ground cells using TRI Reagent (Molecular Research

Center Inc.) (Chomczynski & Sacchi 1987). Cells were lysed in TRI Reagent for 5 min at room temperature. RNA was separated from DNA and protein by extraction with chloroform. RNA was then precipitated with a half volume of isopropanol and centrifuged at 12,000 x g for 15 min at 4^{o}C. The RNA pellet was then washed with 75% ethanol, centrifuged at 7,500 x g for 5 min, and briefly air dried. RNA was then solubilised in diethyl pyrocarbonate (DEPC)-treated water (Sigma-Aldrich). The isolated RNA was subjected to RNase-free DNase I (Fermentas, Quantum Scientific) digestion for 30 min at 37^{o}C in the presence of Mg^{2+}. The reaction was arrested by incubation with 25 mM EDTA at 65^{o}C for 10 min. Genomic DNA contamination was examined/identified by performing a "no-RT" control during RT-PCR using purified RNA samples directly as the templates without adding reverse transcriptase. Samples containing residual genomic DNA were re-digested with RNase-free DNase I and assayed again for DNA contamination. The DNA-free RNA was then stored in 100% ethanol at -80^{o}C until use.

3.2.3.2 Quantitation and visualisation of RNA

The concentration and purity of the isolated total RNA was determined by using a NanoDrop ND-1000 Spectrophotometer (BIOLAB). The purity was determined by referring to absorbance ratios at A_{260}/A_{280}. As the RNA A_{260}:A_{280} ratio is dependant

on both pH and ionic strength (Wilfinger et al. 1997) nano-pure water was used as a dilutant and a blank to assure accurate readings. The integrity of the total RNA was analysed by electrophoresis and ethidium bromide staining on a denatured 1.4% agarose-formaldehyde gel using 3-(N-morpholino)-propanesulfonic acid (MOPS) buffer (Sigma-Aldrich). Visualisation of gels was carried out on an electronic U.V. transilluminator (Science and Technology NZ Ltd). The integrity of the total RNA was judged by the presence and the ratio of 28S and 18S rRNA bands.

3.2.4 cDNA synthesis

Three µg of DNase I-digested RNA template from each sample was reverse transcribed into complementary DNA (cDNA) using the Superscript ^{TM} first strand cDNA synthesis system for RT-PCR (Invitrogen). The total RNA was first incubated with 50 ng of hexamers and 10 mM of dNTP mix for 5 min at 65^{o}C and chilled on ice for another 5 min. A reaction mixture (40 units of RNase inhibitor, 2 µl of 10x RT buffer, 4 µl of 25 mM $MgCl_2$ and 2 µl of 0.1 M DTT) was added to the RNA/hexamer mixture mentioned above and incubated at 25^{o}C for 2 min. Briefly, 50 units (1 µl) of reverse transcriptase (RT) were added to each sample and incubated at 25^{o}C for 10 min followed by incubation at 42^{o}C for 50 min. This reaction was terminated by heating at 70^{o}C for 15 min. The sample was subsequently chilled on ice for 2 min.

Two units (1 µl) of RNase H were added to the synthesised cDNA and incubated for 20 min at 37°C to digest any residual RNA. The cDNA was stored at -20°C prior to PCR amplification. To confirm the efficiency of the first-strand synthesis reaction, a positive control using 50 ng *in vitro* transcribed RNA from the chloramphenicol acetyltransferase (CAT) gene (Invitrogen) was included. A negative control identical to the test assay but excluding the reverse transcriptase reaction was included to check for the presence of genomic DNA contamination.

3.2.4.1 Primer design

Primer design was based on the published *Neurospora crassa* sequence from the Entrez database (accession number CAB91380) obtained from the National Centre for Biotechnology information (NCBI; http://www.ncbi.nlm.nih.gov.). Primers were designed using Primer 3 (http://www.path.com.ac.uk/cgi.bin/primer3.cgi). For each primer pair design, the primer length, melting temperature (Tm), GC content (%) and length of PCR product were taken into consideration. One primer pair was designed for both GAPDH and cofilin genes, with GAPDH being used as an internal reference for calibration and cofilin as the target gene. The amplicons for both genes were around 200 bp in length, with a melting temperature of around 60 °C for all primers thereby permitting simultaneous amplification of the reactions (Table 3.1).

The compatibility of the primers was checked to ensure that no primer dimers were formed using FastPCR software (Kalendar 2004, http://www.biocenter.helsinki.fi/bi/programs/fastpcr.htm). The oligonucleotide primers were then chemically synthesised by Invitrogen.

3.2.4.2 Quantitative expression of *cof1*

Amplification of putative *cof1* fragment was carried out using the SYBR® Green PCR Master Mix Kit (Applied Biosystems). Samples were assayed in 50 µl reaction mixtures containing 25 µl of reaction mix, 3 µl (10 pmol) of each forward and reverse primer, and 3 µl of cDNA. Negative controls without template were used to discount any effects due to contamination. The thermal profile consists of denaturation for 10 min at 95^{o} C followed by 45 cycles of 30 sec at 95^{o}C, 1 min at 55^{o}C and 30 s at 72^{o}C, followed by product melting to check the melting temperature of PCR product (s). Thermal cycling and fluorescence detection were conducted using the STRATAGENE- Mx 3000p system (Stratagene). The copy number of the target gene in the sample was obtained and the ratio of copy numbers between this gene and GAPDH was calculated.

Primers	Nucleotide positions	Sequence (5'→3')	Product size (bp)	Tm (^{o}C)
COF F	222-241	CCG ATA TGC CGT CTA CGA TT	204	59.94
COF R	425-406	TCG TAC TCG ATG TCG TCC TG		59.86
GAPDH F	340-359	GGT GGC AAG AAG GCT ATC AT	203	59.93
GAPDH R	542-523	GTG TAG GAG TGG ACG GTG GT		59.88

Table 3.1 Detail of the primers. The primer length, melting temperature (Tm), GC content (%) and length of PCR product were all taken into consideration when designing primers (F – Forward primer, R – Reverse primer, Tm – melting temperature).

3.2.4.3 Confirmation of PCR product

The product of the RT-PCR reaction was confirmed on a 1.4% (w/v) agarose gel made up with 1x TBE (100 mM Tris Borate EDTA). Three microlitres of the PCR product from each treatment was mixed with 2 µl of orange G loading buffer (30% glycerol, 0.35% orange G). Electrophoresis was carried out at 100 volts for 30 min. Gels were stained in 0.5 µg/ml ethidium bromide solution for 20 min. A single visible band of around 200 bp confirmed the specificity of PCR amplification. The PCR product was then stored at -20˚C until used for sequencing.

3.2.4.4 Sequence analysis of putative *cof1* fragment

PCR products were purified using a FastP Mini column (Eppendorf) and then sequenced directly on an ABI 377 automated DNA sequencer (Perkin-Elmer) using an ABI PRISM BigDye Terminator v3.1 Cycle Sequencing kit (Applied Biosystems). Each sequencing reaction contained 50 ng of purified PCR product, 0.5 µl BigDye Terminator (BDT) reaction mix, 1.75 µl 5x sequencing buffer (containing 350 mM Tris-HCl, pH 9.0 and 2.5 mM $MgCl_2$), 3.2 pmol primer and ddH_2O to a total volume of 10 µl. Thermo-cycling conditions were as follows: 96^{o}C x 10 s, 50^{o}C x 10 s, 60^{o}C x 1 min (25 cycles).

3.3 Results

3.3.1 Immunocytochemistry

To assess the mechanistic details giving rise to the F-actin depleted zone, invasive and non-invasive hyphae were treated with primary antibodies that had been raised against yeast and human cofilin. Both of these primary antibodies showed staining in the tips of invasive hyphae, indicating that a protein that is antigenically related to cofilin is present in hyphae and importantly this is for the most part located in the same regions of the invasive hyphae as the F-actin depleted zone (Figure 3.1A, 3.1B). Eighty two percent of hyphae (n= 44) stained with antibody raised against human cofilin 1 showed a tip high concentration of a protein that is antigenically related to cofilin, whereas the remaining 18% showed no tip high staining. On the other hand, 85% of non-invasive hyphae (n= 39) treated with the human antibody showed no observable tip high localisation of cofilin. Instead, the localisation was mainly observed at the hyphal periphery with some diffuse cytoplasmic staining (Figure 3.1C). The remaining 15% of non-invasive hyphae stained with the human antibody showed a tip high cofilin distribution. Due to insufficient titre, quantitative analysis was not carried out using yeast antibody.

3.3.2 Immunoblotting

The antibody that had been raised against human cofilin was used in immunoblotting of *N. crassa* total cell extracts and this identified a single band of approximately 21kDa (Figure 3.1 D). The size of this protein is within the reported size range of human cofilin 1, 19-21 kDa, the protein which the antibody was raised against. The estimated molecular weight of the hypothetical cofilin gene in *N. crassa* genome was worked out to be around 17 kDa. Due to insufficient titre, immunoblots were unable to be carried out to test the yeast antibody.

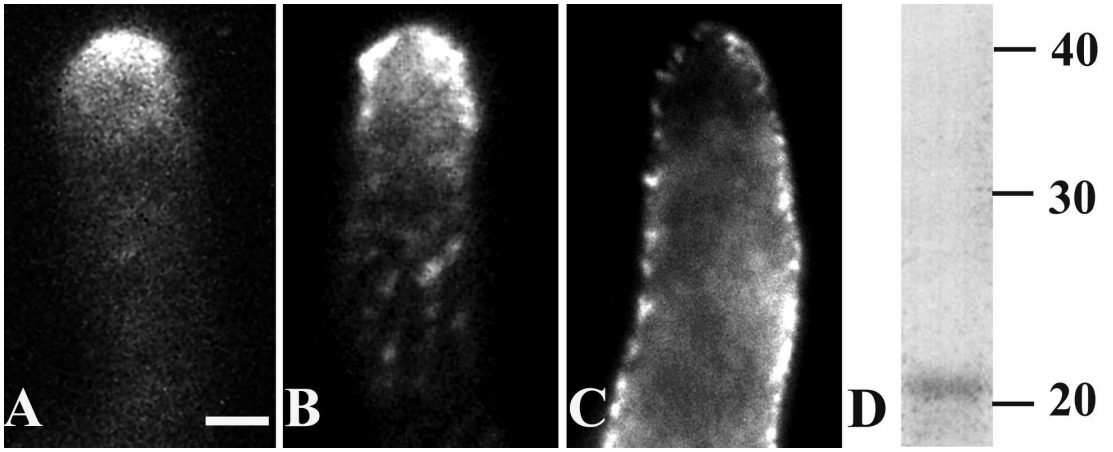

Figure 3.1 Immunostaining and immunoblotting of cofilin.

Invasive hyphae stained with an antibody raised against yeast (A) and human (B) cofilin. Staining is located predominantly at the tips of these hyphae. A more random distribution of stain was seen in non-invasive hyphae that had been exposed to the human cofilin antibody (C). This antibody identified a single band in immunoblots of a whole hyphal fraction that approximated to 21 kDa (D). Hyphae treated with just the secondary antibody alone showed no staining. Hyphae were imaged near the median focal plane Bar= 3.3 μm.

3.3.3 Integrity and purity of total RNA extract

The integrity of extracted RNA from invasive and non-invasive hyphae was first checked by agarose gel electrophoresis (Figure 3.2) before any subsequent experiments were carried out. The results from the agarose gel showed two clear bands at the position of 18s and 28s rRNA for both treatments with a very faded smear. This indicated that RNA extracts had no significant degradation. The RNA was then judged to be ready for the reverse transcription polymerase chain reaction.

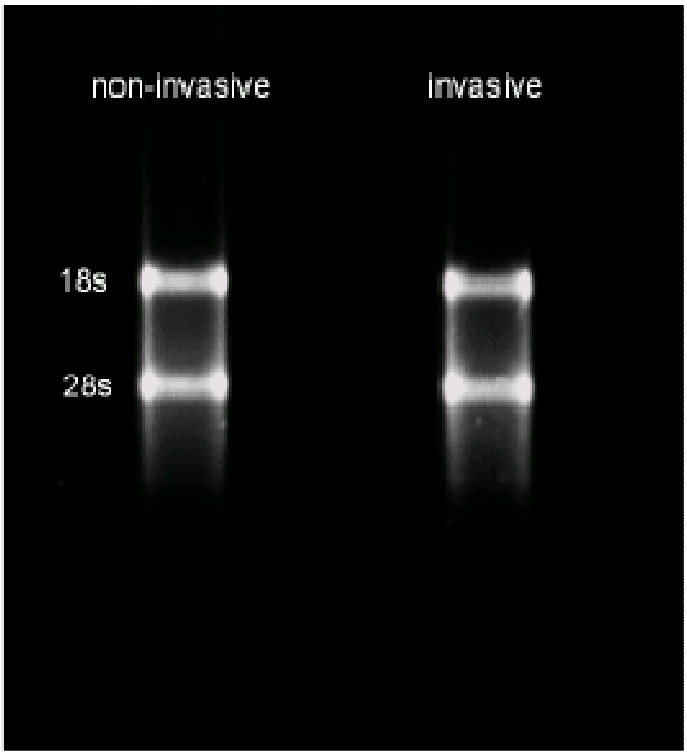

Figure 3.2 Agarose gel detection of total RNA extracted from invasive and non-invasive mycelia of *N. crassa*. The two clear bands of 18s and 28s rRNA obtained from the gel indicate that no significant RNA degradation occurred during extractions. The extracted RNA was thus judged to be suitable for subsequent experimentation.

3.3.4 Quantitative expression of cof1

Expression levels of *cof1*, a cofilin homologue of *N. crassa* were quantified using real-time PCR, with cDNA from invasive and non-invasive hyphae serving as templates. GAPDH (Glyceraldehyde-3-phosphate dehydrogenase) was used in this experiment as an internal control gene. The internal control gene is essential to correct any error introduced for example by unequal amounts of cDNA templates being added to each PCR reaction.

A representative amplification plot is shown in Fig. 3.3A with a dissociation curve in Fig. 3.3B). In the amplification plot (Fig. 3.3A), the horizontal brown line represents the threshold allocated at the elevated level of gene expression that is significant enough for analysis. The plotted curves represent the intensity of fluorescence (y-axis) detected at each cycle (x-axis) for each PCR reaction. Statistical results showed that there was no significant difference ($P>0.05$) between the *cof1* expression levels of invasive (threshold cycle (C_T) = 29) versus non-invasive (C_T = 27.5) hyphae, after having calibrated with the expression levels (C_T = 23.3 for invasive and 24.9 for non-invasive) of the internal control gene, GAPDH. GADPH is one of the most often considered housekeeping genes used as internal standards (Thellin et al. 1999). The dissociation curves (Fig. 3.3B) indicate that the specific amplicons melt at around

88ºC, and with only one peak present it is unlikely that there was any non-specific amplification. The blue curve (Fig 3.3A and 3.3B) represents the negative control, in which there was no sign of amplification, as indicated by the lack of a peak in the dissociation curve.

Although there was only one peak presented in the dissociation curve (Fig. 3.3B), there is still a possibility that there may be more than one amplicon with the same or a very similar melting temperature present in one PCR reaction. For further verification of the specificity of the primers, gel electrophoresis was carried out to separate RT-PCR product(s) by their length (Fig. 3.4). The gels identified only one single band of about 200 bp in the four RT-PCR products of invasive and non-invasive treatments for both the target gene and the reference gene (i.e., invasive *cof1*, non-invasive *cof1*, invasive GAPDH, and non-invasive GAPDH). In addition, the intensity of the bands is quite similar between *cof1* of the two treatments, as well as GAPDH of the two treatments, which further supports the results of no significant difference in their C_T numbers.

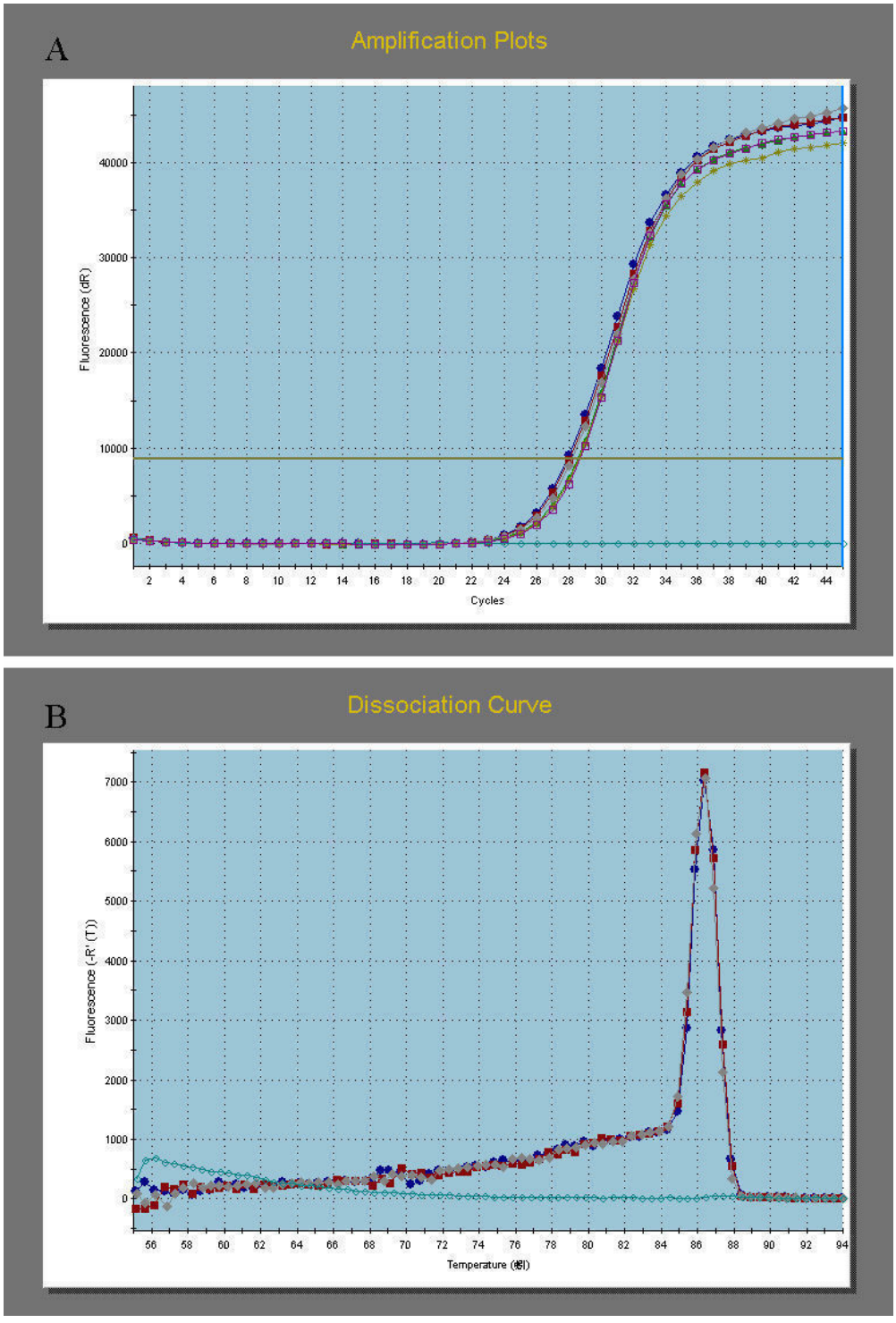

Figure 3.3 Amplification plot (A) and dissociation curve (B) of real-time PCR carried out on hyphal extracts of invasive and non-invasively grown *N. crassa*. Results showed no significant difference between the expression levels (A) of *cof1* in invasive (blue, grey, and red) and non-invasive hyphae (purple, green, and yellow).

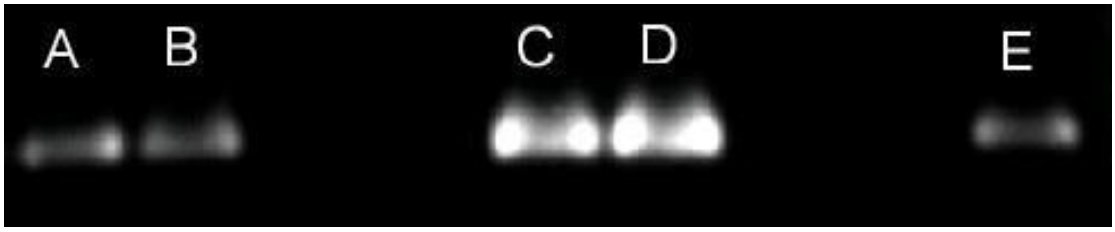

Figure 3.4 Electrophorogram of real-time PCR products. PCR products were analysed on 1.4% (w/v) agarose gels. Each lane contained 3 µl PCR products and 2 µl orange G loading dye. The RT-PCR products of non-invasively (lane A) and invasively (lane B) grown hyphae showed a single band around 200 bp. The products of the house keeping gene GAPDH, from the non-invasive (lane C) and invasively (lane D) grown hyphae, also showed a single band around 200 bp. Lane E shows the DNA ladder of 200 bp.

3.3.5 Sequence analysis of putative fragment

The PCR product was purified and sequenced using the forward and reverse primer (Table 3.1) that had been designed for RT-PCR use. The complementary reverse sequencing result was then aligned with the forward results and with the exception of the primer binding regions, the rest of the sequence completely matched (100%). The sequencing result of the PCR products was then blast searched against the NCBI database (www.ncbi.nlm.nih.gov/BLAST/). The hypothesised cofilin related gene (accession number CAB91380) of *Neurospora crassa* and human *cof1*, showed 100% and 58% positives at the amino acid level, respectively. The results from the blast search showed that the target gene matches with the hypothesised *N. crass*a sequence at amino acid number 80 through to 122. Blasts against the genomic data bank resulted in 14 blast hits on the query sequence, and most of these were from *Saccharomycetes* and ascomycetes. Only two sequences in the query came from *Neurospora crassa*, both of these were referred to as cofilin related genes.

3.4 Discussion

3.4.1 The presence of cofilin in ADZ

If the F-actin cytoskeleton rearranges to allow for increases in tip yielding, then this raises the question of what factors might underlie these rearrangements. There are a large number of actin binding proteins (ABPs) that are capable of facilitating a dynamic cytoskeleton (Dos Remedios et al. 2003). An attractive candidate with respect to an F-actin-depleted zone, given its involvement in actin dynamics in other tip growing systems (Chen et al. 2002; Braun et al. 2004; Jiang et al. 1997a), is the filament severing protein cofilin, also known as actin depolymerising factor (ADF). Ghosh et al (2004) have demonstrated that intracellular cofilin activity may lead to the generation of free barbed ends, the polymerisation of actin, the induction of protrusion, and through the use of a chemically engineered photo-activatable analogue of cofilin (i.e., a light sensitive phospho-cofilin mimic) that it may set the direction of cell migration. These studies have shown that cofilin serves as a dynamic component functioning in cell motility.

The localised staining that is presented at the tips of invasive hyphae, with the use of two cofilin antibodies (raised against yeast and human), occurs in areas where an F-actin depleted zone is present (as detailed in Chapter 2). This apparent

co-localisation would be consistent with cofilin severing F-actin in the tips and creating an F-actin-depleted zone (although caution is advised given that no direct co-localisation studies were conducted due to time constraints). Nevertheless, it is predicted that in double labelling experiment, cofilin will be co-localising the ADZ while actin to be presenting at the bottom of this structure.

With respect to the activity of cofilin, the interaction of cofilin/ADF with actin is enhanced by an alkaline pH (Du & Frieden 1998). It is thus interesting to note the report of a pH gradient in *N. crassa* hyphae with the tips having an alkaline pH (pH8) (Robson et al. 1996). While other publications report no such gradient, they do report a mean cytoplasmic pH for *N. crassa* of 7.6 (Legerton et al. 1983; Parton 1997), which is more alkaline than the value of 7.3 at which actin depolymerisation has been shown to be enhanced by cofilin (Yonezawa et al. 1985).

A maize cofilin, called ZmADF1 (*Zea mays* actin depolymerising factor 1), has been demonstrated to reorganise an F-actin population in *Tradescantia* stamen hair cells (Hussey et al. 1998). In addition, it has been shown that the related protein ZmADF3 plays a similar role (i.e., redistributes F-actin) in the development of maize root hair. While this appears to be coupled with actin reorganization, it should be noted that the

disruption of actin filaments after cytochalasin D treatment led to the appearance of short rods of ZmADF3 and actin in the nucleus. This has led to the suggestion that the main function of ZmADF3 is in the guidance of actin to sites of polymerisation (Jiang et al. 1997b).

In tobacco pollen tubes, Chen *et al* (2002) have shown that over expression of the cofilin NtADF1 (*Nicotiniana tabacum* actin depolymerising factor 1) causes a decrease in fine actin cables and a reduction in growth. When NtADF1 was tagged with GFP, it was found to associate with short actin filaments in the subapical region and with long actin cables in the shank of the pollen tube. The tobacco cofilin may be similar to *N. crassa* in that its *in vitro* activity was enhanced with an alkaline pH. Similar to hyphae, a pH gradient is known to exist in the apical region of elongating pollen tubes. Thus, actin dynamics may be greatly influenced by proton concentrations.

The localisation of cofilin in a zone back from the leading edge has also been seen in other organisms, such as animal neuronal cells and yeast (Moon 1993; Flynn 2007). In other organisms a stable zone of actin was found at their leading edge (Moon 1993; Svitkina and Borisy 1999; Svitkina 2006). This suggests that cofilins have a fairly

common characteristic in that they tend to localise to a region where actin undergoes remodelling.

The immunoblots suggest that the protein recognised by the antibody has a molecular mass of 21 kDa. This matches the mass of human cofilin 1, the protein against which the antibody was raised. The estimated molecular weight of the hypothetical cofilin gene of *N. crassa* is around 17 kDa. Both human cofilin 1 and *N. crassa* cofilin sit on the higher end of the reported size range of cofilin/ADF family (13 to 21 kDa). A homologue of the mammalian cofilin has been identified in yeast, although to the best of our knowledge this is the first indication from immunoblotting data that such a protein in a filamentous species has been identified. Alignment BLAST of human cofilin 1 amino acid sequence against *N. crassa* genome (http://www.broad.mit.edu/annotation/fungi/neurospora_crassa_7) identifies a hypothetical protein (NCU01587.2) that has 33% identity and 58% similarity to the human protein. These levels of identity and similarity are close to those obtained when comparing plant and vertebrate cofilins (typically ~ 40% identity and 60% similarity (Chen et al. 2002). The hypothetical *N. crassa* protein has a predicted mass of just over 17 kDa, slightly less than the 21 kDa that was found in the immunoblots. It is worth noting however that in the published immunoblots of plant pollen tube actin-depolymerising factors,

the molecular weight of the protein identified by immunoblots was ~20 kDa, while the molecular mass predicted by the sequence was ~17 kDa. This disparity may be due to the fact that the salt concentration in higher concentrated protein samples can slightly decrease the motility of the protein (Chen et al. 2003).

3.4.2 Cof1 gene expression in invasive growth

The regulation/expression level of cofilin has been shown to be very important to cell viability and is essential for cell growth (Iida & Yahara 1999). The RT-PCR amplification results indicate that the expression levels of cofilin in invasive and non-invasive hyphae do not differ statistically. This is supported by the earlier reports showing that the level of cofilin expression did not respond to increases in the actin monomer pool (Bamburg et al. 1999), although, while likely, it is not known for definite whether the formation of an ADZ in the invasive hyphae actually leads to an increase in G-actin.

In summary, cofilin/ADF has been shown in this and in other studies to localise at sites where actin remodelling is occurring. In invasive hyphae, this is at the very tip where it may play a role in facilitating greater tip yielding through the breakdown of F-actin.

Chapter 4: The distribution of formin in invasive and non-invasive hyphae

4.1 Introduction

The formins are a family of actin binding proteins that regulate actin dynamics. Most eukaryotes have several formin isoforms, suggesting that the protein may have a diversity of cellular roles. Formin is an actin polymerising protein that co-localises with actin and is thought to participate in a variety of cellular processes that involve the cytoskeleton. These include cytokinesis, septation (Schmitz et al. 2006), and with relevance to the current study, the establishment of cell polarity (reviewed in Tanaka 2000). Formins may also be involved in cell signalling (Habas et al. 2001).

Formins have generated interest with respect to actin biochemistry ever since the discovery of their actin nucleating ability. Their actin nucleation differs from that of the first identified and perhaps best-characterised actin filament initiator, the Arp2/3 complex, as will be described below. Formins are large proteins (~184 kDa in molecular weight, almost double that of Arp2/3) and are comprised of multiple domains. They are involved in actin cable elongation at the barbed end, in contrast

with Arp2/3, which initiates new filament branches at a characteristic 70^{o} angle on the side of a pre-existing filament or at the pointed end (Pollard 2002). Thus, formin-mediated actin cable assembly enables the generation of an alternative set of actin arrangements relative to the Arp2/3 complex. Cells with dysfunctional formins do not assemble actin cables. Conversely, over-activation of formin gene (AgBni1) in *Ashbya gossypii* assembles a dense network of actin cables (Schmitz et al. 2006).

In yeast, the polymerisation of a single microfilament in association with formin has been shown to generate a force of at least 1 pN (Kovar & Pollard 2004). Thus, when turgor is low or absent (see Chapter 5), microfilaments could provide a protrusive force for non-invasive hyphae in a manner similar to that which is responsible for the extension of lamellipodia in animal cells (Heath & Steinberg 1999). On the other hand, this force may not solely be sufficient for achieving invasive growth penetrating through solid media and cell extension is more likely to be dependent upon the fluidity of wall polymers at the cell apex that is governed by wall-weakening enzymes (Money 1999a and 1999b).

A study using the fission yeast, *Schizosaccharomyces pombe*, investigating formin activity using a full-length for3p gene tagged with three tandem copies of GFP

showed that after formins transiently assembled short actin filaments at the cell tip, they are then released from the cortex and move into the cell interior on filaments within the bundle (Martin & Chang 2006). However, the mechanism by which formin 'walk' along the barbed end is not understood in any detail (Kovar 2006).

Formin deletion mutants of the fungus, *Ashbya gossypii*, have shown defects in hyphal growth and vesicle transport, presumably due to defective F-actin assembly. Mutations also result in a lack of septation and changes in branching pattern. More relevant to the current study are the observations that these mutants have an altered tip shape and a loss of a tip high gradient of actin. These findings emphasised the importance of the cooperation of formin and F-actin in hyphal growth (Schmitz et al. 2006).

Structurally, formin isoforms share homology in their C-terminal half, while their N-terminal regions are considered to be far more divergent across species. Formins bear a proline-rich formin homology 1 (FH1) domain in the middle, which is the most conserved region and best characterised. This may mediate interactions with profilin, thus facilitating sequestration of G-actin (Pruyne et al. 2002; Sagot et al. 2002a). Profilin is an abundant actin monomer associated protein, which promotes nucleotide

exchange on actin and increases the rate of formin-mediated elongation (Romero et al. 2004; Kovar et al. 2006). Formins are found to be the only profilin binding proteins in plants (Deeks et al. 2002).

Actin nucleation at the barbed end is mediated by a conserved FH2 domain (Fig 4.1), which has actin binding capacity and tethered-dimer architecture for polarising a growing actin filament (Xu et al. 2004). However, the FH2 core is monomeric, and instead of nucleating, it caps the barbed end to prevent the binding of capping proteins (Lu et al. 2007; Vavylonis et al. 2006; Pruyne et al. 2002). There is a short flexi linker that mediates the dimerisation between FH1 and FH2, forming FH1-FH2, allows FH2 to accelerate *de novo* filamentous nucleation and to alter elongation/depolymerisation rate (Xu et al. 2004). Another property of the FH2 domain is progressive movement along an elongating actin filament, as it does not dissociate or re-associate from the barbed end when adding new monomers. Instead, it travels up the filaments while always maintaining contact (Martin & Chang 2006).

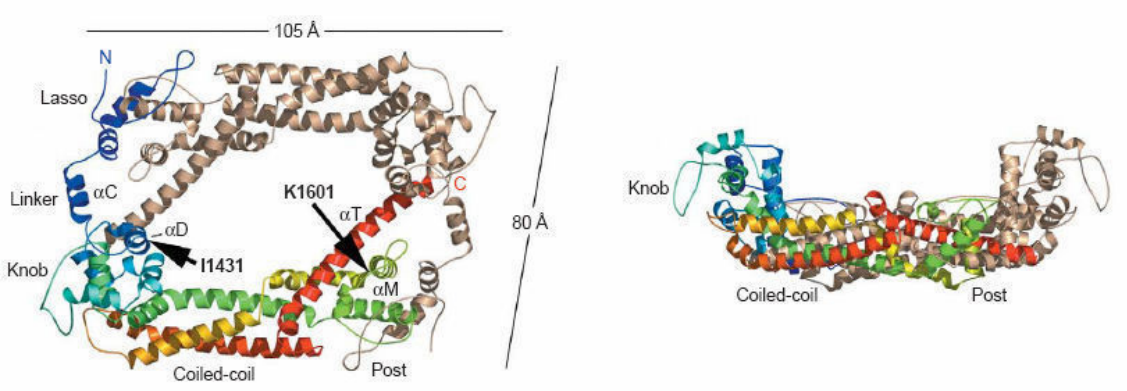

Figure 4.1 Top view (left panel) and side view (right panel) of the crystal structure of the Bni1 FH2 domain homo-dimer. The multi-coloured ribbon indicates one subunit, whereas the brown ribbon represents the other subunit. Each subunit can be classified by four main structure types, which have been called lasso, linker, knob and post from N to C terminal. Arrows indicate the approximate positions of two residues (I1431 and K1601) crucial for actin polymerisation acceleration (Higgs 2005; Xu et al. 2004).

As detailed above, the nucleation process is highly regulated as deletion/over-expression of formins in fungi showed abnormal F-actin patterns compared to wild type strains (Schmitz et al. 2006). More specifically studies using bacterially expressed glutathione-S-transferase (GST) fusion protein containing Bni1pFH1FH2 have shown that deletion of the FH1 domain reduces nucleating activity to 10% of that of the wild type, while deletion of the FH2 domain eliminates nucleating activity. Cleavage of GST to generate isolated FH2 returned nucleation levels back to 50% that of GST-Bni1pFH1FH2 (Pruyne et al. 2002). It has been demonstrated *in vivo* that FH1-profilin interaction is required for FH1-FH2 to function in filament assembly, accelerating ATP hydrolysis, and hence using the derived energy to maintain a much higher constant rate of actin polymerisation (Romero et al. 2004). However, Kovar et al. (2006) suggest that ATP hydrolysis is not required for processive elongation by formin in the presence or absence of profilin. The FH2 is sufficient for nucleating filaments from G-actins, whereas the profilin-actin complex can only be utilised as a substrate by FH1-FH2 (Romero et al. 2004; Higgs 2005; Vavylonis et al. 2006).

The FH3 domain is a loosely conserved motif among formins. This Rho-binding (ras-related GTP-binding protein) domain interacts with GTPases and undergoes

intramolecular association with a short carboxy-terminal domain, which activates actin cable/ring assembly essential for septation (Alberts 2001; Zigmond 2004). The amino acid dissimilarity outside FH1-FH2 suggests the isoforms may possess diverse mechanisms for regulation and cellular localisation. Therefore, how the activity of formins is spatially controlled may have a direct influence in the control the actin cable assembly in the cell. As mentioned in chapter 1, a formin homolog gene (NCU01431) consists of FH2 domain was identified in *Neurospora* genome, which has not been investigated.

The aim of this study is to examine the distribution of a protein that is antigenically related to human formin1 in invasive and non-invasive hyphae of *Neurospora crassa*. With reference to its actin nucleating ability described above and the results presented in Chapter 2, it is hypothesised that formin will be located at the tips of non-invasive hyphae and subapically in invasive hyphae.

4.2 Materials and methods

4.2.1 Antibodies

Formin 1 (T-15) antibody (an affinity purified goat IgG polyclonal antibody raised against formin1 of mouse origin) was purchased from Santa Cruz Biotechnology, Inc, and used as a primary antibody in the immunocytochemistry and immunoblotting. Alexa Fluor® 488 rabbit anti-goat IgG (H+L) conjugate was purchased from Molecular Probes and used as secondary antibody.

4.2.2 Immunocytochemistry and immunoblotting

Methods were the same as described in Chapter 2, except that the cell walls of hyphae were digested for 5 minutes rather than 45 seconds. Hyphae were incubated overnight with primary polyclonal anti-formin (IgG) antibody at a 1:500 dilution and were further incubated with a 1:1000 dilution of Alexa Fluor® 488 rabbit anti goat antibody for secondary against the mouse formin primary. Incubations were carried out at room temperature in the dark. Methods for immunoblotting were as described in Chapter 3, except that the anti-formin antibody was used for staining.

4.3 Results

4.3.1 Distribution of a protein with epitopic similarity to formin1 in invasive and non-invasive hyphae

Immunocytochemical observation of non-invasive hyphae stained with formin 1 antibody showed that 85% (45 out of 53 hyphae) had a prominent staining at the tip of the hypha along with some punctate subapical staining. The remaining 15% showed no tip high formin staining. Those hyphae with a tip high concentration of formin showed two main staining patterns, with stain present as either clouds (Fig. 4.2A, 4.2B) or as a cap (Fig. 4.2C). In some of those hyphae (7 out of 53 hyphae) that displayed a formin cap there was a gap within that cap (Fig. 4.2D).

In contrast to the non-invasive hyphae, 83% (39 out of 47 hyphae) of the invasive hyphae had more random staining throughout the cell, with no apparent tip high concentration (Fig. 4.2E-G), whereas the remaining 17% had prominent staining in the tip. Those hyphae with no tip high concentration showed either random sub-apical staining (Fig. 4.2E), a formin clear zone at the very tip (Fig. 4.2F), or punctate peripheral staining (Fig. 4.2G).

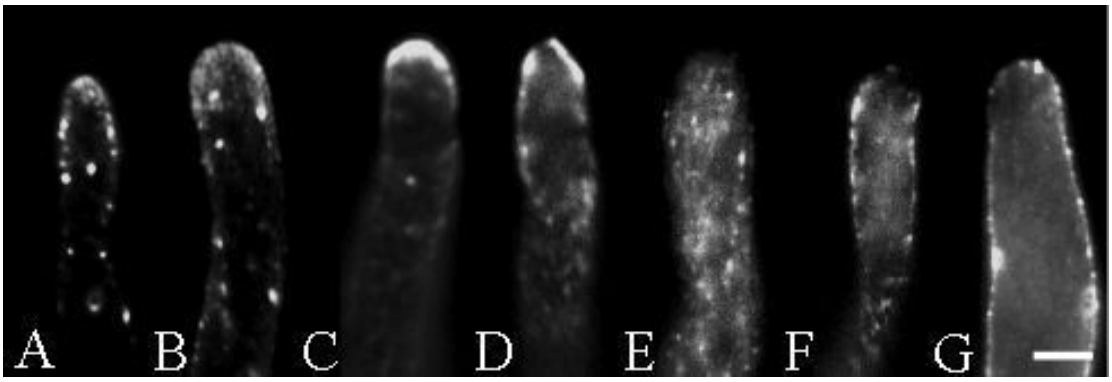

Figure 4.2 Two distinct staining patterns of formin 1 observed in non-invasive (A, B, C and D) and invasive (E, F, and G) hyphae of *Neurospora crassa*. The non-invasive hyphae had prominent clouds of formin 1 staining (A, B), a formin cap (C), and/or a cap with a gap (D). This contrasts with the invasive hyphae, which had no tip high localisation and a more random punctate staining through out the cell (E, F) or peripheral punctate staining at the very tip and through out the cell (G). Control hyphae treated with just the secondary antibody alone showed no staining. Bar = 3μm.

4.3.2 Detection of a protein with epitopic similarity to formin on immunoblotting

In an attempt to identify the protein that was responsible for the immunostaining in hyphae, immunoblotting on total hyphal extracts was carried out using the same antibody as for was used for the immunocytochemistry. Immunoblots indicated only a single band, which had a molecular weight of approximately 180 KDa, as shown in Figure 4.3. The molecular weight of this formin 1-like protein is close to the estimated molecular weight calculated from the amino acid sequence of the hypothetical/ formin related gene in *N. crassa* (197 kDa).

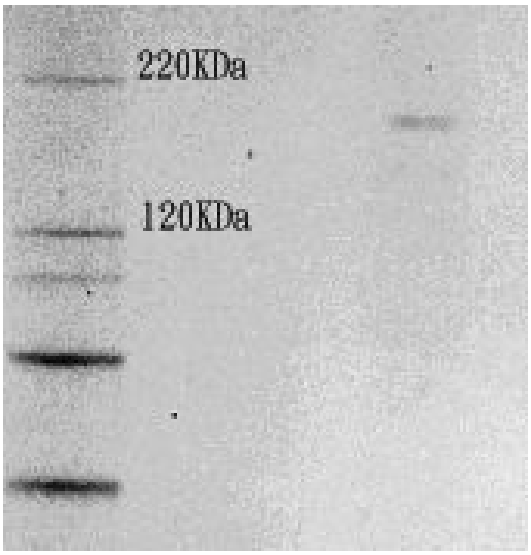

Figure 4.3 Immunoblotting of a protein that is antigenically related to formin1 in total hyphal extracts of *Neurospora crassa*. There was only one band present in total hyphal extracts, which was around 180 KDa.

4.4 Discussion

There have been reports describing two distinct distributions of F-actin in the hyphal apex of *N. crassa* (Suei & Garrill 2008; Chapter 2 this thesis) and in the oomycete *A. bisexualis* (Yu et al. 2004; Walker et al. 2006) and *P. cinnamomi* (Walker et al. 2006). In each of these species, non-invasive hyphae have shown a tip high F-actin distribution, whereas invasive hyphae have shown a tendency for an F-actin depleted zone at the tip. To better understand and address the molecular mechanisms underlying the formation and regulation of this actin-depleted zone, we examined the distribution of cofilin/ADF (in chapter 3 this thesis). We found a protein antigenically related to cofilin present in the same regions where F-actin was depleted. In other words, cofilin localised prominently where it is predicted that there is intensive actin-depolymerisation occurring.

To further understand the dynamics of F-actin in invasive and non-invasive hyphae, the distribution of a protein with epitopic similarity to human formin1, which has a molecular weight of approximately 180 KDa, was examined. This formin-like protein showed prominent localisation at the tips of non-invasive hyphae of *Neurospora crassa*. A different distribution was present in invasive hyphae, with no tip high concentration of antibody staining. Interestingly, the two distinct distributions of

formin immunostaining between invasive and non-invasive hyphae matched with the previously reported distribution of F-actin (Suei & Garrill 2008; Chapter 2 in this thesis). Unfortunately, due to time constraint, no co-localisation experiments were carried out. However, it is predicted that formin will be co-localising with actin in both invasive and non-invasive hyphae, where a redistributed pattern of formin localisation is likely to occur with actin rearrangements. The molecular weight identified from immunoblots was close to one of the three hypothetical formin genes (NCU01431: cytokinesis protein sepA) in *N. crassa* genome.

Schmitz et al (2006) have analysed the relationship between formin and F-actin, as well as its role in vesicle transportation, using mutant strains of the ascomycete *Ashbya gossypii*. One of 3 formins in this organism *Ag*Bni1p was found to locate at hyphal tips. Null mutants lacked actin cables and did not generate hyphae, instead taking the form of large potato shaped cells. These findings suggest an essential role for formin in hyphal tip growth and morphogenesis.

Formin localisation has been studied in other tip growth organisms, such as the model plant, *Arabidopsis thaliana*. Formins have been found to localise to specific cell membrane sub-domains in mature cells, typically at the borders between adjoining

cells (Deeks et al. 2005). This has led to the suggestion that formins function in providing a link between the actin cytoskeleton and the cell exterior, which may play some role analogous to the integrins of animal cells (Heath 2001). These suggestions are intriguing given the purported role that integrin-like proteins may play in tip growth (Kaminskyj & Heath 1995; Sun et al. 2000; Chitcholtan & Garrill 2005). In root hairs, formins are capable of arresting root hair development when placed under the control of an inducible promoter (Deeks et al. 2005). Again these results suggest that F-actin regulation by formins at specific sites associated with the cell membrane may be involved in directing cell polarity and morphological processes.

Kovar et al (2006) compared the activities of formins from budding (Bni1p) and fission (Cdc12p) yeasts. They both nucleate ATP- and ADP-G-actin *in vitro*, while Bni1p had a greater elongation rate (50-75%) than Cdc12p (0%) at free barbed ends over a range of ATP-G-actin concentrations. The difference in rates was due to the capping ability of Cdc12p, while Bni1p elongates and remains bound to the growing barbed end in the presence of monomers. The equilibrium between capped/open may be influenced by the linker length within the formin dimer (Xu et al. 2004), as the Cdc12p linker is short compared to the Bni1p linker. These results suggest that diverse formins are mechanistically similar with respect to actin assembly.

In conclusion, the localisation of a protein with epitopic similarity to formin is consistent with areas where F-actin is present in non-invasive hyphae. In contrast, this protein is absent from areas that normally contain an ADZ in invasive hyphae. These data point to a role for this protein in dynamic changes to the cytoskeleton that may be required for changes in growth strategy in *N. crassa*. On the basis of a similar molecular weight immunoblotting data suggests that this protein is likely to be a member of the formin family.

Chapter 5: Cell pressure

5.1 Introduction

Previous chapters in this thesis have suggested that F-actin rearrangements, facilitated by ABPs, may be necessary for invasive hyphal growth. F-actin has long been described as a tip growth regulator (Picton & Steer 1982) affecting the cell wall and the extensibility of the tip, which will yield due to the force of turgor pressure. Also, F-actin is likely to not just affect the rate of growth, but will also be responsible for the tip shape (Jackson & Heath 1990, 1993). Reports of oomycete hyphae growing in zero turgor or at least at levels of turgor below the lower limit of that which is measurable (Kaminskyj et al. 1992; Money & Harold 1993) have also led to suggestions that F-actin may also serve as a driving force providing a protrusive force for cell expansion and not just acting as a regulator (Harold et al. 1996; Heath 1990; Heath 1995). This raises the question of whether or not the re-distribution of F-actin that is observed in invasive hyphae is a result of a different level of turgor in these hyphae. Thus, if turgor were increased, might there be a need for less of a protrusive force from F-actin, and thus might there be lower concentrations of F-actin at the tip (i.e., an ADZ).

5.1.1 What is turgor pressure and turgor regulation?

Generally speaking, most organisms contain a higher concentration of solutes in the cytosol than the surrounding medium. This causes an influx of water down the resultant water gradient. In cells that do not have a cell wall, this would cause cells to burst if mechanisms were not in place to counter such influx. These mechanisms include the Na^+/K^+ ATPase of animal cells, one function of which is to reduce the cellular ion concentration and the contractile vacuoles of certain protists that function to expel water. In walled cells, such as fungal and oomycete hyphae and in plant cells, the increase in cell volume that occurs with water influx is countered by the resistive capabilities of the cell wall. The pressing of the plasma membrane against the cell wall generates an internal hydrostatic pressure referred to as turgor pressure. At equilibrium, turgor forces as much water out as what enters.

Fungi and plants are capable of maintaining their turgor pressure at a constant value in the face of changes to their external conditions. This is particularly evident in species such as sea grasses that live in estuarine environments, where tidal/river movements ensure that the external ion concentrations are never constant (Garrill et al. 1994). For an organism that may be reliant upon constant turgor for growth, there is clearly a need to respond to external solute changes (Jennings & Burke 1990; Lew et al. 2004).

To maintain turgor under such conditions, they must adjust to a hyperosmotic stress by accumulating ions/osmolytes and adjust to a hypoosmotic stress by secreting them to ease cell swelling and prevent bursting. Direct pressure probe measurements (discussed in more detail below) have shown that *N. crassa* can respond to hyperosmotic stress and return turgor to an original value over a time frame of 30 minutes - 1 hour. Hypoosmotic stresses are technically more difficult to create, but suggestions are that the hyphal response to such challenge may be instantaneous with turgor appearing to remain constant (i.e., without any measurable changes).

5.1.2 Turgor pressure and cell growth

Turgor pressure has been described as the driving force for cell wall expansion. By exerting pressure on the plastic wall at the hyphal tip, it causes deformation and localised extension at this specific site. However, while it may well be driving growth in the oomycetes, it is debatable whether turgor plays any role in the regulation of their cell growth (Money 1997, 1999). As mentioned above, reports have shown that these hyphae can grow in the absence of measurable turgor (Kaminskyj et al. 1992; Money & Harold 1993). In such cases, regulation of growth has been suggested to be due to changes in tip extensibility rather than a change in the actual driving force. What is clear is that in these organisms, the relationship between turgor and growth

rates is very complicated. There is also a complex relationship between turgor and morphology as hyphae can assume a plasmodial type appearance under hyperosmotic stress (Money & Harold 1993). The oomycetes also present a complicated scenario in that they are different from the fungi, unable to turgor regulate, which would further argue that tip extensibility is the key to cell growth rather than turgor itself.

This is not such an issue for fungi as they appear able to turgor regulate. Indeed, alterations in net ion channel fluxes, which will affect internal solute concentrations, might act as one of the potential survival tricks for the fungal kingdom and also in higher plants (Lew et al. 1992; Lew 1998; Silverman-Gavrila & Lew 2001; Shabala & Lew 2002; Levina & Lew 2006; Lew 2007). Another way to compensate is via the accumulation of osmotically active metabolites, such as glycerol (and other sugar alcohols), amino acids, their derivatives, and other metabolites (Jennings 1995; Money 1997; Davis et al. 2000), which were found with an increase in turgor pressure (Money & Howard 1996).

5.1.3 Detecting turgor pressure

Turgor pressure can be measured directly using a single cell pressure probe. However, this has been found to be technically difficult when working with fungal species with

particularly small hyphal diameters (Money 1990; Money & Harold 1992). Turgor can be estimated indirectly using incipient plasmolysis (Jennings 1995; Kaminskyj et al. 1992; Money 1990), which might not be suitable for cells that can turgor regulate. Lew *et al* (2004) examined turgor regulation in fungal species and found that *N. crassa* recovered its turgor over time, with half of the original turgor recovered around 30 minutes after osmotic challenge. In comparison, the turgor of the oomycete, *A. bisexualis*, fell from a level of around 6 bars to nearly zero upon hyperosmotic shock and transiently climbed up to ~ 2 bars and failed to recover further overnight.

These studies suggest that fungi can, but oomycetes can not, regulate turgor, yet they appear to have similar morphologies and both extend by hyphal tip growth. Therefore, the role of turgor in hyphal tip growth might differ between fungi and oomycetes and turgor driven growth might therefore not be a universal feature of hyphal organisms. As the fungi do turgor regulate, however, it is likely that turgor will play some role in driving growth and this raises the question of whether turgor increases when fungi are growing invasively and require a greater protrusive force.

This chapter examines the role of turgor by measuring and comparing turgor pressure directly and indirectly in invasive and non-invasive hyphae of *N. crassa*.

5.2 Materials and Methods

5.2.1 Pressure probe (direct pressure measurement)

Direct pressure measurements were made using a pressure probe designed and built by Professor Steve Tyerman, University of Adelaide, Australia. The pressure transducer in the probe was capable of measuring up to a maximum of 20 bars. The pressure probe and attached micropipette were filled with low viscosity silicon oil (WACKER AS4, Wacker-Chemie, Germany). Borosilicate glass capillaries (Harvard Apparatus Ltd., U.K.) were used to make the micropipettes. These had an external diameter of 1.0 mm and an internal diameter of 0.58 mm. The pipettes were pulled on a Narashige PC-10 pipette puller (Narashige Co. Ltd., Japan) on a one step setting at the heater level of 65. The pressure probe was attached to the micromanipulator (Lang GMBH & Co. K6, Type STM3), which were in turn attached to a Zeiss IM35 microscope with a Zeiss F-LD20/O, 25 Phase objective. The turgor pressures of both invasive and non-invasive *N. crassa* hyphae were measured. These measurements were obtained by inserting the micropipette into a hypha no more than approximately 300 µm from the apex of the cell. Upon entry of the micropipette into the cell, the oil-cytoplasm interface moved into the pipette. To measure the hydrostatic pressure of the cell, the meniscus was moved to the point at which the micropipette entered the cell wall.

For measurements of turgor in invasive hyphae, this necessitated moving the pipette through the agar media. Care was taken to ensure that oil was able to move out of the tip of the pipette and thus eliminated the possibility that agar was blocking the tip of the pipette prior to insertion into the cell.

5.2.2 Incipient plasmolysis (indirect pressure measurement)

Indirect pressure measurements were made using the technique of incipient plasmolysis for both invasive and non-invasive hyphae. Hyphae were initially prepared as described in Chapter 2. Vogel's broth was replaced after an hour of recovery by Vogel's broth supplemented with either 0 M, 0.5 M, 1 M, 1.5 M, 2 M, 2.5 M, 3 M, 4 M, 5 M, 6 M or 7 M sorbitol (Sigma Chemical Co., USA). Hyphae were left to plasmolyse for 30 minutes. An additional set of experiments was carried out utilizing a different time interval of 3 minutes incubation in Vogel's broth supplemented with 0, 0.5 and 1M sorbitol. Fifty hyphae in each well-plate were then assessed for plasmolysis (with 3 replicates) using a Zeiss IM35 microscope with a Zeiss F-LD20/O, 25phase objective.

Data was plotted as % of hyphae plasmolysed versus sorbitol concentration. Standard curves were fitted to the data using a logistic regression analysis of the form:

$$y = \frac{a}{1 + \left(\frac{X}{X_o}\right)^b}$$

Equation 5.1

This was carried out using the program Sigma Plot 2000. The concentration of sorbitol that caused 50% of the hyphae to plasmolyse was calculated by the rearrangement of the above equation. As described by Money (1990), hyphae will decrease in volume as they approach incipient plasmolysis, thus, the protoplasm will be much more concentrated than when the cells are at full turgor. Therefore, a correction factor of 0.63 is applied to approximate the internal osmotic potential in order to avoid underestimation. Turgor was then calculated as the difference between the osmotic potential of Vogel's broth and the internal potential using the following equation:

$$\psi_p = \psi_\pi^o - \psi_\pi^i \qquad \text{Equation 5.2}$$

Where "ψ_p" represents turgor pressure, "ψ_π^o" represents the osmotic potential of the media and "ψ_π^i" represents the osmotic potential of the internal environment. The osmolarity of Vogel's broth 283 mOsmol kg^{-1}, was obtained using a Wescor vapour pressure osmometer (Model 5100C). This value was converted into bars using the

Van't Hoff equation:

$$\psi_s = - \text{í}RTc_s \qquad \text{Equation 5.3}$$

As "ψ_s" represents the osmotic potential (in bars), "R" represents the gas constant (0.0832 bar L mol^{-1} K^{-1}), "T" represents the absolute temperature (in degrees Kelvin) and "c_s" represents the solute concentration of the solution, expressed as osmolarity (mole of total dissolved solutes per litre of water [mol L^{-1}]). The minus sign indicates that the dissolved solute reduces the water potential of a solution. As sorbitol will not dissociate in solution the Van't Hoff factor (í) is taken to be 1 and is thus omitted from the above equation.

5.2.3 Burst pressure

Measurements of the burst pressure of invasive and non-invasive hyphae of *N. crassa* were carried out using the pressure probe as described above, except that the insertion of the micropipette into the hypha was made closer to the tip. Initial turgor measurements were made on hyphae prior to attempts to burst the hyphae. Bursting was carried out by injecting silicon oil into the cells and increasing the internal pressure through the continued injection of silicon oil until the hyphae burst. The pressure was recorded when the tip burst.

5.3 Results

5.3.1 Direct pressure measurement

To make direct measurements of turgor pressure for invasive and non-invasive hyphae, a cell pressure probe was employed. Upon the initial immersion of the pipette into Vogel's broth, the broth was forced by surface tension into the pipette. Pressure was then applied to the pipette via the pressure probe until the meniscus, which formed at the hydrophobic (silicon oil) –hydrophilic (sorbitol broth) interface, moved back to the tip of the micropipette. The pressure required for this action was used as the zero (offset) pressure and was subtracted from hyphal pressure reading in order to acquire the net or actual turgor pressure within the cell.

Upon impalement of a hypha with the pipette the meniscus was forced back (about 200~400 μm) by the turgor pressure away from the tip of the pipette. Positive pressure was then applied to bring the meniscus back to the cell wall. A reading of the amount of positive pressure required to do this was measured using the pressure transducer and subsequently used to approximate the hyphal turgor pressure. After measurement, it was normal to see cytoplasm leak from the impalement site when withdrawing the pipette out of the cell. This leakage was taken as an indication that no wound response, which would lead to plugging of the micropipette, had occurred. A wound response is

quite common when pressure probe measurements are made with oomycetes (Lew et al. 2004; Walker et al. 2006) and can severely compromise recordings leading to overestimates of pressure.

The impalement techniques were slightly easier with invasive hyphae due to the agar which essentially held hyphae in place as the pipette was pressed against and then forced into the hypha. With the non-invasive hyphae impalement could at times be more problematic as pressing the pipette against the hyphae caused significant movement (as there was effectively no supporting lattice, only solution surrounding the hyphae) and thus penetration was difficult. On the other hand, it was more straightforward for the micropipette to reach the non-invasive hyphae as the pipette was moving through solution and not through agar.

The direct estimation of turgor pressure for non-invasive (5.13 $\pm$ SEM 0.44 bars, n=20) and invasive (6.97 $\pm$ SEM 0.34 bars, n=23) hyphae was obtained from this experiment. The respective turgor pressure measurements were significantly different ($P<0.001$). Results are summarised in table 5.1. Twenty replicates of non-invasive (range from 2.04 to 8.92) and twenty-three replicates of invasive measurements (range from 3.65 to 10.24) were carried out.

Growth type	Range (bars) (lowest-highest)	Average (bars)	± SEM
Non-invasive (n=20)	2.04- 8.92	5.13	0.44
Invasive (n=23)	3.65- 10.24	6.97	0.34

Table 5.1 Pressure probe data table

5.3.2 Indirect pressure measurement

This experiment was carried out to determine the internal osmotic potential of the hyphae. Plasmolysis data for hyphae incubated in sorbitol broth for 30 minutes were plotted to obtain sigmoidal curves (Fig. 5.1) for both invasive and non-invasive hyphae). The sorbitol concentration added to the Vogel's media at which 50% of hyphae were plasmolysed for non-invasive and invasive hyphae were 2.76 ± 0.28 M (non-invasive hyphae) and 2.51 ± 0.13 M (invasive hyphae). The osmotic pressure for non-invasive (3.07 mol kg^{-1}) and invasive (2.82 mol kg^{-1}) treatments at that specific concentration was then calculated using the equation obtained from the graph of osmotic pressure (Fig. 5.2). The hyphal turgor pressures obtained (using equation 5.2 and 5.3) were 40.32 bars for the non-invasive and 36.36 bars for the invasive hyphae. Statistically, there was no significant difference in turgor pressures between non-invasive and invasive hyphae. These pressures are extremely high and as

described in the Discussion section for this Chapter are unlikely to be accurate. One source of experimental error in this experiment may be the fact that *N. crassa* shows significant turgor recovery 30 minutes after being subjected to hyperosmotic challenge (Lew et al. 2004).

In view of the above, another set of experiments were carried out in which hyphae were left in sorbitol broth for only 3 minutes. These showed a somewhat different trend compared to those that were left in sorbitol broth for 30 minutes. The sorbitol concentration in Vogel's media that caused 50% of the non-invasive hyphae to plasmolyse was 0.77 $\pm$ 0.3 M. In contrast, the invasive hyphae showed a similar trend as those that had been left in the sorbitol broth for 30 minutes. The hyphal turgor of non-invasive hyphae that were left in sorbitol broth for 3 minutes was 9.45 bars. Despite being significantly lower than that obtained in the previous set of experiments, this is still an extremely high value and likely to be an overestimation of the true value.

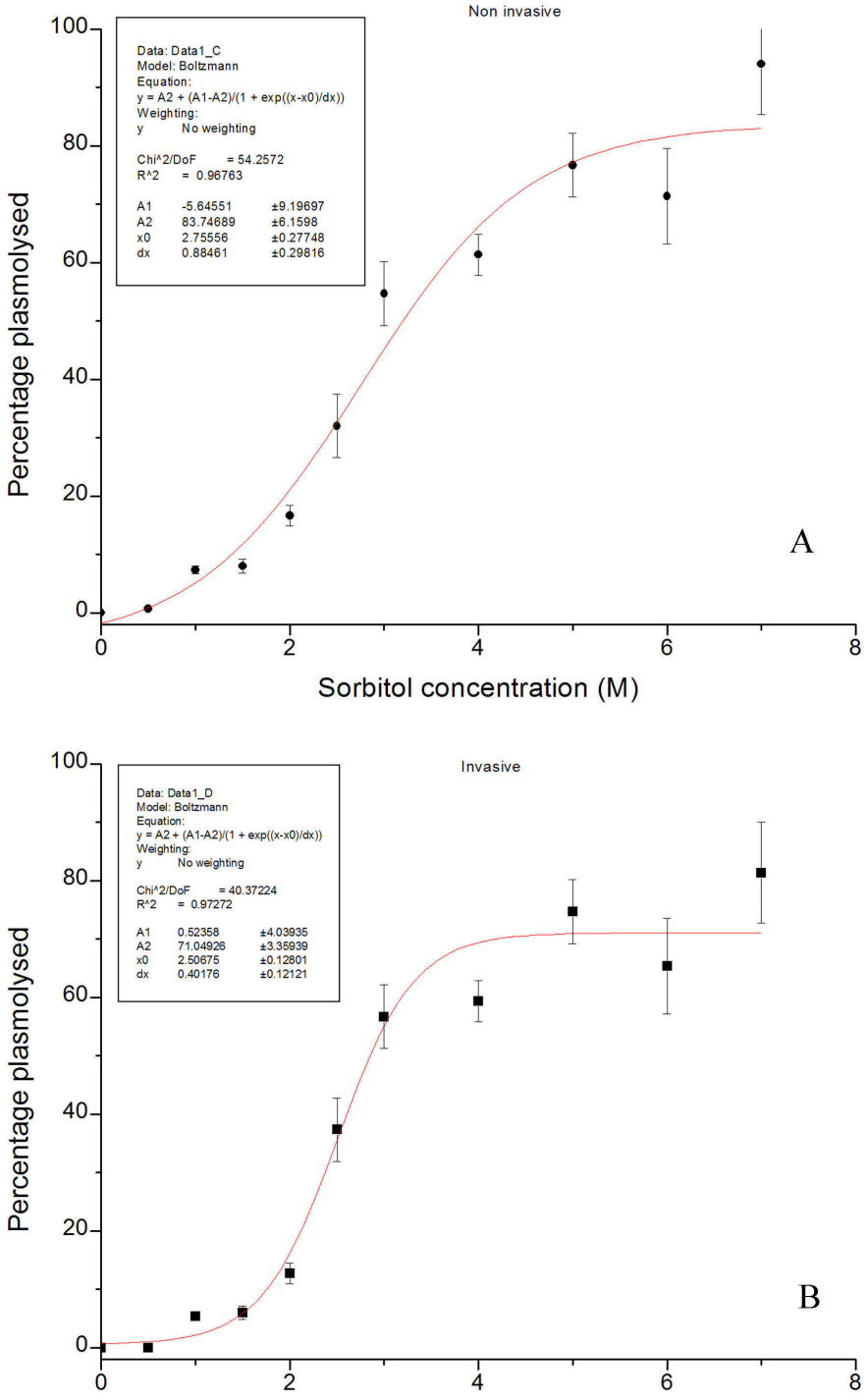

Figure 5.1 Incipient plasmolysis data for non-invasive (A) and invasive (B) hyphae of *Neurospora crassa*. The sigmoidal curves showed that the sorbitol concentration required for 50% of the hyphae to plasmolyse was 2.76 $\pm$ 0.28 M for non-invasive hyphae and 2.51 $\pm$ 0.13 M for invasive hyphae.

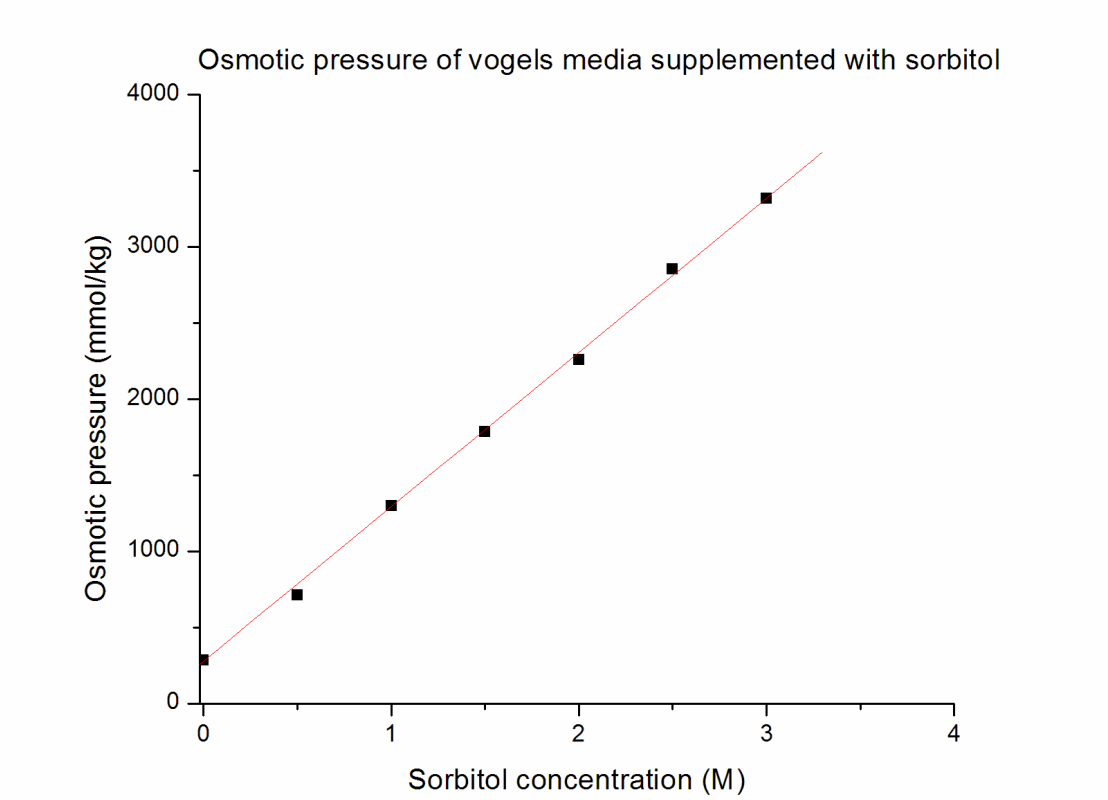

Figure 5.2 Plot of osmotic pressure of various concentrations of sorbitol in Vogel's media. Data is plotted with the line of best fit. The equation of the line of best fit (y=1013x+280) was calculated from the graph, where y represents the osmotic pressure in mOsmol kg^{-1}, x represents the sorbitol concentration in Vogel's media in M.

5.3.3 Burst pressure measurement

Bursting pressure measurements of invasive and non-invasive hyphae of *N. crassa* were attempted using the pressure probe in order to indirectly approximate cell wall strength. The initial turgor pressure was obtained prior to the bursting as described in the Materials and Methods section (section 5.3). The hyphal pressure was then increased upon the injection of silicon oil into the hyphae. Theoretically, silicon oil should be continually injected into the cell up to the point when bursting occurred at the apex of the hyphal tip and at which point the pressure will then be recorded.

Unfortunately, presumably due to the extremely small size of the hyphae of *N. crassa* (5-10 μm diameter), these experiments were extremely difficult and no actual bursting measurements were possible. After initial turgor measurements, it was typical to see cytoplasm leak from the impalement site when applying more pressure. Both invasive and non-invasive hyphae almost always "leaked" at the impalement sites. In some extreme cases, the apex of hyphae appeared extremely turgid or alternately extremely compliant in that they would burst as the micropipette touched the hypha prior to impalement.

In order to check that the failure to obtain measurements was due to technical

difficulties associated with working with small hyphae, bursting pressure measurements were made with the oomycete, *Achlya bisexualis*, which has relatively large hyphae (diameters around 15-20 μm). These hyphae were grown in 0.3M sorbitol and gave initial readings for turgor of 2.2 and 2.45 bars, and burst pressures of 5.70 and 4.88 bars, respectively. This suggests that the failure to obtain data for *N. crassa* was likely to be due to the technical limitations imposed by the size of the hyphae.

5.4 Discussion

5.4.1 Pressure probe

The findings presented in this Chapter indicate that invasive hyphae possess a significantly higher turgor pressure (6.97 bars) compared to non-invasive hyphae (5.13 bars). If turgor is the main driving force for growth, it could be suggested that the higher turgor would result in a higher growth rate. However, as described in Chapter 2 both invasive and non-invasive hyphae show a similar growth rate, despite these different levels of turgor. However, according to previous reports (Kaminskyj et al. 1992), increases in turgor are not directly related to increases in growth rates and there is clearly a complex relationship between turgor and growth. Jennings (1995) has also suggested that turgor may actually drive growth but that growth rates are likely to be largely dependent on the extensibility of the hyphal apex. There is also restraint offered by the agar media for invasive hyphae and this may be slowing growth.

With respect to extensibility and in line with arguments presented at various junctures in this thesis, actin seems to play a role in restraining tip yielding under normal turgor (i.e., the turgor level that cells maintain in un-supplemented liquid media). Gupta and Heath (1997) found that the disruption of actin with latrunculin causes a growth

acceleration of normal turgor hyphae. This finding is consistent with previous work in which irradiation-induced damage to the apical actin, resulted in rapid growth acceleration (Jackson & Heath 1993b). Therefore, apical actin does appear to function in restraining tip growth. This conclusion may well apply to our findings in Chapter 2 with the dynamic rearrangement of actin at the apical region resulting in an ADZ, creating less restraint at the tip and greater tip yielding in invasive hyphae. This then raises an anomaly, as with greater turgor and less resistance at the tip it might be argued that invasive hyphae should grow faster than their non-invasive counterparts, yet our data indicate that this is not the case. As noted above, however, the relationship between turgor and growth rates is complex and the amount of turgor required to enable the hyphae to penetrate the agar media rather than simply overcoming the resistive properties of the hyphal apex is not clear.

The discovery that tip growth persists in oomycete hyphae with significantly reduced or not measurable turgor/no turgor (Kaminskyj et al. 1992; Money & Harold 1993) has led to suggestions that actin may function as a driving force for cell growth. This hypothesis is further supported by Gupta and Heath (1997) who found that the disruption of actin in low turgor hyphae causes the growth rate to decrease. These findings both point to a potential role of F-actin functioning in tip protrusion, at least

in those hyphae growing under conditions of low turgor. However, contrary to these assertions, Harold *et al* (1996) found actin to be absent from the apical region in these cells. This raises the possibility that the hyphae were growing not in the absence of turgor but at levels of turgor that were below the level of detection by the pressure probe (Gupta & Heath 1997). Therefore, with lower turgor, the reduction of apical actin might be indicative of a more compliant tip that is still able to extend forward despite the low level of turgor. This would act in collaboration with cell wall weakening by endoglucanases. Thus, in such a circumstance, turgor would be the driving force for growth and not apical protrusion by actin filaments.

Other workers have examined the force exerted by invasive hyphae and the relevance of this to the penetration of solid media (Ravishankar et al. 2001; MacDonald et al. 2002; Money et al. 2004). Their results suggested that invasive hyphae of two oomycetes would be unable to penetrate solid tissue with just the force exerted by turgor pressure alone. This process would also require the concerted activity of secreted enzymes. However, it is suggested that this conclusion is somewhat controversial, as it is possible to question whether the hypha that were examined were actually growing invasively.

Force measurements were made using a micro-strain gauge, which was placed in solution just next to the agar through which the hyphae were growing. The force exerted by the hypha was measured using the displacement of the gauge, but to actually displace the gauge, the hyphae had to grow out of the agar and thus were in effect growing non-invasively at the time of displacement. In order to maintain the same growth rate, the force exerted by hyphae penetrating through solid media is more likely to be greater than that of those growing in liquid broth (non-invasive). Another point of contention is that the hyphae were pushing against the silicon beam, where they appeared to bulge and then flatten (Ravishankar et al. 2001). This suggests that growing/pushing against an obstacle is not an identical action to penetrating through agar media.

Mechanisms that a fungus may use to increase its turgor when growing invasively include the uptake of ions. This is a mechanism utilised by fungi as well as higher plants in response to hyperosmotic challenge (Lew et al. 1992; Lew 1998; Silverman-Gavrila & Lew 2001; Shabala & Lew 2002; Levina & Lew 2006; Lew 2007). Another mechanism that would increase turgor (or maintain it at a constant level given osmotic challenge) would be the accumulation of osmotically active metabolites. Changes in levels of sugar alcohols such as glycerol and mannitol have been reported, with

glycerol synthesis reportedly being controlled through the osmotically sensitive MAP kinase signal cascade in *N. crassa* (Shabala & Lew 2002). Other molecules such as amino acids, their derivatives, and other secondary metabolites also play a part (Jennings 1995; Money & Howard 1996; Money 1997; Davis et al. 2000).

5.4.2 Incipient plasmolysis

In a comparative study of various methodologies, Money (1990) has suggested that there is usually a good agreement between turgor values determined directly using a pressure probe and indirectly using incipient plasmolysis. These comparisons were made using oomycetes. However, results obtained in this chapter showed disagreement when applied to the ascomycete, *N. crassa*.

N. crassa growing in Vogel's broth supplemented with sorbitol for 30 minutes has an estimated turgor pressure of 36.36 and 40.32 bars for invasive and non-invasive hyphae, respectively. This is much higher than the previously reported values of 12.4-17.5 bars measured straight after flooding with osmolytes (~0-3 min) (Robertson & Rizvi, 1968). The difference between measurements is likely due to the osmolyte incubation time period with the problem in measurement likely to be due to recovery of turgor as previously observed by Lew *et al* (2004). They showed that turgor

dropped dramatically upon hyperosmotic treatment (i.e., measured directly after osmotic shock) with recovery to almost half the original value after 30 minutes. These observations suggest that the recovery has a striking impact on the measurement of turgor by incipient plasmolysis. In other words, when recovery commences after osmotic shock, cells are likely to return to normal while counting of/searching for plasmolysed cells is still in process and most hyphae will have recovered (i.e., have deplasmolysed) with a longer time period. This is further supported by the difference in turgor obtained from 30 minutes incubation (36.36 bars) and 3 minutes after flooding (9.45 bars) for non-invasive, but not invasive hyphae. Measurement obtained from the shorter incubation was slightly lower than the results obtained by Robertson and Rizvi (1968) observed directly after flooding (12-17 bars). These are still almost double to triple those obtained directly using a pressure probe (Lew et al. 2004). In contrast to the non-invasive hyphae, there was no significant difference between values obtained with the two incubation intervals for invasive hyphae. Reasons for this difference are unclear.

Taken together, these arguments suggest that incipient plasmolysis is not the best methodology to indirectly estimate the turgor pressure of invasive and non-invasive hyphae of *N. crassa*.

5.4.3 Bursting pressure

Measurements of bursting pressure were not possible due to the small size/diameter of the hyphal tip. In addition, the hyphal tips were easily burst upon insertion of the micropipette into hyphae, also by any small movement of the micropipette when applying pressure and injection of oil. Bursting experiments were subsequently carried out on an oomycete, *Achlya bisexualis*, which have a much bigger hyphal diameter to check that it was indeed technical difficulties relating to the small size of *N. crassa* hyphae that precluded any measurements being taken. Attempts were successful with non-invasive hyphae of *A. bisexualis* grown on 0.3M sorbitol-PYG media, which had bursting pressures, typically between 6-8 bars. This suggests that it was the small size of the hyphae that precluded similar measurements with *N. crassa*.

In conclusion, results in this chapter showed that invasively growing hyphae have a significantly larger turgor than non-invasive hyphae. This has an important implication for invasive hyphae as it may enable, along with an ADZ, the provision of a greater protrusive force. Incipient plasmolysis is not a reliable method for indirect turgor measurement due to the turgor regulation of *N. crassa*. Bursting experiments were unsuccessful due to technical difficulties.

Chapter 6: Conclusion

6.1 The presence of ADZ

Tip growth has been described as a growth process characterised by localised extension at the cell apex and is present in a variety of cell types such as fungal and oomycete hyphae, pollen tubes, and root hairs. Actin was previously thought to be mainly located at the cell apex or growing edge in many of these tip growing cells.

However, results obtained from Chapter 2 showed the presence of an actin-depleted zone (ADZ) at the apex. This appears to be a prevalent feature in invasive hyphae of the fungus *N. crassa*. Recent work on other organisms, such as oomycetes and pollen tubes, also show that F-actin may not necessarily be located preferentially at the tip (Yu et al. 2004; Lovy-Wheeler et al. 2005; Walker et al. 2006). Notably, an ADZ is also present in non-invasive hyphae, although in these, tip high localisation was still the most common feature. It is suggested for various reasons (see below) that the ADZ is likely to be a true dynamic structure and may be a factor that enables hyphae to grow invasively. Faint actin staining was present at the apex of hyphae with an ADZ, at sites where the Spitzenkörper was expected to be present. This difference in

actin staining patterns among species further supported the existence of an ADZ, since oomycetes do not have Spitzenkörper.

The fact that invasive growth occurs through agar and non-invasive growth occurs on top of agar, or through liquid media meant that *in situ* fixation of growing hyphae was effectively carried out under different conditions. This raises the possibility that the ADZ is not a true structural component of the F-actin cytoskeleton, but is in fact an artefact of different fixation regimes. In order to eliminate the possibility that the ADZ might be an artefact, a series of experiments were carried out (i.e., the effect of fixation on morphology, the quality of F-actin staining, the penetration of antibody through agar, and a comparison of different fixatives) with all results pointing to the ADZ as a true dynamic structure. A difference in actin distribution between invasive and non-invasive hyphae raises the prospect of an alternative mechanism of tip growth that enables hyphae to grow at the same rate under these two different conditions.

The presence of the ADZ resulting from actin rearrangement as hyphae grow invasively is consistent with the hypothesis that actin plays a role in restraining the tip. With less tip restraint, more of the turgor pressure is available for protrusive force,

which enables the hyphae to grow through solid media. Nevertheless, it is worth remembering that definitive demonstration of this dynamic structure awaits the development of a GFP-actin strain in *N. crassa*, which will enable live hyphal imaging. A recent study on cytoskeletal actin revealed an actin patch-depleted zone at the hyphal tip (Upadhyay & Shaw 2008), a structure similar to the ADZ demonstrated by immunostaining in this thesis (Chapter 2). Notably, this is the first successful GFP labelling of actin in an ascomycete, although the native actin gene is also present. The localisation of the native actin is left unresolved, which might be one of the potential pitfalls with this approach. However, actin organisation could be further investigated by immunostaining. Moreover, Wilson et al. (2006) demonstrated the ability of GFP-labelled probes to cause aberrations and to obstruct pollen tube growth. These examples imply that even though GFP-probing is a power approach, caution needs to be taken into account in their usage and analysis.

Further investigations were carried out to better understand the mechanism underlying ADZ formation. Actin binding proteins play important roles in regulating actin dynamics and thus are key candidates that are likely to contribute to the rearrangement of actin resulting in an ADZ.

Immunostaining showed that a protein which shares epitopic similarity to formin1 has

a similar distribution to actin in invasive and non-invasive hyphae. This protein was also shown to have a molecular weight of approximately 180 KDa by immunoblotting, which is very similar to the molecular weight of the mouse formin1 (184 KDa) that this antibody was raised against. The concurrent distribution of formin and actin probably reflects the actin nucleating function that formin possesses. As would be expected, as the ADZ is present at the tip of invasive hyphae, formin tends to be less concentrated there in comparison to non-invasive hyphae, which less frequently exhibits the ADZ.

The distribution of cofilin, which is an actin depolymerising protein, is of interest particularly in relation to the ADZ in invasive hyphae. Cofilin was shown to accumulate largely in the same region as the ADZ in invasive hyphae, while the distribution was more dispersed in non-invasive hyphae as shown by immunostaining. The protein that was likely to be responsible for this staining was shown by immunoblotting to have a mass of around 21 KDa, a value that sits at the upper end of the size range of this protein family (Carlier et al. 2003). The tip high concentration of cofilin at the same location as the ADZ in invasive hyphae is consistent with it playing a role in the dynamic remodelling of actin at the tip. It is important, however, to note that cofilin not only functions to sever F-actin at the pointed end, it is also

responsible for the recycling of G-actin, which under certain circumstances will promote barbed end actin polymerisation (Paavilainen et al. 2004, Carlier & Pantaloni 1997, Chen 2000, Maciver & Weeds 1994; Blanchoin et al. 2000).

The RT-PCR results suggest that the difference in distribution of cofilin does not arise from a difference in cofilin gene expression levels between invasive and non-invasive hyphae. Nevertheless, the level of gene expression does not determine the actual activity of cofilin. The activity of cofilin is controlled by the phosphorylation state of the protein (reviewed in Bamburg 1999a). In addition, Andrianantoandro and Pollard (2006) suggest that the action of cofilin in cells will depend on the local concentration of active cofilins, where low concentrations favour severing and high concentrations favour nucleation (as detailed in the preceding paragraph).

6.2 Turgor pressure is found to be higher in invasive hyphae

Hyphal tip growth is thought to result from a balance of tip extensibility and a protrusive force, where one is restraining and the other protruding. Tip extensibility is likely to result from the combined contribution of the cell wall and the actin cytoskeleton. The protrusive force has typically been thought to be solely dependant on turgor although it should be remembered that turgor levels have been found to show a complex relationship with growth rate (Kaminskyj et al. 1992).

Direct turgor pressure measurement obtained using the pressure probe showed that invasive hyphae possess significantly higher turgor than non-invasive hyphae. This difference in turgor may have provided the extra protrusive force that invasive hyphae require to penetrate through agar and maintain a growth rate similar to that when they grow non-invasively. Thus, even if turgor is not directly controlling growth, it is still providing a protrusive force for growth and is thus strongly influencing it. This, coupled with observations of the ADZ would suggest that under normal turgor/invasive growth conditions F-actin does not play a role in actually driving growth (i.e., providing a protrusive force). This correlates with the conclusions of Money who calculated that 1 million polymerising microfilaments were required for a hypha with a diameter of 10 μm to exert a force of 0.2 bars (Money 1995).

6.3 Summary

Data presented in this thesis argue for the presence of an F-actin depleted zone in invasive hyphae and it is suggested that this may play a role in invasive hyphal tip growth. The F-actin remodelling necessary for this structure may occur due to the activity of the actin binding protein cofilin. The reduction of F-actin is likely to reduce restraint and hence increase extensibility at the cell apex. This in turn will enable the provision of a greater protrusive force by turgor. A schematic representation of these processes are shown in detail in Fig 6.1.

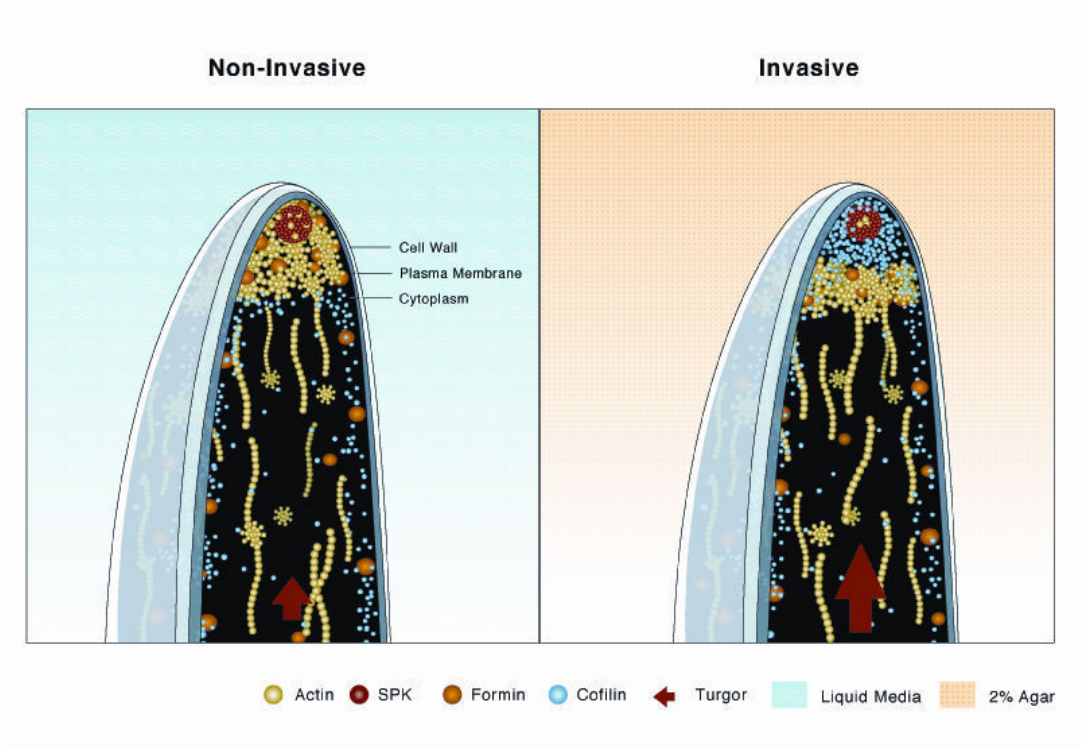

Figure 6.1 Illustrative summaries of the mechanistics of invasive and non-invasive hyphal tip growth of *N. crassa*. Actin rearrangement occurs creating an ADZ in invasive hyphae, this is largely absent from non-invasive hyphae. A Spitzenkörper is present under both growth conditions, it is slightly larger in invasive hyphae but this size difference is insufficient to account for the exclusion of actin from the tip. The presence of cofilin in the same area as the ADZ suggests its participation in cytoskeletal rearrangement required for invasive growth. A protein that is antigenically related to formin showed a similar distribution to actin in non-invasive hyphal tips. Turgor pressure is found to be significantly larger in invasive than non-invasive hyphae.

References

Alberts AS (2001) Identification of a Carboxyl-terminal Diaphanous-related Formin Homology Protein Autoregulatory Domain. Journal of Biological Chemistry 276(4): 2824-2830.

Allwood EG, Smertenko AP, Hussey PJ (2001) Phosphorylation of plant actin-depolymerising factor by calmodulin-like domain protein kinase. FEBS Letters 499(1-2): 97-100.

Andrianantoandro E, Pollard TD (2006) Mechanism of Actin Filament Turnover by Severing and Nucleation at Different Concentrations of ADF/Cofilin. Molecular Cell 24(1): 13-23.

Atkinson HA, Daniels A, Read ND (2002) Live-cell imaging of endocytosis during conidial germination in the rice blast fungus, *Magnaporthe grisea*. Fungal Genetics and Biology 37(3): 233-244.

Ayscough KR (1998) In vivo functions of actin-binding proteins. Current Opinion in Cell Biology 10(1): 102-111.

Bachewich CL, Heath IB (1997) The Cytoplasmic pH Influences Hyphal Tip Growth and Cytoskeleton-Related Organization. Fungal Genetics and Biology 21(1): 76-91.

Balcer HI, Goodman AL, Rodal AA, Smith E, Kugler J, Heuser JE Goode BL (2003) Coordinated Regulation of Actin Filament Turnover by a High-Molecular-Weight Srv2/CAP Complex, Cofilin, Profilin, and Aip1. Current Biology 13(24): 2159-2169.

Baluška F, von Witsch M, Peters M, Hlavačka A, Volkmann D (2001) Mastoparan Alters Subcellular Distribution of Profilin and Remodels F-Actin Cytoskeleton in Cells of Maize Root Apices. Plant and Cell Physiology 42(9): 912-922.

Bamburg JR (1999a) Proteins of the ADF/Cofilin Family: Essential Regulators of

Actin Dynamics. Annual Review of Cell and Developmental Biology 15(1): 185-230.

Bamburg JR (1999b) Special interest subgroups at the ASCB: Regulation of actin dynamics by ADF/cofilins *in vivo* and *in vitro*. Trends in Cell Biology 9(3): 118-118.

Bamburg JR, McGough A, Ono S (1999) Putting a new twist on actin: ADF/cofilins modulate actin dynamics. Trends in Cell Biology 9(9): 364-370.

Bartnicki-Garcia S, Hergert F, Gierz G (1989) Computer simulation of fungal morphogenesis and the mathematical basis for hyphal (tip) growth. Protoplasma 153(1): 46-57.

Bartnicki-Garcia S, Bartnicki DD, Gierz G, Lopez-Franco R, Bracker CE (1995) Evidence That Spitzenkorper Behavior Determines the Shape of a Fungal Hypha: A Test of the Hyphoid Model. Experimental Mycology 19(2): 153-159.

Blanchoin L, Pollard TD, Mullins RD (2000) Interactions of ADF/cofilin, Arp2/3 complex, capping protein and profilin in remodeling of branched actin filament networks. Current Biology 10(20): 1273-1282.

Bobkov AA, Muhlrad A, Shvetsov A, Benchaar S, Scoville D, Almo SC, Reisler E (2004) Cofilin (ADF) Affects Lateral Contacts in F-actin. Journal of Molecular Biology 337(1): 93-104.

Borisy GG, Svitkina TM (2000) Actin machinery: pushing the envelope. Current Opinion in Cell Biology 12(1): 104-112.

Borkovich KA, Alex LA, Yarden O, Freitag M, Turner GE, Read ND, Seiler S, Bell-Pedersen D, Paietta J, Plesofsky N (2004) Lessons from the genome sequence of Neurospora crassa: tracing the path from genomic blueprint to multicellular organism. Microbiology and Molecular Biology Reviews 68(1): 1-108.

Bourett TM, Howard RJ (1991) Ultrastructural immunolocalization of actin in a fungus. Protoplasma 163(2): 199-202.

Bowman GD, Nodelman IM, Hong Y, Chua NH, Lindberg U, Schutt CE (2000) A comparative structural analysis of the ADF/Cofilin family. Proteins Structure Function and Genetics 41(3): 374-384.

Braun M, Baluška F, von Witsch M, Menzel D (1999) Redistribution of actin, profilin and phosphatidylinositol-4, 5-bisphosphate in growing and maturing root hairs. Planta 209(4): 435-443.

Braun M, Hauslage J, Czogalla A, Limbach C (2004) Tip-localized actin polymerization and remodeling, reflected by the localization of ADF, profilin and villin, are fundamental for gravity-sensing and polar growth in characean rhizoids. Planta 219(3): 379-388.

Bruno KS, Aramayo R, Minke PF, Metzenberg RL, Plamann M (1996) Loss of growth polarity and mislocalization of septa in a Neurospora mutant altered in the regulatory subunit of cAMP-dependent protein kinase. EMBO Journal 15(21): 5772-5782.

Campbell NA, Reece JB (2005) Biology: Benjamin Cummings.

Carlier M-F, Pantaloni D (1996) Chapter 2 Actin polymerization: Regulation by divalent metal ion and nucleotide binding, ATP hydrolysis and actin binding proteins. In: Bittar EE, Bittar N, editors. Principles of Medical Biology: Elsevier. pp. 43-57.

Carlier M-F, Pantaloni D (1997) Control of actin dynamics in cell motility. Journal of Molecular Biology 269(4): 459-467.

Carlier M-F (1998) Control of actin dynamics. Current Opinion in Cell Biology 10(1): 45-51.

Carlier M-F, Wiesner S, Le Clainche C, Pantaloni D (2003) Actin-based motility as a self-organized system: mechanism and reconstitution in vitro. Comptes Rendus Biologies 326(2): 161-170.

Chen H, Bernstein BW, Bamburg JR (2000) Regulating actin-filament dynamics in vivo. Trends in Biochemical Sciences 25(1): 19-23.

Chen CY, Wong EI, Vidali L, Estavillo A, Hepler PK, Wu H, Cheung AY (2002) The Regulation of Actin Organization by Actin-Depolymerizing Factor in Elongating Pollen Tubes. Plant Cell 14(9): 2175-2190.

Chen YC, Cheung AY, Wu H (2003) Actin-Depolymerizing Factor Mediates Rac/Rop GTPase regulated Pollen Tube Growth. Plant Cell 15(1): 237-249.

Chitcholtan K, Garrill A (2005) A [beta]4 integrin-like protein co-localises with a phosphotyrosine containing protein in the oomycete *Achlya bisexualis*: Inhibition of tyrosine phosphorylation slows tip growth. Fungal Genetics and Biology 42(6): 534-545.

Chomczynski P, Sacchi N (1987) Single-step method of RNA isolation by acid guanidinium thiocyanate-phenol-chloroform extraction. Analytical Biochemistry 162(1): 156-159.

Cole L, Orlovich DA, Ashford AE (1998) Structure, Function, and Motility of Vacuoles in Filamentous Fungi. Fungal Genetics and Biology 24(1-2): 86-100.

Colot HV, Park G, Turner GE, Ringelberg C, Crew CM et al. (2006) A high-throughput gene knockout procedure for Neurospora reveals functions for multiple transcription factors. Proceedings of the National Academy of Sciences of the United States of America 103(27): 10352.

Cooper JA (1991) The Role of Actin Polymerization in Cell Motility. Annual Review of Physiology 53(1): 585-605.

Cooper JA, Schafer DA (2000) Control of actin assembly and disassembly at filament ends. Current Opinion in Cell Biology 12(1): 97-103.

Courvoisier A, Isel F, Francois J, Maaloum M (1998) End-Adsorbed Telechelic Polymer Chains at Surfaces: Bridging and Elasticity. Langmuir 14(14): 3727-3729.

Davis DJ, Burlak C, Money NP (2000) Osmotic pressure of fungal compatible osmolytes. Mycological Research 104(07): 800-804.

Dedova IV, Nikolaeva OP, Mikhailova VV, dos Remedios CG, Levitsky DI (2004) Two opposite effects of cofilin on the thermal unfolding of F-actin: a differential scanning calorimetric study. Biophysical Chemistry 110(1-2): 119-128.

Deeks MJ, Hussey PJ, Davies B (2002) Formins: intermediates in signal-transduction cascades that affect cytoskeletal reorganization. Trends in Plant Science 7(11): 492-498.

Deeks MJ, Cvrckova F, Machesky LM, Mikitova V, Ketelaar T, Zarsky V, Davies B, Hussey PJ (2005) Arabidopsis group Ie formins localize to specific cell membrane domains, interact with actin-binding proteins and cause defects in cell expansion upon aberrant expression. New Phytologist 168(3): 529-540.

Degousee N, Gupta GD, Lew RR, Heath IB (2000) A Putative Spectrin-Containing Membrane Skeleton in Hyphal Tips of *Neurospora crassa*. Fungal Genetics and Biology 30(1): 33-44.

Djafarzadeh S, Niggli V (1997) Signaling Pathways Involved in Dephosphorylation and Localization of the Actin-Binding Protein Cofilin in Stimulated Human Neutrophils. Experimental Cell Research 236(2): 427-435.

Dominguez R (2004) Actin-binding proteins - a unifying hypothesis. Trends in Biochemical Sciences 29(11): 572-578.

Dong CH, Xia GX, Hong Y, Ramachandran S, Kost B, Chua NH (2001) ADF Proteins Are Involved in the Control of Flowering and Regulate F-Actin Organization, Cell Expansion, and Organ Growth in Arabidopsis. Plant Cell 13(6): 1333-1346.

Du J, Frieden C (1998) Kinetic studies on the effect of yeast cofilin on yeast actin polymerization. Biochemistry 37(38): 13276-13284.

Feijó JA, Costa SS, Prado AM, Becker JD, Certal AC (2004) Signalling by tips. Current Opinion in Plant Biology 7(5): 589-598.

Fischer-Parton S, Parton RM, Hickey PC, Dijksterhuis J, Atkinson HA, Read ND (2000) Confocal microscopy of FM 4-64 as a tool for analysing

endocytosis and vesicle trafficking in living fungal hyphae. Journal of Microscopy 198(3): 246-259.

Flynn K, Pak C, Bamburg JR (2007) Regulation of Growth Cone Initiation and Actin Dynamics by ADF/Cofilin. In: Curtis Id, editor. Intracellular Mechanisms for Neuritogenesis: Springer US. pp. 25-56.

Freitag M, Hickey PC, Raju NB, Selker EU, Read ND (2004) GFP as a tool to analyze the organization, dynamics and function of nuclei and microtubules in *Neurospora crassa*. Fungal Genetics and Biology 41(10): 897-910.

Garrill A, Tyerman SD, Findlay GP (1994) Ion channels in the plasma membrane of protoplasts from the halophytic angiosperm *Zostera muelleri*. The Journal of Membrane Biology 142(3): 381-393.

Garrill A (2000) Eusocial hyphae? Mycological Research 104: 514-515.

Geitmann A, Emons AMC (2000) The cytoskeleton in plant and fungal cell tip growth. Journal of Microscopy 198(3): 218-245.

Ghosh M, Song X, Mouneimne G, Sidani M, Lawrence DS, Condeelis JS (2004) Cofilin promotes actin polymerization and defines the direction of cell motility. Science 304(5671): 743-746.

Gibbon BC, Kovar DR, Staiger CJ (1999) Latrunculin B Has Different Effects on Pollen Germination and Tube Growth. The Plant Cell Online 11(12): 2349.

Glass NL, Rasmussen C, Roca MG, Read ND (2004) Hyphal homing, fusion and mycelial interconnectedness. Trends in Microbiology 12(3): 135-141.

Gow NA (1989) Control of extension of the hyphal apex. Current Topics in Medical Mycology 3: 109-152.

Gupta GD, Heath IB (1997) Actin Disruption by Latrunculin B Causes Turgor-Related Changes in Tip Growth of *Saprolegnia ferax* Hyphae. Fungal Genetics and Biology 21(1): 64-75.

Gupta GD, Heath IB (2000) A Tip-High Gradient of a Putative Plasma Membrane SNARE Approximates the Exocytotic Gradient in Hyphal Apices of the

Fungus *Neurospora crassa*. Fungal Genetics and Biology 29(3): 187-199.

Habas R, Kato Y, He X (2001) Wnt/Frizzled Activation of Rho Regulates Vertebrate Gastrulation and Requires a Novel Formin Homology Protein Daam1. Cell 107(7): 843-854.

Harold RL, Money NP, Harold FM (1996) Growth and morphogenesis in *Saprolegnia ferax*: Is turgor required? Protoplasma 191(1): 105-114.

Harold FM (2002) Force and compliance: rethinking morphogenesis in walled cells. Fungal Genetics and Biology 37(3): 271-282.

Heath IB (1990) The roles of actin in tip growth. International Review of Cytology 123: 95-127.

Heath IB (1995a) Integration and regulation of hyphal tip growth. Canadian Journal of Botany 73(S1): 131-139.

Heath IB (1995b) The cytoskeleton. The Growing Fungus: 99–134.

Heath IB, Steinberg G (1999) Mechanisms of Hyphal Tip Growth: Tube Dwelling Amebae Revisited. Fungal Genetics and Biology 28(2): 79-93.

Heath IB (2000) Chapter 16: Organisation and functions of actin in hyphal tip growth. In: C. J. Staiger, F. Baluška, D. Volkmann, Barlow P, editors. Actin: A Dynamic Framework for Multiple Plant Cell Functions. Dordrecht: Academic Press. pp. 275-300.

Heath IB, Gupta G, Bai S (2000) Plasma Membrane-Adjacent Actin Filaments, but Not Microtubules, Are Essential for both Polarization and Hyphal Tip Morphogenesis in *Saprolegnia ferax* and *Neurospora crassa*. Fungal Genetics and Biology 30(1): 45-62.

Heath IB (2001) Bridging the divide: cytoskeleton-plasma membrane-cell wall interactions in growth and development. In: Howard R, Gow N, editors. The Mycota VIII Biology of the Fungal Cell Springer-Verlag, Berlin. pp. 201-223.

Heath IB, Skalamera D (2001) Regulation of tip morphogenesis by the cytoskeleton

and calcium ions: Cell biology of plant and fungal tip growth. In: Geitmann A. CM, Heath IB editor. Cell Biology of Plant and Fungal Tip growth. Siena, Italy: Amsterdam–Berlin–Oxford–Tokyo–Washington: IOS Press. pp. 37-54.

Heath IB, Bonham M, Akram A, Gupta GD (2003) The interrelationships of actin and hyphal tip growth in the ascomycete *Geotrichum candidum*. Fungal Genetics and Biology 38(1): 85-97.

Hickey PC, Jacobson DJ, Read ND, Louise Glass N (2002) Live-cell imaging of vegetative hyphal fusion in *Neurospora crassa*. Fungal Genetics and Biology 37(1): 109-119.

Higgs HN, Pollard TD (2001) Regulation of Actin Filament Network Formation Through ARP 2/3 Complex: Activation by a Diverse Array of Proteins 1. Annual Review of Biochemistry 70(1): 649-676.

Higgs HN (2005) Formin proteins: a domain-based approach. Trends in Biochemical Sciences 30(6): 342-353.

Hoch HC, Staples RC (1985) The microtubule cytoskeleton in hyphae of Uromyces phaseoli germlings: Its relationship to the region of nucleation and to the F-actin cytoskeleton. Protoplasma 124(1): 112-122.

Holdaway-Clarke TL, Hepler PK (2003) Control of pollen tube growth: role of ion gradients and fluxes. New Phytologist 159(3): 539-563.

Howard RJ (1981) Ultrastructural analysis of hyphal tip cell growth in fungi: Spitzenkorper, cytoskeleton and endomembranes after freeze-substitution. Journal of Cell Science 48(1): 89-103.

Howard RJ, Ferrari MA, Roach DH, Money NP (1991) Penetration of Hard Substrates by a Fungus Employing Enormous Turgor Pressures. Proceedings of the National Academy of Sciences of the United States of America 88(24): 11281-11284.

Huang TY, DerMardirossian C, Bokoch GM (2006) Cofilin phosphatases and regulation of actin dynamics. Current Opinion in Cell Biology 18(1): 26-31.

Hussey PJ, Yuan M, Calder G, Khan S, Lloyd CW (1998) Microinjection of

pollen-specific actin-depolymerizing factor, ZmADF 1, reorientates F-actin strands in Tradescantia stamen hair cells. The Plant Journal 14(3): 353-357.

Iida K, Yahara I (1999) Cooperation of two actin-binding proteins, cofilin and Aip1, in *Saccharomyces cerevisiae*. Genes Cells 4: 21-32.

Jackson SL, Heath IB (1990) Evidence that actin reinforces the extensible hyphal apex of the oomycete *Saprolegnia ferax*. Protoplasma 157(1): 144-153.

Jackson SL, Heath IB (1993) UV microirradiation implicates F-actin in reinforcing growing hyphal tips. Protoplasma 175(1): 67-74.

Jennings DH, Burke RM (1990) Compatible solutes-the mycological dimension andtheir role as physiological buffering agents. New Phytology 116: 277-283.

Jennings DH (1995) The Physiology of Fungal Nutrition: Cambridge University Press.

Jiang CJ, Weeds AG, Hussey PJ (1997a) The maize actin-depolymerizing factor, ZmADF 3, redistributes to the growing tip of elongating root hairs and can be induced to translocate into the nucleus with actin. The Plant Journal 12(5): 1035-1043.

Jiang CJ, Weeds AG, Khan S, Hussey PJ (1997b) F-actin and G-actin binding are uncoupled by mutation of conserved tyrosine residues in maize actin depolymerizing factor (*ZmADF*). Proceedings of the National Academy of Sciences of the United States of America 94(18): 9973.

Kalendar R (2004) FastPCR, PCR primer design, DNA and protein tools, repeats and own database searches program. URL http://www biocenter helsinki fi/bi/bare-1_html/fastpcr htm.

Kaminskyj SGW, Garrill A, Heath IB (1992) The relation between turgor and tip growth in *Saprolegnia ferax*: Turgor is necessary, but not sufficient to explain apical extension rates. Experimental Mycology 16(1): 64-75.

Kaminskyj SGW, Heath IB (1996) Studies on Saprolegnia ferax suggest the general importance of the cytoplasm in determining hyphal morphology. Mycologia

88(1): 20-37.

Kaminskyj SGW, Hamer JE (1998) hyp Loci Control Cell Pattern Formation in the Vegetative Mycelium of Aspergillus nidulans. Genetics 148(2): 669-680.

Kovar DR, Pollard TD (2004) Insertional assembly of actin filament barbed ends in association with formins produces piconewton forces. Proceedings of the National Academy of Sciences of the United States of America 101(41): 14725-14730.

Kovar DR, Harris ES, Mahaffy R, Higgs HN, Pollard TD (2006) Control of the Assembly of ATP- and ADP-Actin by Formins and Profilin. Cell 124(2): 423-435.

Kovar DR (2006a) Cell Polarity: Formin on the Move. Current Biology 16(14): R535-R538.

Kumar KS, Dayananda S, Subramanyam C (2005) Copper alone, but not oxidative stress, induces copper-metallothionein gene in *Neurospora crassa*. FEMS Microbiology Letters 242(1): 45-50.

Kwon YH, Hoch HC, Staples RC (1991) Cytoskeletal organization in Uromyces urediospore germling apices during appressorium formation. Protoplasma 165(1): 37-50.

Lappalainen P, Drubin DG (1997) Cofilin promotes rapid actin filament turnover in vivo. Nature 389(6637): 78-82.

Lee JY, Yoo BC, Harmon AC (1998) Kinetic and calcium-binding properties of three calcium-dependent protein kinase isoenzymes from soybean. Biochemistry 37(19): 6801-6809.

Legerton TL, Kanamori K, Weiss RL, Roberts JD (1983) Measurements of cytoplasmic and vacuolar pH in Neurospora using nitrogen-15 nuclear magnetic resonance spectroscopy. Biochemistry 22(4): 899-903.

Levina NN, Lew RR (2006) The role of tip-localized mitochondria in hyphal growth. Fungal Genetics and Biology 43(2): 65-74.

Lew RR, Garrill A, Covic L, Heath IB, Serlin BS (1992) Novel ion channels in the protists, Mougeotia and Saprolegnia, using sub-gigaseals. FEBS Letters 310(3): 219-222.

Lew RR (1998) Mapping Fungal Ion Channel Locations. Fungal Genetics and Biology 24(1-2): 69-76.

Lew RR, Levina NN, Walker SK, Garrill A (2004) Turgor regulation in hyphal organisms. Fungal Genetics and Biology 41(11): 1007-1015.

Lew RR (2007) Ionic currents and ion fluxes in *Neurospora crassa* hyphae. Journal of Experimental Botany 58(12): 3475.

Li Y, Uruno T, Haudenschild C, Dudek SM., Garcia JGN, Zhan X (2004) Interaction of cortactin and Arp2/3 complex is required for sphingosine-1-phosphate-induced endothelial cell remodeling. Experimental Cell Research 298(1): 107-121.

Lopez I, Anthony RG, Maciver SK, Jiang CJ, Khan S, Weeds AG, Hussey PJ (1996) Pollen specific expression of maize genes encoding actin depolymerizing factor-like proteins. Proceedings of the National Academy of Sciences of the United States of America 93(1): 7415-7420.

Lopez-Franco R, Bartnicki-Garcia S, Bracker CE (1994) Pulsed Growth of Fungal Hyphal Tips. Proceedings of the National Academy of Sciences of the United States of America 91(25): 12228-12232.

Löpez-Franco R, Bracker CE (1996) Diversity and dynamics of the Spitzenkoper in growing hyphal tips of higher fungi. Protoplasma 195(1): 90-111.

Lovy-Wheeler A, Wilsen KL, Baskin TI, Hepler PK (2005) Enhanced fixation reveals the apical cortical fringe of actin filaments as a consistent feature of the pollen tube. Planta 221(1): 95-104.

Lu J, Meng W, Poy F, Maiti S, Goode BL, Eck MJ (2007) Structure of the FH2 Domain of Daam1: Implications for Formin Regulation of Actin Assembly. Journal of Molecular Biology 369(5): 1258-1269.

Ma H, Snook LA, Tian C, Kaminskyj SGW, Dahms TES (2006) Fungal surface remodelling visualized by atomic force microscopy. Mycological Research 110(8): 879-886.

MacDonald E, Millward L, Ravishankar JP, Money NP (2002) Biomechanical interaction between hyphae of two Pythium species (Oomycota) and host tissues. Fungal Genetics and Biology 37(3): 245-249.

Machesky LM (1994) Purification of a cortical complex containing two unconventional actins from Acanthamoeba by affinity chromatography on profilin-agarose. The Journal of Cell Biology 127(1): 107-115.

Maciver SK, Weeds AG (1994) Actophorin preferentially binds monomeric ADP-actin over ATP-bound actin: consequences for cell locomotion. FEBS Letters 347(2-3): 251-256.

Martin SG, Chang F (2006) Dynamics of the Formin For3p in Actin Cable Assembly. Current Biology 16(12): 1161-1170.

McDaniel DP, Roberson RW (1998) γ-Tubulin is a component of the Spitzenkorper and centrosomes in hyphal-tip cells of Allomyces macrogynus. Protoplasma 203(1): 118-123.

McDaniel DP, Roberson RW (2000) Microtubules Are Required for Motility and Positioning of Vesicles and Mitochondria in Hyphal Tip Cells of *Allomyces macrogynus*. Fungal Genetics and Biology 31(3): 233-244.

McGough A, Chiu W (1999) ADF/Cofilin weakens lateral contacts in the actin filament. Journal of Molecular Biology 291(3): 513-519.

Miller DD, Lancelle SA, Hepler PK (1996) Actin microfilaments do not form a dense meshwork in Lilium longiflorum pollen tube tips. Protoplasma 195(1): 123-132.

Mogilner A, Oster G (2003a) Force Generation by Actin Polymerization II: The Elastic Ratchet and Tethered Filaments. Biophysical Journal 84(3): 1591-1605.

Mogilner A, Oster G (2003b) Polymer Motors: Pushing out the Front and Pulling up the Back. Current Biology 13(18): 721-733.

Money NP (1990) Measurement of hyphal turgor. Experimental Mycology 14(4): 416-425.

Money NP, Harold FM (1992) Extension Growth of the Water Mold *Achlya*: Interplay of Turgor and Wall Strength. Proceedings of the National Academy of Sciences of the United States of America 89(10): 4245-4249.

Money NP, Harold FM (1993) Two water molds can grow without measurable turgor pressure. Planta 190(3): 426-430.

Money NP (1994) Osmotic adjustment and the role of turgor in mycelial fungi. The Mycota 1: 67–88.

Money NP, Howard RJ (1996) Confirmation of a Link between Fungal Pigmentation, Turgor Pressure, and Pathogenicity Using a New Method of Turgor Measurement. Fungal Genetics and Biology 20(3): 217-227.

Money NP (1997) Wishful Thinking of Turgor Revisited: The Mechanics of Fungal Growth. Fungal Genetics and Biology 21(2): 173-187.

Money NP, Hill TW (1997) Correlation between endoglucanase secretion and cell wall strength in oomycete hyphae: implications for growth and morphogenesis. Mycologia 89(5): 777-785.

Money NP (1999a) To Perforate a Leaf of Grass. Fungal Genetics and Biology 28(3): 146-147.

Money NP (1999b) Biophysics: Fungus punches its way in. Nature 401(6751): 332-333.

Money NP (1999c) On the origin and functions of hyphal walls and turgor pressure. Mycological Research 103(10): 1360-1360.

Money NP (2001) Functions and Evolutionary Origin of Hyphal Turgor Pressure;

Geitmann A, Cresti M, Heath IB, editors: IOS Press. pp.161-170

Money NP, Davis CM, Ravishankar JP (2004) Biomechanical evidence for convergent evolution of the invasive growth process among fungi and oomycete water molds. Fungal Genetics and Biology 41(9): 872-876.

Moon AL (1993) Cofilin is an essential component of the yeast cortical cytoskeleton. The Journal of Cell Biology 120(2): 421-435.

Mourino-Perez RR, Roberson RW, Bartnicki-Garcia S (2006) Microtubule dynamics and organization during hyphal growth and branching in *Neurospora crassa*. Fungal Genetics and Biology 43(6): 389-400.

Mullins RD (2000) How WASP-family proteins and the Arp2/3 complex convert intracellular signals into cytoskeletal structures. Current Opinion in Cell Biology 12(1): 91-96.

Nishida E, Maekawa S, Sakai H (1984) Cofilin, a protein in porcine brain that binds to actin filaments and inhibits their interactions with myosin and tropomyosin. Biochemistry 23(22): 5307-5313.

Oh KB, Nishiyama T, Sakai E, Matsuoka H, Kurata H (1997) Flow sensing in mycelial fungi. Journal of Biotechnology 58(3): 197-204.

Ojala PJ, Paavilainen V, Lappalainen P (2001) Identification of yeast cofilin residues specific for actin monomer and PIP2 binding. Biochemistry 40(51): 15562-15569.

Paavilainen VO, Bertling E, Falck S, Lappalainen P (2004) Regulation of cytoskeletal dynamics by actin-monomer-binding proteins. Trends in Cell Biology 14(7): 386-394.

Pantaloni D, Clainche CL, Carlier MF (2001) Mechanism of Actin-Based Motility. Science 292(5521): 1502-1506.

Parton RM (1997) Pronounced cytoplasmic pH gradients are not required for tip growth in plant and fungal cells. Journal of Cell Science 110(10): 1187-1198.

Parton RM, Fischer-Parton S, Watahiki MK, Trewavas AJ (2001) Dynamics of the apical vesicle accumulation and the rate of growth are related in individual pollen tubes. Journal of Cell Science 114(14): 2685-2695.

Pernodet N, Maaloum M, Tinland B (1997) Pore size of agarose gels by atomic force microscopy. Electrophoresis 18(1): 55-58.

Picton JM, Steer MW (1982) A model for the mechanism of tip extension in pollen tubes. Journal of Theoretical Biology 98(1): 15-20.

Pierson ES (1988) Rhodamine-phalloidin staining of F-actin in pollen after dimethylsulphoxide permeabilization. Sexual Plant Reproduction 1(2): 83-87.

Pollard TD, Cooper JA (1986) Actin and Actin-Binding Proteins. A Critical Evaluation of Mechanisms and Functions. Annual Review of Biochemistry 55(1): 987-1035.

Pollard TD (2002) Formins initiate new actin filaments. Nature Cell Biology 4(8):626-631.

Pollard TD, Borisy GG (2003) Cellular Motility Driven by Assembly and Disassembly of Actin Filaments. Cell 112(4): 453-465.

Prehoda KE, Scott JA, Mullins RD, Lim WA (2000) Integration of Multiple Signals Through Cooperative Regulation of the N-WASP-Arp2/3 Complex. pp. 801-806.

Pruyne D, Evangelista M, Yang C, Bi E, Zigmond S, Bretscher A, Boone C (2002) Role of Formins in Actin Assembly: Nucleation and Barbed-End Association. Science 297(5581): 612-615.

Ravishankar JP, Davis CM, Davis DJ, MacDonald E, Makselan SD, Millward L, Money NP (2001) Mechanics of Solid Tissue Invasion by the Mammalian Pathogen Pythium insidiosum. Fungal Genetics and Biology 34(3): 167-175.

Read ND, Kalkman ER (2003) Does endocytosis occur in fungal hyphae? Fungal Genetics and Biology 39(3): 199-203.

Riquelme M, Reynaga-Pena CG, Gierz G, Bartnicki-Garcia S (1998) What Determines Growth Direction in Fungal Hyphae? Fungal Genetics and Biology 24(1-2): 101-109.

Riquelme M, Bartnicki-Garcia S (2004) Key differences between lateral and apical branching in hyphae of *Neurospora crassa.* Fungal Genetics and Biology 41(9): 842-851.

Roberson RW (1992) The actin cytoskeleton in hyphal cells of Sclerotium rolfsii. Mycologia 84(1): 41-51.

Roberson RW, Vargas MM (1994) The tubulin cytoskeleton and its sites of nucleation in hyphal tips of Allomyces macrogynus. Protoplasma 182(1): 19-31.

Robertson NF, Rizvi SRH (1968) Some observations on the water-relations of the hyphae of *Neurospora crassa*. Annals of Botany 32: 279-291.

Robinson RC, Turbedsky K, Kaiser DA, Marchand JB, Higgs HN, Choe S, Pollard TD (2001) Crystal Structure of Arp2/3 Complex. Science 294(5547): 1679.

Robson GD, Prebble E, Rickers A, Hosking S, Denning DW, Trinci APJ, Robertson W (1996) Polarized Growth of Fungal Hyphae Is Defined by an Alkaline pH Gradient. Fungal Genetics and Biology 20(4): 289-298.

Romero S, Le Clainche C, Didry D, Egile C, Pantaloni D, Carlier M-F (2004) Formin Is a Processive Motor that Requires Profilin to Accelerate Actin Assembly and Associated ATP Hydrolysis. Cell 119(3): 419-429.

Roos UP, Turian G (1977) Hyphal tip organization inAllomyces arbuscula. Protoplasma 93(2): 231-247.

Sagot I, Rodal AA, Moseley J, Goode BL, Pellman D (2002a) An actin nucleation mechanism mediated by Bni1 and profilin. Nature Cell Biology 4(8): 626-631.

Sagot I, Klee SK, Pellman D (2002b) Yeast formins regulate cell polarity by controlling the assembly of actin cables. Nature Cell Biology 4(1): 42-50.

Schafer DA, Welch MD, Machesky LM, Bridgman PC, Meyer SM, Cooper JA (1998) Visualization and Molecular Analysis of Actin Assembly in Living Cells. The Journal of Cell Biology 143(7): 1919-1930.

Schmitz HP, Kaufmann A, Kohli M, Laissue PP, Philippsen P (2006) From Function to Shape: A Novel Role of a Formin in Morphogenesis of the Fungus *Ashbya gossypii*. Molecular Biology of the Cell 17(1): 130-145.

Shabala SN, Lew RR (2002) Turgor Regulation in Osmotically Stressed *Arabidopsis* Epidermal Root Cells. Direct Support for the Role of Inorganic Ion Uptake as Revealed by Concurrent Flux and Cell Turgor Measurements. Plant Physiology 129(1): 290.

Silverman-Gavrila LB, Lew RR (2001) Regulation of the tip-high [Ca2+] gradient in growing hyphae of the fungus *Neurospora crassa*. European Journal of Cell Biology 80(6): 379-390.

Sone T, Griffiths AJF (1999) The frost Gene of Neurospora crassa Is a Homolog of Yeast cdc1 and Affects Hyphal Branching via Manganese Homeostasis. Fungal Genetics and Biology 28(3): 227-237.

Steer MW, Heath IB (1990) Tip Growth in Plant and Fungal Cells: Academic Press San Diego, California.

Steinberg G (1998) Organelle Transport and Molecular Motors in Fungi. Fungal Genetics and Biology 24(1-2): 161-177.

Steinberg G (2007) Hyphal Growth: a Tale of Motors, Lipids, and the Spitzenkorper. Eukaryotic Cell 6(3): 351-360.

Suei S, Garrill A (2008) An F-actin-depleted zone is present at the hyphal tip of invasive hyphae of *Neurospora crassa* Protoplasma 232: 165-172.

Suelmann R, Fischer R (2000) Nuclear migration in fungi-different motors at work. Research in Microbiology 151(4): 247-254.

Sun Y, Han Y, Zhao JF, Bai J, Hao MP, Sun DY (2000) The effect of integrin-like

proteins on pollen germiantion and tube growth of Nicotiana tabacum. Shi Yan Sheng Wu Xue Bao 33(3): 255-62.

Svitkina TM, Borisy GG (1999) Arp2/3 Complex and Actin Depolymerizing Factor/Cofilin in Dendritic Organization and Treadmilling of Actin Filament Array in Lamellipodia. The Rockefeller University Press. pp. 1009-1026.

Svitkina T (2006) Structural organization and dynamics of the cytoskeletal network. American Physical Society, APS March Meeting, March 13-17, 2006, abstract# R1 001.

Tanaka K (2000) Formin Family Proteins in Cytoskeletal Control. Biochemical and Biophysical Research Communications 267(2): 479-481.

Thellin O, Zorzi W, Lakaye B, De Borman B, Coumans B et al. (1999) Housekeeping genes as internal standards: use and limits. Journal of Biotechnology 75(2-3): 291-295.

Tokuraku K, Okamoto S, Katsuki M, Nakagawa H, Kotani S (2001) The actin-depolymerizing factor destrin has an actin-stabilizing domain. Biochemistry and Cell Biology 79(6): 773-778.

Torralba S, Raudaskoski M, Pedregosa AM, Laborda F (1998) Effect of cytochalasin A on apical growth, actin cytoskeleton organization and enzyme secretion in Aspergillus nidulans. Microbiology 144(1): 45-53.

Torralba S, Heath IB, Ottensmeyer FP (2001) Ca2+ Shuttling in Vesicles During Tip Growth in *Neurospora crassa*. Fungal Genetics and Biology 33(3): 181-193.

Torralba S, Heath IB (2001) Cytoskeletal and Ca2+ regulation of hyphal tip growth and initiation. Current Topics in Developmental Biology: Academic Press. pp. 135-187.

Torralba S, Heath IB (2002) Analysis of three separate probes suggests the absence of endocytosis in *Neurospora crassa* hyphae. Fungal Genetics and Biology 37(3): 221-232.

Trewavas A (1999) Le calcium, c'est la vie: calcium makes waves. Plant Physiology 120(1): 1-6.

Upadhyay, S., and Shaw, B. D. (2008) The role of actin, fimbrin and endocytosis in growth of hyphae in *Aspergillus nidulans*. Molecular Microbiology 68(3): 690-705.

van der Honing HS, Emons AMC, Ketelaar T (2007) Actin based processes that could determine the cytoplasmic architecture of plant cells. BBA-Molecular Cell Research 1773(5): 604-614.

Vavylonis D, Kovar DR, O'Shaughnessy B, Pollard TD (2006) Model of Formin-Associated Actin Filament Elongation. Molecular Cell 21(4): 455-466.

Vidali L, Hepler PK (2001) Actin and pollen tube growth. Protoplasma 215(1): 64-76.

Virag A, Griffiths AJF (2004) A mutation in the *Neurospora crassa* actin gene results in multiple defects in tip growth and branching. Fungal Genetics and Biology 41(2): 213-225.

Vogel HJ (1956) A convenient growth medium for *Neurospora* (Medium N). . Microbiological Genetic Bulletin 13: 42-43.

Vogel HJ (1964) Distribution of Lysine Pathways Among Fungi: Evolutionary Implications. The American Naturalist 98(903): 435-446.

Volkmann N, Amann KJ, Stoilova-McPhie S, Egile C, Winter DC, Hazelwood L, Heuser JE, Li R, Pollard TD, Hanein D (2001) Structure of Arp2/3 Complex in Its Activated State and in Actin Filament Branch Junctions. Science 293(5539): 2456-2459.

Vorobiev S, Strokopytov B, Drubin DG, Frieden C, Ono S, Condeelis J, Rubenstein PA, Almo SC (2003) The structure of nonvertebrate actin: Implications for the ATP hydrolytic mechanism. Proceedings of the National Academy of Sciences of the United States of America 100(10): 5760-5765.

Walker SK, Chicholtan K, Suei S, Garrill A (2006) Do F-actin Rearrangements Accompany Invasive Tip Growth? In: Meyer W, Pearce C, editors. 8th International Mycological Congress: Medimond - International Proceedings. pp. 279-284.

Walker SK, Chitcholtan K, Yu Y, Christenhusz GM, Garrill A (2006) Invasive hyphal growth: An F-actin depleted zone is associated with invasive hyphae of the oomycetes *Achlya bisexualis* and *Phytophthora cinnamomi*. Fungal Genetics and Biology 43(5): 357-365.

Walker SK, Garrill A (2006) Actin microfilaments in fungi. Mycologist 20(1): 26-31.

Watanabe N, Higashida C (2004) Formins: processive cappers of growing actin filaments. Experimental Cell Research 301(1): 16-22.

Wear MA, Schafer DA, Cooper JA (2000) Actin dynamics: Assembly and disassembly of actin networks. Current Biology 10(24): 891-895.

Welch MD, Rosenblatt J, Skoble J, Portnoy DA, Mitchison TJ (1998) Interaction of Human Arp2/3 Complex and the *Listeria monocytogenes* ActA Protein in Actin Filament Nucleation. Science 281(5373): 105.

Wendland J, Ayad-Durieux Y, Knechtle P, Rebischung C, Philippsen P (2000) PCR-based gene targeting in the filamentous fungus *Ashbya gossypii*. Gene 242(1-2): 381-391.

Wendland J (2001) Comparison of Morphogenetic Networks of Filamentous Fungi and Yeast. Fungal Genetics and Biology 34(2): 63-82.

Wessels JGH (1993) Tansley Review No. 45 Wall growth, protein excretion and morphogenesis in fungi. New Phytologist 123(3): 397-413.

Wilsen KL, Lovy-Wheeler A, Voigt B, Menzel D, Kunkel JG et al. (2006) Imaging the actin cytoskeleton in growing pollen tubes. Sexual Plant Reproduction 19(2): 51-62.

Winder SJ (2003) Structural insights into actin-binding, branching and bundling

proteins. Current Opinion in Cell Biology 15(1): 14-22.

Xiang X, Morris NR (1999) Hyphal tip growth and nuclear migration. Current Opinion in Microbiology 2(6): 636-640.

Xu Y, Moseley JB, Sagot I, Poy F, Pellman D, Goode BL, Eck MJ (2004) Crystal Structures of a Formin Homology-2 Domain Reveal a Tethered Dimer Architecture. Cell 116: 711-723.

Yonezawa N, Nishida E, Sakai H (1985) pH control of actin polymerization by cofilin. Journal of Biological Chemistry 260(27): 14410-14412.

Yu YP, Jackson SL, Garrill A (2004) Two Distinct Distributions of F-actin are Present in the Hyphal Apex of the Oomycete *Achlya bisexualis*. Plant and Cell Physiology 45(3): 275-280.

Zigmond SH (2004) Formin-induced nucleation of actin filaments. Current Opinion in Cell Biology 16(1): 99-105.

Appendices

Appendix 1.1: Actin sequence homology among organisms

1. *N. crassa* vs. *A. nidulans*

Sequence 1: *N. crassa* [Length = 375 aa]

Sequence 2: *A. nidulans* [Length = 376 aa]

Score = 747 bits (1928), Expect = 0.0

Identities = 370/373 (99%), Positives = 373/373 (100%), Gaps = 0/373 (0%)

```
Query  3    EEVAALVIDNGSGMCKAGFAGDDAPRAVFPSIVGRPRHHGIMIGMGQKDSYVGDEAQSKR  62

            EEVAALVIDNGSGMCKAGFAGDDAPRAVFPSIVGRPRHHGIMIGMGQKDSYVGDEAQSKR

Sbjct  4    EEVAALVIDNGSGMCKAGFAGDDAPRAVFPSIVGRPRHHGIMIGMGQKDSYVGDEAQSKR  63


Query  63   GILTLRYPIEHGVVTNWDDMEKIWHHTFYNELRVAPEEHPVLLTEAPINPKSNREKMTQI  122

            GILTLRYPIEHGVVTNWDDMEKIWHHTFYNELRVAPEEHPVLLTEAPINPKSNREKMTQI

Sbjct  64   GILTLRYPIEHGVVTNWDDMEKIWHHTFYNELRVAPEEHPVLLTEAPINPKSNREKMTQI  123
```

```
Query  123  VFETFNAPAFYVSIQAVLSLYASGRTTGIVLDSGDGVTHVVPIYEGFALPHAIARVDMAG  182
            VFETFNAPAFYVSIQAVLSLYASGRTTGIVLDSGDGVTHVVPIYEGFALPHAI+RVDMAG
Sbjct  124  VFETFNAPAFYVSIQAVLSLYASGRTTGIVLDSGDGVTHVVPIYEGFALPHAISRVDMAG  183

Query  183  RDLTDYLMKILAERGYTFSTTAEREIVRDIKEKLCYVALDFEQEIQTAAQSSSLEKSYEL  242
            RDLTDYLMKILAERGYTFSTTAEREIVRDIKEKLCYVALDFEQEIQTA+QSSSLEKSYEL
Sbjct  184  RDLTDYLMKILAERGYTFSTTAEREIVRDIKEKLCYVALDFEQEIQTASQSSSLEKSYEL  243

Query  243  PDGQVITIGNERFRAPEALFQPSVLGLESGGIHVTTFNSIMKCDVDVRKDLYGNIVMSGG  302
            PDGQVITIGNERFRAPEALFQPSVLGLESGGIHVTTFNSIMKCDVDVRKDLYGNIVMSGG
Sbjct  244  PDGQVITIGNERFRAPEALFQPSVLGLESGGIHVTTFNSIMKCDVDVRKDLYGNIVMSGG  303

Query  303  TTMYPGLSDRMQKEITALAPSSMKVKIIAPPERKYSVWIGGSILASLSTFQQMWISKQEY  362
            TTMYPG+SDRMQKEITALAPSSMKVKIIAPPERKYSVWIGGSILASLSTFQQMWISKQEY
Sbjct  304  TTMYPGISDRMQKEITALAPSSMKVKIIAPPERKYSVWIGGSILASLSTFQQMWISKQEY  363

Query  363  DESGPSIVHRKCF  375
            DESGPSIVHRKCF
Sbjct  364  DESGPSIVHRKCF  376
```

2. *N. crassa* vs. *A. bisexualis*

Sequence 1: *N. crassa* [Length = 375 aa]

Sequence 2: *A. bisexualis* [Length = 376 aa]

Score = 659 bits (1699), Expect = 0.0

Identities = 308/374 (82%), Positives = 351/374 (93%), Gaps = 0/374 (0%)

```
Query  2    EEEVAALVIDNGSGMCKAGFAGDDAPRAVFPSIVGRPRHHGIMIGMGQKDSYVGDEAQSK  61
            +++V ALV+DNGSGMCKAGFAGDDAPRAVFPSIVGRP+H GIM+GM QKD+YVGDEAQSK
Sbjct  3    DDDVQALVVDNGSGMCKAGFAGDDAPRAVFPSIVGRPKHPGIMVGMDQKDAYVGDEAQSK  62

Query  62   RGILTLRYPIEHGVVTNWDDMEKIWHHTFYNELRVAPEEHPVLLTEAPINPKSNREKMTQ  121
            RG+LTL+YPIEHG+VTNWDDMEKIWHHTFYNELRVAPEEHPVLLTEAP+NPK+NRE+MTQ
Sbjct  63   RGVLTLKYPIEHGIVTNWDDMEKIWHHTFYNELRVAPEEHPVLLTEAPLNPKANRERMTQ  122

Query  122  IVFETFNAPAFYVSIQAVLSLYASGRTTGIVLDSGDGVTHVVPIYEGFALPHAIARVDMA  181
            I+FETFN PA YV+IQAVLSLYASGRTTG VLDSGDGV+H VPIYEG+ALPHAI R+D+A
Sbjct  123  IMFETFNVPAMYVNIQAVLSLYASGRTTGCVLDSGDGVSHTVPIYEGYALPHAIVRLDLA  182

Query  182  GRDLTDYLMKILAERGYTFSTTAEREIVRDIKEKLCYVALDFEQEIQTAAQSSSLEKSYE  241
```

```
            GRDLTDY+MKIL ERGY+F+TTAEREIVRDIKEKL Y+ALDF+QE++TAA+SS LEKSYE

Sbjct  183  GRDLTDYMMKILTERGYSFTTTAEREIVRDIKEKLTYIALDFDQEMKTAAESSGLEKSYE  242


Query  242  LPDGQVITIGNERFRAPEALFQPSVLGLESGGIHVTTFNSIMKCDVDVRKDLYGNIVMSG  301

            LPDG V+ IGNERFR PE LFQP+++G E+ GIH  TF +IMKCDVD+RKDLY NIV+SG

Sbjct  243  LPDGNVLVIGNERFRTPEVLFQPALIGKEASGIHDCTFQTIMKCDVDIRKDLYCNIVLSG  302


Query  302  GTTMYPGLSDRMQKEITALAPSSMKVKIIAPPERKYSVWIGGSILASLSTFQQMWISKQE  361

            GTTMYPG+S+RM KE+TALAPS+MK+K++APPERKYSVWIGGSIL+SLSTFQQMWISK E

Sbjct  303  GTTMYPGISERMTKELTALAPSTMKIKVVAPPERKYSVWIGGSILSSLSTFQQMWISKAE  362


Query  362  YDESGPSIVHRKCF  375

            YDESGPSIVHRKCF

Sbjct  363  YDESGPSIVHRKCF  376
```

3. *N. crassa* vs. *S. cerevisiae*

Sequence 1: *N. crassa* [Length = 375 aa]

Sequence 2: *S. cerevisiae* [Length = 299 aa]

Score = 559 bits (1440), Expect = 2e-157

Identities = 272/299 (90%), Positives = 290/299 (96%), Gaps = 0/299 (0%)

```
Query  43   IMIGMGQKDSYVGDEAQSKRGILTLRYPIEHGVVTNWDDMEKIWHHTFYNELRVAPEEHP  102
            IM+GMGQKDSYVGDEAQSKRGILTLRYPIEHG+VTNWDDMEKIWHHTFYNELRVAPEEHP
Sbjct  1    IMVGMGQKDSYVGDEAQSKRGILTLRYPIEHGIVTNWDDMEKIWHHTFYNELRVAPEEHP  60

Query  103  VLLTEAPINPKSNREKMTQIVFETFNAPAFYVSIQAVLSLYASGRTTGIVLDSGDGVTHV  162
            VLLTEAP+NPKSNREKMTQI+FETFN PAFYVSIQAVLSLY+SGRTTGIVLDSGDGVTHV
Sbjct  61   VLLTEAPMNPKSNREKMTQIMFETFNVPAFYVSIQAVLSLYSSGRTTGIVLDSGDGVTHV  120

Query  163  VPIYEGFALPHAIARVDMAGRDLTDYLMKILAERGYTFSTTAEREIVRDIKEKLCYVALD  222
            VPIY GF+LPHAI R+D+AGRDLTDYLMKIL+ERGY+FSTTAEREIVRDIKEKLCYVALD
Sbjct  121  VPIYAGFSLPHAILRIDLAGRDLTDYLMKILSERGYSFSTTAEREIVRDIKEKLCYVALD  180

Query  223  FEQEIQTAAQSSSLEKSYELPDGQVITIGNERFRAPEALFQPSVLGLESGGIHVTTFNSI  282
            FEQE+QTAAQSSS+EKSYELPDGQVITIGNERFRAPEALF PSVLGLES GI  TT+NSI
```

```
Sbjct  181  FEQEMQTAAQSSSIEKSYELPDGQVITIGNERFRAPEALFHPSVLGLESAGIDQTTYNSI  240


Query  283  MKCDVDVRKDLYGNIVMSGGTTMYPGLSDRMQKEITALAPSSMKVKIIAPPERKYSVWI  341

             MKC  DVRK+LYGNIVMSGGTTM+PG+++RMQKEITALAPSSMKVKIIAPPERKYSVWI

Sbjct  241  MKCXXDVRKELYGNIVMSGGTTMFPGIAERMQKEITALAPSSMKVKIIAPPERKYSVWI  299
```

4. *N. crassa* vs. skeletal muscle alpha-actin of *Homo sapiens*

Sequence 1: *N. crassa* [Length = 375 aa]

Sequence 2: *Homo sapiens* [Length = 377 aa]

Score = 681 bits (1756), Expect = 0.0

Identities = 325/374 (86%), Positives = 352/374 (94%), Gaps = 0/374 (0%)

```
Query  2    EEEVAALVIDNGSGMCKAGFAGDDAPRAVFPSIVGRPRHHGIMIGMGQKDSYVGDEAQSK  61

            E+E  ALV DNGSG+ KAGFAGDDAPRAVFPSIVGRPRH G+M+GMGQKDSYVGDEAQSK

Sbjct  4    EDETTALVCDNGSGLVKAGFAGDDAPRAVFPSIVGRPRHQGVMVGMGQKDSYVGDEAQSK  63


Query  62   RGILTLRYPIEHGVVTNWDDMEKIWHHTFYNELRVAPEEHPVLLTEAPINPKSNREKMTQ  121

            RGILTL+YPIEHG++TNWDDMEKIWHHTFYNELRVAPEEHP LLTEAP+NPK+NREKMTQ

Sbjct  64   RGILTLKYPIEHGIITNWDDMEKIWHHTFYNELRVAPEEHPTLLTEAPLNPKANREKMTQ  123


Query  122  IVFETFNAPAFYVSIQAVLSLYASGRTTGIVLDSGDGVTHVVPIYEGFALPHAIARVDMA  181

            I+FETFN PA YV+IQAVLSLYASGRTTGIVLDSGDGVTH VPIYEG+ALPHAI R+D+A

Sbjct  124  IMFETFNVPAMYVAIQAVLSLYASGRTTGIVLDSGDGVTHNVPIYEGYALPHAIMRLDLA  183


Query  182  GRDLTDYLMKILAERGYTFSTTAEREIVRDIKEKLCYVALDFEQEIQTAAQSSSLEKSYE  241

            GRDLTDYLMKIL ERGY+F TTAEREIVRDIKEKLCYVALDFE E+ TAA SSSLEKSYE
```

```
Sbjct  184  GRDLTDYLMKILTERGYSFVTTAEREIVRDIKEKLCYVALDFENEMATAASSSSLEKSYE  243


Query  242  LPDGQVITIGNERFRAPEALFQPSVLGLESGGIHVTTFNSIMKCDVDVRKDLYGNIVMSG  301

            LPDGQVITIGNERFR PE LFQPS +G+ES GIH TT+NSIMKCD+D+RKDLY N VMSG

Sbjct  244  LPDGQVITIGNERFRCPETLFQPSFIGMESAGIHETTYNSIMKCDIDIRKDLYANNVMSG  303


Query  302  GTTMYPGLSDRMQKEITALAPSSMKVKIIAPPERKYSVWIGGSILASLSTFQQMWISKQE  361

            GTTMYPG++DRMQKEITALAPS+MK+KIIAPPERKYSVWIGGSILASLSTFQQMWI+KQE

Sbjct  304  GTTMYPGIADRMQKEITALAPSTMKIKIIAPPERKYSVWIGGSILASLSTFQQMWITKQE  363


Query  362  YDESGPSIVHRKCF  375

            YDE+GPSIVHRKCF

Sbjct  364  YDEAGPSIVHRKCF  377
```

Appendix 1.2: Cofilin sequence homology among organisms

1. N. crassa vs. *A. nidulans*

Sequence 1: *N. crassa* [Length = 154]

Sequence 2: *A. nidulas* [Length = 161]

Score = 105 bits (263), Expect = 1e-21
Identities = 63/163 (38%), Positives = 97/163 (59%), Gaps = 20/163 (12%)

```
Query  4    SGVQVDPECRRAFDKLM------SRQLRYIIYKLSDDFKEIVIESTSEGATENYDEFREK  57
            SGVQV  EC  AF+ L          + ++II+K+SDD K++V++ TS+    +Y+ F  K
Sbjct  5    SGVQVQDECITAFNNLRMTGGQKGSKPKFIIFKISDDKKQVVVDETSDDP--DYETFLNK  62

Query  58   LVNAQTKSASGAISKGPRYAVYDFEYKLASGEGSRNKVTFIAWSPDDAGIKS-------K  110
            L +A  K A+G     PRYAVYD EY L  GEG+R+K+ FI+W P    I +
Sbjct  63   LGDA--KDANG--KPAPRYAVYDVEYDLGGGEGTRSKIIFISWVPSGTSINAAHKEQQWS  118

Query  111  MVYASSKEALKRSLSGIAVELQANEQDDIEYEQIIKTVSKGTA  153
            M+YAS++E LK +L+ +   + A+++ D+ ++ I+  VS G A
Sbjct  119  MIYASTREVLKNALN-VVTSIHADDKGDLAWKSILAEVSGGKA  160
```

2. N. crassa vs. *S. cerevisiae*

Sequence 1: *N. crassa* [Length = 154]

Sequence 2: *S. cerevisiae* [Length = 143]

Score = 116 bits (290), Expect = 7e-25
Identities = 60/155 (38%), Positives = 97/155 (62%), Gaps = 14/155 (9%)

```
Query  1    MSQSGVQVDPECRRAFDKL-MSRQLRYIIYKLSDDFKEIVIESTSEGATENYDEFREKLV  59
            MS+SGV V  E   AF+ L + ++ ++I++ L+D  EIV++ TS     +YD F EKL
Sbjct  1    MSRSGVAVADESLTAFNDLKLGKKYKFILFGLNDAKTEIVVKETS--TDPSYDAFLEKLP  58

Query  60   NAQTKSASGAISKGPRYAVYDFEYKLASGEGSRNKVTFIAWSPDDAGIKSKMVYASSKEA  119
                          YA+YDFEY++   EG R+K+ F  WSPD A ++SKMVYASSK+A
Sbjct  59   ENDCL----------YAIYDFEYEINGNEGKRSKIVFFTWSPDTAPVRSKMVYASSKDA  107

Query  120  LKRSLSGIAVELQANEQDDIEYEQIIKTVSKGTAA  154
            L+R+L+G++ ++Q  +  ++ Y+ +++ VS+G  +
Sbjct  108  LRRALNGVSTDVQGTDFSEVSYDSVLERVSRGAGS  142
```

3. N. crassa vs. *Homo sapiens*

Sequence 1: *N. crassa* [Length = 154]

Sequence 2: *Homo sapiens* [Length = 166]

Score = 71.6 bits (174), Expect = 2e-11
Identities = 40/121 (33%), Positives = 71/121 (58%), Gaps = 5/121 (4%)

```
Query  20   MSRQLRYIIYKLSDDFKEIVIESTSEGATENYDEFREKLVNAQTKSASGAISKGPRYAVY  79
            + ++ + +++ LS+D K I++E   EG      +  + + +           K  RYA+Y
Sbjct  29   VKKRKKAVLFCLSEDKKNIILE---EGKEILVGDVGQTVDDPYATFVKMLPDKDCRYALY  85

Query  80   DFEYKLASGEGSRNKVTFIAWSPDDAGIKSKMVYASSKEALKRSLSGIAVELQANEQDDI  139
            D  Y+  + E  +  + FI W+P+ A +KSKM+YASSK+A+K+ L+GI  ELQAN  +++
Sbjct  86   DATYE--TKESKKEDLVFIFWAPESAPLKSKMIYASSKDAIKKKLTGIKHELQANCYEEV  143

Query  140  E  140
            +
Sbjct  144  K  144
```

Appendix 1.3: Formin sequence homology among organisms

1. N. crassa vs. *A. nidulans*

Sequence 1: *N. crassa* [Length = 1790]

Sequence 2: *A. nidulans* [Length = 1790]

```
 Score =  973 bits (2514),  Expect = 0.0
 Identities = 552/974 (56%), Positives = 697/974 (71%), Gaps = 43/974 (4%)

Query  50    ASTHTARSSRHYRDSSVISLD-RPDTPESGLNMTAGVVTTIPYDPVSPDNRSPVALDHLP  108
             +S    +RSSR+ + SS+ S+D    D    S L+ +AG +T+IP++ +S D +SP+ +D+L
Sbjct  44    SSAAGSRSSRYSKRSSIQSVDFGADIDPSLLSTSAGPITSIPFESLSTDTQSPIPVDYLS  103

Query  109   RPDQMPLRRELVPHHLNKGTGDFHQYPTIDQSPSSPYNGQSPSASSSRSTLATANITMAS  168
             + +  P R+E  P HL KG GDFHQYP  D S    +  Q    +  R     A + M+S
Sbjct  104   KAETSP-RKEPSPGHLAKGVGDFHQYPAWDPSAMRNHQ-QFSHPTGPRPPPHAAGVAMSS  161

Query  169   TG---RQAQFQQWGPPRESSLPGYNSRGHSYMTT-------RSSGDNASIYSGRDGHYQE  218
             +    + A++QQWG P  S+  G     H   +T       R S D ASI+S    + +
Sbjct  162   SATGDKGARYQQWGRPGSSA--GNAGLSHHSSSTVDSSTNSRMSIDQASIHSSLSSNTRG  219

Query  219   APGTS-HRSSRIGLPSTSSQSSYLSPHAHKDRDTQRLTKVAAGH---QGSEGFNFPKPDD  274
             +  S   SSR  LPS S+  S      +  R +     +      Q +E +   +P D
Sbjct  220   SSYISTDGSSRTTLPSHSNDRSNYYAAMNSGRGSSAQGAIPPAQPRVQNTEQY-LTRPRD  278

Query  275   DNVIEQMFINLMQKRGWHNLPDQAKRQMIAYPAAKKWTLIYQDRLTEWQGEQKRRQTAKI  334
             D V++Q+F+ LMQKRGW NLP+QA+RQM+AYPA+KKWTL++QDRLTE QGEQKR+Q A+
Sbjct  279   DRVVDQLFLELMQKRGWQNLPEQARRQMMAYPASKKWTLVHQDRLTELQGEQKRKQKARE  338

Query  335   --GQYSNVDITQSSDDEGSPEWYVRKVMENALDSKGLGGLEVNLRTQQIGWVKRFIDCQG  392
               G      I + +D+EGSPEWYV+KVM++ + SK L  L V+LRTQ I WVK F++ QG
Sbjct  339   THGYDGPSGILERADEEGSPEWYVKKVMDDTITSKQLASLSVSLRTQPISWVKAFVEAQG  398
```

```
Query  393  QIALTNVLLKMNRKTAYGPAQ-PDNGRLDKNLDREYDIVKCLKALMNNKFGADDALAHQQ  451
            QIALTNVL+K+NRK  GP  P +G  DK+LDREYDIVKCLKALMNNK+GADDALAHQQ
Sbjct  399  QIALTNVLVKINRKKVTGPVPAPPSG--DKDLDREYDIVKCLKALMNNKYGADDALAHQQ  456

Query  452  VIVALATSLISPRLTTRKLVSEVLTFLCHWGEGKGHVKVIEAMDVVKAQQGENGRFDAWM  511
            +IVAL +SL+SPRL TRKLVSEVLTFLCHW EG+GH +V++AMD VK  QGE GRFDAWM
Sbjct  457  IIVALISSLLSPRLNTRKLVSEVLTFLCHWAEGQGHERVLQAMDHVKNHQGETGRFDAWM  516

Query  512  RLVEVTVDGRGKMGSLVGASEEVRSGGIGMENLLMEYAVATLILVNMLVDAPEKDLQLRI  571
            R+VEVT+DGRGKMGSLVGASEE RSGGIGMENLLMEYAV+T+IL+NMLVDAPE DLQLR
Sbjct  517  RIVEVTIDGRGKMGSLVGASEEYRSGGIGMENLLMEYAVSTMILINMLVDAPENDLQLRC  576

Query  572  HIRAQFTACGIRRILNKMEAFQYELIDKQIERFRSNEAIDYEDMLERENSSIKDSIEGEV  631
            HIRAQF +CGI+R+L+KME FQYE+IDKQIE FR NEAIDYED+L+RE+SS KDSIEGEV
Sbjct  577  HIRAQFISCGIKRLLSKMEGFQYEVIDKQIEHFRENEAIDYEDLLQRESSSTKDSIEGEV  636

Query  632  KDLNDPVQIVDAIQQRLNGTKTQDYFVSALQHLLLIRDNDGEERLRMFQLVDSMLSYVAM  691
            KD+ DP+QI DAI  RLNGT+  DYF+SALQHLLLIR+N GE+ LRM+QLVD+MLSYVAM
Sbjct  637  KDMTDPLQITDAIASRLNGTRAHDYFLSALQHLLLIRENSGEDGLRMYQLVDAMLSYVAM  696

Query  692  DRRLPDMDLKQSLNFTVQSLLDKLHTDSEARQALDEALEARQIADAAMAERDEMKERLAL  751
            DRRLPD+DL+Q L FTVQSLLD+LHTD+EAR+A DE+LEARQIA+AA+AERDEMK ++ L
Sbjct  697  DRRLPDLDLRQGLTFTVQSLLDRLHTDAEARRAYDESLEARQIAEAALAERDEMKAQVEL  756

Query  752  GADGLVAKLQKQIDEQAMFIEAQKRRAEGLKSELASLQTLRAKEAQRYELETRELYLMLR  811
            GADGLV KLQKQI+EQ  IE Q R+ E LK+ELA +Q LRA+E QR ELETRELYLMLR
Sbjct  757  GADGLVRKLQKQIEEQTGIIELQSRQNEMLKAELADVQRLRAQELQRNELETRELYLMLR  816

Query  812  DAQDVAASNATKGNAKLGEEDVARMQGILDRERLLERLQMQIERQKTQFKLEGRVWGEVI  871
            DAQD+AASNA K N    E D A M+GILDRE+LL RL+ Q+ER KTQFKLEG+VWG+
Sbjct  817  DAQDIAASNAKKSNMGEAETDPAHMRGILDREKLLTRLEKQLERTKTQFKLEGKVWGQ-H  875

Query  872  GPSDRLRALREEMDGFGDDTPEVVPPKDFTNSMLGSVKRSTRIPRKPVGS---RSDHVED  928
             PSDRLR LRE+MDG      +  P + F       +   +  PVGS   +  +++
Sbjct  876  DPSDRLRELREQMDG------DAGPREAFEE------QARLNLSLNPVGSVYRKKTYIQG  923

Query  929  VLEESDVEIGD-DGEIVYEKPRVVKIRRPVVDPKQTNGMFNELTGKVRRYDASDSEEGDG  987
            + + +  E+G  D E+VY K R+V + RP +DP+Q  G+  E+  KV + DA D+++ +G
```

```
Sbjct  924   MEDTATEELGQTDDEVVYAKARLVDLHRPRMDPEQATGLLGEIAAKVPKIDADDAKD-EG  982

Query  988   ITTGPSHPSMESQT  1001
               T    P+  + T
Sbjct  983   KPTESEQPAEGAAT  996
```

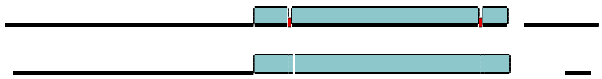

```
 Score =  658 bits (1697),  Expect = 0.0
 Identities = 356/498 (71%), Positives = 418/498 (83%), Gaps = 4/498 (0%)

Query  1119  GLPTTNSVGLPVVRPKKKLKAFHWDKVDTPLATHWAAHTPSPESREEKYHELSKKGILDE  1178
              G P+     +  +RPKKKLKA HWDKVDTP  T WA H  +P+ +EEKY EL+K+G+LDE
Sbjct  1133  GAPSHAIPVMSSIRPKKKLKALHWDKVDTPQVTVWATHGTTPQEKEEKYVELAKRGVLDE  1192

Query  1179  VEKLFMAKE--IKKLGGGGAKKDDKKQIISNDLRKAFEIALAKFSQFPVEKVVQMIIHCD  1236
              VE+LFMAKE  I   G    ++ DKKQIISNDL K F+IAL+KFSQFP E+VV+ IIHCD
Sbjct  1193  VERLFMAKETRIFGGGVAAKQRKDKKQIISNDLSKNFQIALSKFSQFPAEEVVRRIIHCD  1252

Query  1237  KDVLDNPVVMDFLQKDDLCNISDNTAKVMAPYSKDWTGPDAGKDTREQDPNELTRQDQIY  1296
               ++LDN VVM+FLQ+D++C + +N +K+MAPYSKDWTGPDA     REQDP+ELTR+DQIY
Sbjct  1253  AEILDNMVVMEFLQRDEMCTVPENVSKLMAPYSKDWTGPDAANTEREQDPSELTREDQIY  1312

Query  1297  LYTAFELHHYWKSRMRALALTRSFEQEYEEITEKMRAVVAVSESLRDSVSLMNVLGLILD  1356
              LYTAFEL+HYWK+RMRALALTRSFE +YE I+ K+R VV VSESLRDSVSLMNVLGLILD
Sbjct  1313  LYTAFELNHYWKARMRALALTRSFEPDYEHISAKLREVVRVSESLRDSVSLMNVLGLILD  1372

Query  1357  IGNYMNDANKQARGFKLSSLARLGMVKDDKNESTLADLVERIVRQQYPEWEDFAKDIEGV  1416
              IGN+MNDANKQA+GFKLSSLARLGMVKDDKNE+T ADLVERIVR QYPEWEDF + I GV
Sbjct  1373  IGNFMNDANKQAQGFKLSSLARLGMVKDDKNETTFADLVERIVRNQYPEWEDFTEQISGV  1432

Query  1417  IAAQKINIEQLQADAKRYIDNIKNVQMSLDSGNLSDPKKFHPQDRVSQIVQRVMKDARFK  1476
              I  QK+N++QL+ DAK+YIDNIKNVQ SLD+GNLSDPKKFHPQDRVSQI QR MKDAR K
Sbjct  1433  IGLQKLNVDQLRTDAKKYIDNIKNVQASLDAGNLSDPKKFHPQDRVSQITQRSMKDARRK  1492

Query  1477  AEQMQLYLEEMVRTYNDIMVFYGEDPSDDNARREFFSKLASFITEWKRSREKNIQLEEQR  1536
```

```
            AEQMQLYLEEMV+TY+DIMVFYGED +DD ARR+FF+KLA+F+ EWK+S+EKNI LEE R
Sbjct  1493 AEQMQLYLEEMVKTYDDIMVFYGEDNTDDGARRDFFAKLAAFLQEWKKSKEKNIALEEAR  1552

Query  1537 KRNEASMKRKNAQFKALQASEAQG--PASPTSTGAMDSLLEKLRAAAPQTRDQRDRRRRA  1594
            +R EAS+ RK          + A G  P SP ++GAMDSLLEKLRAAAPQ +DQRDRRRRA
Sbjct  1553 RRTEASLARKRINVGLANGAGAAGDAPVSPATSGAMDSLLEKLRAAAPQAKDQRDRRRRA  1612

Query  1595 RLKDRHQVRIASGQQVPD  1612
            RLK+RHQVR+ASGQ++PD
Sbjct  1613 RLKERHQVRVASGQKIPD  1630
```

2. N. crassa vs. *S. cerevisiae*

Sequence 1: *N. crassa* [Length = 1790]

Sequence 2: *S. cerevisiae* [Length = 1953]

```
 Score =  311 bits (797),  Expect = 7e-82
 Identities = 181/474 (38%), Positives = 270/474 (56%), Gaps = 22/474 (4%)

Query  1120  LPTTNSVGLPVVRPKKKLKAFHWDKVDTPLATHWAAHTPSPESREEKY-HELSKKGILDE  1178
             LP + S+     RP KKLK  HW+K+D    + W         + EK+  +L +KG+L +
Sbjct  1341  LPQSPSLFEKYPRPHKKLKQLHWEKLDCTDNSIWGT------GKAEKFADDLYEKGVLAD  1394

Query  1179  VEKLFMAKEIKKLGGGGAKKDDKKQIISNDLRKAFEIALAKFSQFPVEKVVQMIIHCDKD  1238
             +EK F A+EIK L     +   K   +S D+ + F I L  +S   V  +V+ I++CD+D
Sbjct  1395  LEKAFAAREIKSLASKRKEDLQKITFLSRDISQQFGINLHMYSSLSVADLVKKILNCDRD  1454

Query  1239  VLDNPVVMDFLQKDDLCNISDNTAKVMAPYSKDWTGPDAGKDTR--EQDPNELTRQDQIY  1296
              L  P V++FL K ++  +S N A+  APYS DW G    +D +  E+DPN+L R DQIY
Sbjct  1455  FLQTPSVVEFLSKSEIIEVSVNLARNYAPYSTDWEGVRNLEDAKPPEKDPNDLQRADQIY  1514

Query  1297  LYTAFELHHYWKSRMRALALTRSFEQEYEEITEKMRAVVAVSESLRDSVSLMNVLGLILD  1356
             L     L  YW SRMRAL +  S+E+EY E+  K+R V     +L++S +L NV  +IL
Sbjct  1515  LQLMVNLESYWGSRMRALTVVTSYEREYNELLAKLRKVDKAVSALQESDNLRNVFNVILA  1574

Query  1357  IGNYMNDANKQARGFKLSSLARLGMVKDDKNESTLADLVERIVRQQYPEWEDFAKDIEGV  1416
             +GN+MND +KQA+GFKLS+L RL  +KD  N  T  + VE+IVR  YP + DF  ++E V
Sbjct  1575  VGNFMNDTSKQAQGFKLSTLQRLTFIKDTTNSMTFLNYVEKIVRLNYPSFNDFLSELEPV  1634

Query  1417  IAAQKINIEQLQADAKRYIDNIKNVQMSLDSGNLSDPKKFHPQDRVSQIVQRVMKDARFK  1476
             +   K++IEQL  D K +  +I NV+ S++ GNLSD  KFHP D+V      V+ +AR K
Sbjct  1635  LDVVKVSIEQLVNDCKDFSQSIVNVERSVEIGNLSDSSKFHPLDKVLIKTLPVLPEARKK  1694

Query  1477  AEQMQLYLEEMVRTYNDIMVFYGEDPSDDNARREFFSKLASFITEWKRSREKNIQLEEQR  1536
              + ++  ++  +  +  +M  YGED  D  A+  FF K A FI E+K+++ +N+  EE+
```

```
Sbjct  1695  GDLLEDEVKLTIMEFESLMHTYGEDSGDKFAKISFFKKFADFINEYKKAQAQNLAAEEEE  1754

Query  1537  K-----RNEASMKRKNAQFKALQASEAQGPASPTS--------TGAMDSLLEKL  1577
             +     +     ++K AQ K  Q   +  P+S  +            MD LLE+L
Sbjct  1755  RLYIKHKKIVEEQQKRAQEKEKQKENSNSPSSEGNEEDEAEDRRAVMDKLLEQL  1808
```

```
 Score =  231 bits (589),  Expect = 9e-58
 Identities = 163/575 (28%), Positives = 285/575 (49%), Gaps = 60/575 (10%)

Query  352  PEWYVRKVMENALDSKGLGGLEVNLRTQQIGWVKRFIDCQGQIALTNVLLKMNRKTAYGP  411
            P  YV++++ + L S  +  L V LRT+Q+ WV  FID QG IA+ NVL+    KTA
Sbjct  338  PIHYVQRILADKLTSDEMKDLWVTLRTEQLDWVDAFIDHQGHIAMANVLMNSIYKTA---  394

Query  412  AQPDNGRLDKNLDREYDIVKCLKALMNNKFGADDALAHQQVIVALATSLISPRLTTRKLV  471
              P       + L++E    KC + L     G  +  H+ +   +A  L S +L TRK+
Sbjct  395  --PRENLTKELLEKENSFFKCFRVLSMLSQGLYEFSTHRLMTDTVAEGLFSTKLATRKMA  452

Query  472  SEVLTFLCHWGEGKGHVKVIEAMDVVKAQQGENGRF----------------------D  508
            +E+   +            V+ ++D  K + G+N
Sbjct  453  TEIFVCMLEKKNKSRFEAVLTSLDK-KFRIGQNLHMIQNFKKMPQYFSHLTLESHLKIIQ  511

Query  509  AWMRLVEVTVDGRGKMGSLVGASEEVRSGGIGMENLLMEYAVATLILVNMLVDAPEKDLQ  568
            AW+  VE T+DGRGKMGSLVGAS+E ++GG   EN ++EY   T++ +N L    + ++
Sbjct  512  AWLFAVEQTLDGRGKMGSLVGASDEFKNGG--GENAILEYCQWTMVFINHLCSCSD-NIN  568

Query  569  LRIHIRAQFTACGIRRILNKMEAFQYELIDKQIERFRSNEAIDYEDMLERENSSIKDSIE  628
             R+ +R +   CGI RI+NK++   Y+ +  QIE + +N+  D+   LE  N +
Sbjct  569  QRMLLRTKLENCGILRIMNKIKLLDYDKVIDQIELYDNNKLDDFNVKLEANNKAFN----  624

Query  629  GEVKDLNDPVQIVDAIQQRLNGTKTQDYFVSALQHLLL-----IRDNDGEERL-RMFQLV  682
                DL+DP+ ++  +     GT+ +   VS +QHL L      I +N     +L +  +L+
Sbjct  625  ---VDLHDPLSLLKNLWDICKGTENEKLLVSLVQHLFLSSSKLIEENQNSSKLTKQLKLM  681

Query  683  DSMLSYVAMDRRLPDMDLKQSLNFTVQSLLDKLHTDSEARQALDEALEARQIADAAMAER  742
```

```
            DS+++ V++        D + ++N  +Q L D + TD  AR+A+ E+    +  +   AER
Sbjct  682  DSLVTNVSV---ASTSDEETNMNMAIQRLYDAMQTDEVARRAILESRALTKKLEEIQAER  738

Query  743  DEMKERLALGADGLVAKLQKQIDEQAMFIEAQKRRAEGLKSELASLQTLRAKEAQRYELE  802
            D + E+L+    GLV +L+ ++ E+   +   +R  + L++EL  L+     E  + E+E
Sbjct  739  DSLSEKLSKAEHGLVGQLEDELHERDRILAKNQRVMQQLEAELEELKKKHLLEKHQQEVE  798

Query  803  TRELYLML--RDAQDVAASNATKG-NAKLGEEDVARMQGILDRERLLERLQMQIERQKTQ  859
             R++  +L  R  +    +  T+G N+ L   + A +Q +          LQ  + R K
Sbjct  799  LRKMLTILNSRPEESFNKNEGTRGMNSSLNSSEKANIQKV---------LQDGLSRAKKD  849

Query  860  FKLEGRVWGEVIGPSDRLRALREEMDGFGDDTPEV  894
            +K + + +G  + P+ RL+ LR +M+   ++  ++
Sbjct  850  YKDDSKKFGMTLQPNKRLKMLRMQMENIENEARQL  884
```

3. N. crassa vs. *Homo sapiens*

Sequence 1: *N. crassa* [Length = 1790]

Sequence 2: *Homo sapiens* [Length = 1722]

```
 Score = 63.5 bits (153),  Expect = 3e-07
 Identities = 85/432 (19%), Positives = 177/432 (40%), Gaps = 69/432 (15%)
Query  1142  WDKVDTP-LATHWAAHTPSPESREEKYHELSKKGILDEVEKLFMAKEIKKLGGGGAKKDD  1200
             W+K++ P +  H      S  + +E+     KK I D + K   AK++
Sbjct  1315  WEKIEEPSIDCHEFEELFSKTAVKER-----KKPISDTISKT-KAKQVV----------  1357

Query  1201  KKQIISNDLRKAFEIALAKFSQFPVEKVVQMIIHCDKDVLDNPVVMDFL----QKDDLCN  1256
               +++SN   +A  I ++      ++ +   +++ D  V+D   +        Q D+L
Sbjct  1358  --KLLSNKRSQAVGILMSSL-HLDMKDIQHAVVNLDNSVVDLETLQALYENRAQSDELEK  1414

Query  1257  ISDNTAKVMAPYSKDWTGPDAGKDTREQDPNELTRQDQIYLYTAFELHHYWKSRMRALAL  1316
             I  +                 G+ +++++  +   + + +LY    + ++   R+  +
Sbjct  1415  IEKH-----------------GRSSKDKENAKSLDKPEQFLYELSLIPNF-SERVFCILF  1456

Query  1317  TRSFEQEYEEITEKMRAVVAVSESLRDSVSLMNVLGLILDIGNYMNDANK---QARGFKL  1373
               +F +    I  K+  +  + E+L++  +L  VLGL+L  GNYMN  NK   QA GF L
Sbjct  1457  QSTFSESICSIRRKLELLQKLCETLKNGPGVMQVLGLVLAFGNYMNGGNKTRGQADGFGL  1516

Query  1374  SSLARLGMVKDDKNESTLADLVERIVRQQYPEWEDFAK--------DIEGVIAAQKINIE  1425
               L +L  VK   N  +L   +     + +   ED  K         + + +  A ++  E
Sbjct  1517  DILPKLKDVKSSDNSRSLLSYIVSYYLRNFD--EDAGKEQCLFPLPEPQDLFQASQMKFE  1574

Query  1426  QLQADAKRYIDNIKNVQMSLDSGNLSDPKKFHPQDRVSQIVQRVMKDARFKAEQMQLYLE  1485
               Q D ++   ++K  +  +++G +              + +++ +  A+   E  +  L
Sbjct  1575  DFQKDLRKLKKDLKACE--VEAGKVYQVSSKEHMQPFKENMEQFIIQAKIDQEAEENSLT  1632

Query  1486  EMVRTYNDIMVFY------GEDPSDDNARREFFSKLASFITEWKR--SREKNIQLEEQRK  1537
             E  + + +   ++      GE     NA   FFS    F +++K    +E  + L+E+ K
Sbjct  1633  ETHKCFLETTAYFFMKPKLGEKEVSPNA---FFSIWHEFSSDFKDFWKKENKLLLQERVK  1689
```

```
Query  1538  RNEASMKRKNAQ  1549
               E  ++K  +
Sbjct  1690  EAEEVCRQKKGK  1701
```

Appendix 2: Vogel's minimal medium

Ingredients (50X stock solution)

Chemicals	g/L
Na_3 citrate $2H_2O$	125
KH_2PO_4	250
NH_4NO_3	100
$MgSO_4.7H_2O$	10
$CaCl_2.2H_2O$	5
Distilled water	750
Biotin (Vitamin H)	5
Trace element solution	5

Trace element stock solution

Chemicals	g/100ml
Citric acid.1H_2O	5
$ZnSO_4.7H_2O$	5
$Fe(NH_4)_2(SO_4)_2.6H_2O$	1
$CuSO_4.5H_2O$	0.25
$MnSO_4.1H_2O$	0.05
H_3BO_3	0.05
$Na_2MoO_4.2H_2O$	0.05